Online Monitoring-Based Methodologies to Assess Microaerobic 2,3-Butanediol Production

Methoden zur Evaluierung der microaeroben 2,3-Butandiol Produktion basierend auf Online-Prozessüberwachungstechnologien

Von der Fakultät für Maschinenwesen der Rheinisch-Westfälischen Technischen Hochschule Aachen zur Erlangung des akademischen Grades eines Doktors der Naturwissenschaften genehmigte Dissertation

vorgelegt von

Benedikt Heyman

Berichter: Universitätsprofessor Dr.-Ing. Dr. h. c. (Osaka) Jochen Büchs
Privatdozent Dr. rer. nat. habil. Ulf Prüße

Tag der mündlichen Prüfung: 13.12. 2019

Danksagung

Die vorliegende Dissertation wurde während meiner Tätigkeit als wissenschaftlicher Mitarbeiter am Lehrstuhl für Bioverfahrenstechnik der RWTH Aachen verfasst. Die Arbeit wurde im Rahmen des Exzellenzclusters „Tailor-Made Fuels from Biomass" (TMFB) angefertigt, welcher durch die deutschen Bundes- und Länderregierungen finanziert wurde. Zusätzlich durfte ich als Kollegiat am Graduiertenkolleg „Selectivity in Chemo- and Biocatalysis" (SeleCa) teilnehmen, welches durch die Deutsche Forschungsgemeinschaft (DFG) finanziert wurde.

Mein besonderer Dank gilt Prof. Jochen Büchs für die Betreuung der Arbeit und für die Möglichkeit am Lehrstuhl für Bioverfahrenstechnik zu promovieren. Seine Unterstützung und Anregungen, sowie die immer vertrauensvolle und konstruktive Zusammenarbeit waren Voraussetzung für das Gelingen dieser Arbeit. Die Promotionszeit war eine spannende, herausfordernde und lehrreiche Zeit, in der ich mich wissenschaftlich und persönlich weiterentwickeln konnte. Außerdem möchte ich Dr. Ulf Prüße danken, dass er das Koreferat meiner Arbeit übernommen hat. Prof. Christoph Broeckmann danke ich für die Übernahme des Prüfungsvorsitzes.

Bei allen Kooperationspartnern innerhalb und außerhalb von TMFB und SeleCa möchte ich mich für die gute Zusammenarbeit bedanken. Der interdisziplinäre Austausch hat meine Arbeit sehr bereichert.

Ich danke Prof. Eiichiro Fukusaki, Ass.-Prof. Sastia Putri, Teruko Matsuo und Moyu Taniguchi an der Osaka Universität in Japan. Sie haben mich herzlich an der Osaka Universität empfangen und haben keine Mühen gescheut, mir die japanische Kultur und Küche näherzubringen. Außerdem möchte ich Birthe Halmschlag und Tobias Schindler für die unvergessliche gemeinsame Zeit bei unserem Forschungsaufenthalt in Osaka danken.

Die gesamte Promotionszeit war von der Zusammenarbeit mit den Kolleginnen und Kollegen der BioVT geprägt, denen ich für die gute und freundschaftliche Arbeitsatmosphäre danken möchte. Besonders Robin Lamm danke ich für die zahlreichen Diskussionen und für die Freundschaft, die in den vielen gemeinsamen Stunden entstanden ist. Bei Dirk Kreyenschulte und Lars Regestein möchte ich mich für die gute und herzliche Unterstützung vor allem zu Beginn der Promotionszeit bedanken. Ein weiterer Dank gilt Bertram Geinitz, Nina Ihling, Tobias Habicher, Timm Keil, Markus Müller, Elena Herweg, Kira Kauffmann, Kyra Hoffmann, Judith Loogen, Christoph Scheeren und Georg Wandrey für die schöne gemeinsame Zeit bei und neben der Arbeit. Außerdem danke ich Tamara Sous, René Petri, Stefan Taubert und Elena Wolf, deren Arbeit unerlässlich ist, um den reibungslosen Ablauf des Lehrstuhls zu gewährleisten.

Bei meinen Studierenden Hannah Tulke, Katharina Miebach, Katja Rohr, Vanessa Schmitt, Damarice Wandji und Patrick Lichtner möchte ich mich dafür bedanken, dass sie mich durch ihre Arbeiten unterstützt haben. Das hat mich sowohl wissenschaftlich als auch persönlich sehr bereichert.

Meinen Freunden und meiner Familie möchte ich dafür danken, dass sie mir immer geholfen haben, Abstand von der Arbeit zu gewinnen und einen Ausgleich zu schaffen. Ganz besonderes danke ich Nina, für die bedingungslose Unterstützung auf unserem gemeinsamen Weg.

Aachen, im Dezember 2019 Benedikt Heyman

Zusammenfassung

Die biotechnologische Produktion von Plattformchemikalien aus erneuerbaren Ressourcen trägt dazu bei, den Verbrauch fossiler Rohstoffe in der chemischen Industrie zu senken. Häufig werden reduzierte Plattformchemikalien wie 2,3-Butandiol in mikroaeroben Prozessen hergestellt. Bei diesen sauerstofflimitierten Kultivierungen muss die Sauerstoffverfügbarkeit präzise eingestellt werden, um die gewünschte Stoffwechselaktivität zu erreichen.

In dieser Arbeit wurde die 2,3-Butandiolproduktion mit *Bacillus licheniformis* als Modell-Bioprozess verwendet, um basierend auf Online-Prozessüberwachungstechnologien Methoden zur Beurteilung und Optimierung mikroaerober Kultivierungen zu entwickeln. Durch die Anwendung eines definierten zweistufigen Kultivierungsprofils und eines neuen Ansatzes zur Bestimmung der maximalen 2,3-Butandiolkonzentration wurde eine einfache und zuverlässige Methode zur Bestimmung der optimalen Sauerstoffverfügbarkeit entwickelt. Ein genereller Nachteil bei der Entwicklung von mikroaeroben Kultivierungen ist die begrenzte Verfügbarkeit von Online-Prozessüberwachungstechnologien zur Bestimmung der Stoffwechselaktivität in Abhängigkeit von der Sauerstoffverfügbarkeit. Daher wurden Online-Messungen des Respiratorischen Quotienten mit stöchiometrischen Analysen kombiniert, um die metabolische Aktivität in verschiedenen Kultivierungsphasen zu entschlüsseln. Darüber hinaus wurde die Messung des Redoxpotentials zur Bestimmung sehr geringer Gelöstsauerstoffkonzentrationen (DOT) eingesetzt. Der Einfluss von DOT, pH-Wert und Medienkomponenten auf das Redoxpotential wurde in abiotischen Experimenten charakterisiert und quantifiziert. Durch entsprechende Korrektur des Redoxpotentials können geringe Änderungen der DOT während der Kultivierung auch bei schwankenden pH-Werten isoliert gemessen werden.

Die entwickelten Methoden sind auf andere Mikroorganismen übertragbar und steigern den Informationsgewinn durch Online-Prozessüberwachung bei mikroaeroben Kultivierungen. Der Respiratorische Quotient und das Redoxpotential liefern detaillierte und komplementäre Informationen über die Stoffwechselaktivität. Zusammen mit dem Konzept zur Untersuchung der Sauerstoffverfügbarkeit trägt dies entscheidend zur Entwicklung verbesserter mikroaerober Kultivierungsprozesse für die Herstellung verschiedener biobasierter Produkte bei.

Abstract

Biotechnological production of platform chemicals from renewable carbon sources is a promising measure to decrease the consumption of fossil resources in the chemical industry and the fuel sector. Reduced platform chemicals like 2,3-butanediol are often produced in microaerobic cultivation processes. Under these oxygen-limited conditions, the precise adjustment of the oxygen availability is crucial to obtain the desired metabolic activity.

In this thesis, 2,3-butanediol production with *Bacillus licheniformis* was used as model bioprocess to develop online monitoring-based methodologies to assess microaerobic cultivations. A fast and reliable shake flask methodology is presented to determine the optimum oxygen availability. Comparable results and well-characterized experimental conditions were obtained by application of a defined two-stage cultivation profile and a novel technique to determine the maximum 2,3-butanediol concentration. As the obtained results are applicable to stirred tank reactor cultivations, the product and by-product spectrum can be optimized at reduced effort and costs. Still, a drawback for microaerobic process development is the limited availability of online monitoring techniques to determine the metabolic activity with respect to oxygen availability. Therefore, online monitoring of the respiratory quotient was combined with stoichiometric analyses to reveal the metabolic activity during distinct cultivation phases. Furthermore, monitoring of the redox potential was used to monitor the dissolved oxygen tension (DOT) at trace levels that cannot be resolved with conventional DOT probes. The influence of DOT, pH and media components on the redox potential was characterized and quantified in abiotic experiments. On this basis, a corrected redox potential is obtained that solely reflects changes of the DOT, even if the pH strongly fluctuates during the cultivation.

Overall, the developed methodologies are transferable to other microorganisms or products and increase the information content from online monitoring during microaerobic cultivations. Respiratory quotient and redox potential provide detailed and complementary information on the metabolic activity during microaerobic cultivations. Together with the presented approach to investigate the effects of oxygen availability, this contributes to the development of improved microaerobic cultivation processes for the production of diverse bio-based compounds.

Funding and publications

This work was performed as part of the Cluster of Excellence “Tailor-Made Fuels from Biomass” EXC 236, which is funded by the Excellence Initiative by the German federal and state governments to promote science and research at German universities. Additional funding was received from the German Research Foundation (DFG) through the International Research Training Group “Selectivity in Chemo- and Biocatalysis” (SeleCa).

Parts of this thesis have been published previously, or are in preparation for submission:

- Heyman, B., Tulke, H., Putri, S.P., Fukusaki, E. Büchs, J. **2020**. Online monitoring of the respiratory quotient reveals metabolic phases during microaerobic 2,3-butanediol production with *Bacillus licheniformis*. *Eng Life S*ci, 20, 133-144.

- Heyman, B., Lamm, R., Tulke, H., Regestein, L., Büchs, J. **2019**. Shake flask methodology for assessing the influence of the maximum oxygen transfer capacity on 2,3-butanediol production. *Microb Cell Fact*, 18(78).

Contributions to further publications during the preparation of this thesis:

- Lamm, A., Jäger, V.D., Heyman, B., Berg, C., Cürten, C., Krauss, U., Jaeger, K.E., Büchs, J. **2020**. Detailed small-scale characterization and scale-up of active YFP inclusion body production with *Escherichia coli* induced by a tetrameric coiled coil domain. J *Biosci Bioeng.*

- Eggert, A., Maßmann, T., Kreyenschulte, D.H., Becker, M., Heyman, B., Büchs, J., Jupke, A. **2019**. Integrated in-situ product removal process concept for itaconic acid

by reactive extraction, pH-shift back extraction and purification by pH-shift crystallization. *Sep Purif Technol,* 215, 463-472.

- Regestein, L., Klement, T., Grande, P.M., Kreyenschulte, D.H., Heyman, B., Maßmann, T., Eggert, A., Sengpiel, R.G., Wang, Y., Wierckx, N., Blank, L.M., Spiess, A.C., Leitner, W., Bolm, C., Weßling, M., Jupke, A., Agler-Rosenbaum, M., Büchs, J. **2018**. From beech wood to itaconic acid: case study on biorefinery process integration. *Biotech Biofuels*, 11, 279-289.

- Kreyenschulte*, D.H., Heyman*, B., Eggert, A., Maßmann, T., Kalvelage, C., Kossack, R., Regestein, L., Jupke, A., Büchs, J. **2018.** In situ reactive extraction of itaconic acid during fermentation of *Aspergillus terreus*. *Biochem Eng J,* 135, 133-141.

- Drabo, P., Tiso, T., Heyman, B., Sarikaya, E., Gaspar, P., Förster, J., Büchs, J., Blank, L.M., Delidovich, I. **2018.** Anionic extraction for efficient recovery of biobased 2,3-butanediol - a platform for bulk and fine chemicals. *Chem Sus Chem,* 16, 3252-3259.

*These authors contributed equally to the publication.

Contents

Nomenclature

List of abbreviations

Abbreviation	Description
ADP	Adenosine diphosphate
ATP	Adenosine triphosphate
CTR	Carbon dioxide transfer rate
DOT	Dissolved oxygen tension
FAD	Flavin adenine dinucleotide (quinone form)
$FADH_2$	Flavin adenine dinucleotide (hydroquinone form)
HPLC	High performance liquid chromatography
k_La	Volumetric mass transfer coefficient
MEK	Methyl-ethyl-ketone
MES	2-(*N*-morpholino) ethanesulfonic acid
NAD^+	(Oxidized) nicotinamide adenine dinucleotide
NADH	(Reduced) nicotinamide adenine dinucleotide
OD_{600}	Optical density at a wavelength of 600 nm
ORP	Oxidation reduction potential
OTR	Oxygen transfer rate
OTR_{max}	Maximum oxygen transfer capacity
RAMOS	Respiration Activity Monitoring System
rpm	Rounds per minute
RQ	Respiratory quotient
TMFB	Cluster of Excellence “Tailor-Made Fuels from Biomass”
TCA cycle	Tricarboxylic acid cycle
vvm	Volume specific aeration rate per minute

List of symbols

Abbreviation	Description	Unit
$(\Delta log_{10}(DOT)/\Delta E_h)_{calib}$	Slope of the logarithmic DOT against the redox potential	1/V
a_{O2}	Activity of oxygen	-
DOT_{calc}	Calculated DOT	%
DOT_{calib}	Calibrated DOT	%
$DOT_{measured}$	Measured DOT	%
e^-	Electrons	-
E^0	Standard redox potential referred to normal hydrogen electrode	V
E_h	Redox potential	V
$E_{h_{cor}}$	Corrected redox potential (independent of the pH)	V
$E_{h_{measured}}$	Measured redox potential	V
F	Faraday constant	C/mol
j	Amount of oxygen that serves as electron acceptor	mol
m	Amount of transferred protons	mol
n	Amount of transferred electrons	mol
Ox	Oxidant in a redox reaction	mol
R	Universal gas constant	$kg \cdot m^2/(s^2 \cdot mol \cdot K)$
Red	Reductant in a redox reaction	mol
T	Absolute temperature	K
ν_i	Stoichiometric coefficient of compound i	-
ΔE_{But}	Redox potential shift caused by 2,3-butanediol changes	V/(g/L)
ΔE_{DOT}	Redox potential shift caused by DOT changes	V/log(DOT)
ΔE_{Glu}	Redox potential shift caused by glucose changes	V/(g/L)
ΔE_h	Redox potential shift	V
ΔE_{medium}	Redox potential shift caused by medium composition changes	V
ΔE_{pH}	Redox potential shift caused by the pH changes	V

List of figures

Chapter 1

Introduction

In 2018, nearly 85% of the global primary energy used for electricity production originated from fossil resources (BP, 2019). However, climate change, resource depletion and political concerns are strong driving forces to develop alternative concepts for reduced fossil resource utilization. A promising approach is the replacement of fossil resources by renewable alternatives with lower carbon footprint. In this scenario, utilization of lignocellulosic biomass or organic waste streams for biotechnological production of platform chemicals can improve the sustainability of the chemical industry and the fuel sector (Blaschek et al., 2010; Hermann and Patel, 2007; Koutinas et al., 2016). Especially for fuel production, reduced products like fatty acids (e.g. in biodiesel) or alcohols are attractive due to their high specific energy (Antoni et al., 2007). Production of these reduced compounds in bioprocesses is usually achieved by reduction of the oxygen supply (Liu et al., 2013; Parawira et al., 2004; Saisaard et al., 2011; Wu et al., 2019). Consequently, microaerobic or completely anaerobic cultivation processes have gained increasing attention for biofuel production (Liu et al., 2013).

1.1 Microaerobic cultivation conditions

Bioprocesses can be categorized as anaerobic, microaerobic or aerobic based on the availability of oxygen. In aerobic bioprocesses, the energy demand to ensure sufficient oxygen supply by

agitation and aeration significantly contributes to the overall energy consumption (Kreyenschulte et al., 2016). Consequently, cultivation processes with reduced oxygen transfer are economically attractive. However, microaerobic conditions often result in enhanced biomass and accelerated product formation compared to completely anaerobic cultivations (Nguyen and Khanal, 2018; Saisaard et al., 2011).

Microaerobic conditions are achieved, when the oxygen transfer from the gaseous to the aqueous phase is lower than the microorganisms' oxygen demand. Consequently, the dissolved oxygen tension (DOT) is in the range of the organism's K_m value, which is usually close to zero. As depicted in Figure 1-1, the organism adapts to reduced oxygen availability by activation of anaerobic pathways (Partridge et al., 2007). Thereby, a relative oxygen availability of one indicates fully aerobic conditions without oxygen limitation. Anaerobic conditions are present at a relative oxygen availability of zero and microaerobic conditions at values between zero and one. As long as some oxygen is available, respiratory pathways remain active as this is the most efficient way to generate energy and to maintain the NADH/NAD^+ balance (Zeng and Deckwer, 1996). However, the intracellular NADH/NAD^+ balance cannot solely be maintained by oxidation of NADH in the respiratory chain under microaerobic conditions. Consequently, the formation of reduced metabolites or organic acids via anaerobic pathways is favored to regenerate NAD^+ to maintain energy production via glycolysis (Zeng et al., 1994). This metabolic adaption to microaerobic conditions can be utilized for biotechnological production processes. Prominent examples for products that are obtained from microaerobic cultivations are organic acids (Li et al., 2015b; Tian et al., 2015) or alcohols like ethanol (Franzén, 2003; Pham et al., 2008; Saisaard et al., 2011) and 2,3-butanediol (cf. Section 1.2). Furthermore, microaerobic cultivation conditions are often beneficial for the biotechnological production of various products including amino acids, vitamins, polysaccharides, antibiotics, vaccines and enzymes (Zeng and Deckwer, 1996).

Despite the benefits for many production processes, the limited availability of online process monitoring and control possibilities is a general challenge in microaerobic cultivations. Even though changes in the oxygen availability severely influence the cultivation performance (Figure 1-1), online monitoring is often restricted to pH measurement (Liu et al., 2013). In contrast, the DOT, which is often used as control parameter in aerobic cultivations, is close to zero (in the range of the K_m-value for oxygen) under microaerobic conditions. In this range, the

DOT cannot be monitored with DOT probes. Additionally, the oxygen transfer rate (OTR) is constant at the level of the maximum oxygen transfer capacity (OTR_{max}). Therefore, many metabolic phenomena like diauxic effects, limitations and inhibitions that affect the course of the OTR in aerobic cultivations cannot be observed (Anderlei and Büchs, 2001). However, measurements of the respiratory quotient (RQ) (Franzén, 2003; Zeng et al., 1991b; Zeng et al., 1994) and the redox potential (Kjaergaard, 1977; Liu et al., 2013) have been applied to monitor and control the metabolic activity under microaerobic cultivation conditions. Therefore, the application of these measurement techniques was investigated in this thesis and is introduced in detail in Chapter 4 and 5, respectively.

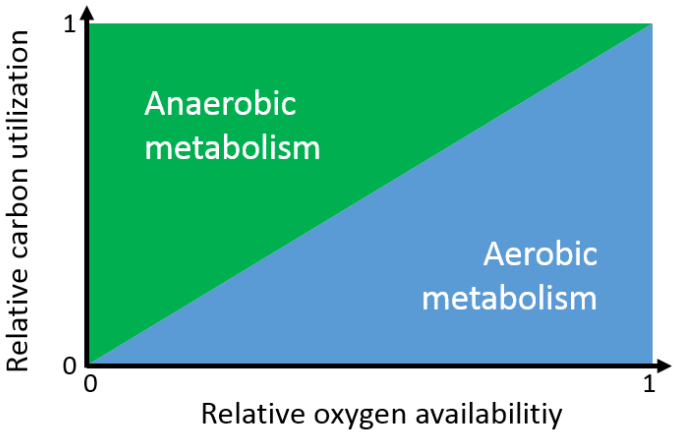

Figure 1-1: Schematic presentation of the metabolic response to microaerobic conditions. The oxygen availability defines if anaerobic (0), microaerobic (0-1) or completely aerobic (1) conditions are present. Thereby, an oxygen availability of one indicates that the organism's oxygen demand is lower than the amount of oxygen that is supplied to the cultivation broth.

1.2 2,3-Butanediol production

2,3-Butanediol is a widely used platform chemical with numerous applications in the chemical and pharmaceutical industry. Amongst others, it is used for 1,3-butadiene or methyl-ethyl-ketone (MEK) synthesis and is a basis for several resins, solvents, fuels, polymers, food additives, plasticizers, cosmetics and drugs (Bialkowska, 2016; Celinska and Grajek, 2009; Ji et al., 2011; Penner et al., 2017). As bivalent alcohol with two chiral centers, three stereoisomers

of 2,3-butanediol exist, two optically active isomers (referred to as D- and L-2,3-butanediol) and the optically inactive meso-2,3-butanediol (Figure 1-2). However, in many applications achiral products like 1,3-butadiene or MEK are derived from all 2,3-butanediol stereoisomers since the stereo-confirmation does not affect the conversion (Drabo et al., 2017).

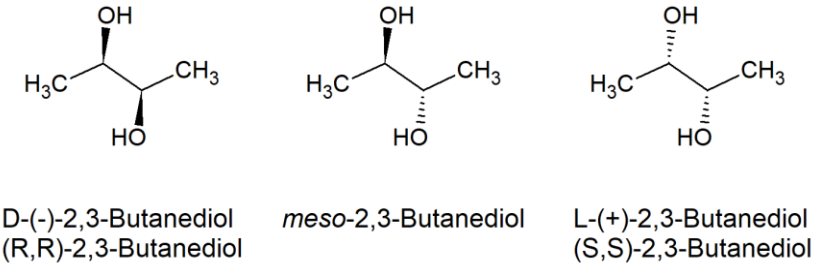

Figure 1-2: Chemical structure and nomenclature of the 2,3-butanediol stereoisomers.

2,3-Butanediol was identified as promising intermediate for fuel production within the Cluster of Excellence "Tailor-Made Fuels from Biomass" (TMFB) at RWTH Aachen University. TMFB was initiated in 2007 as part of the Excellence Initiative of the German Research Foundation (DFG). The aim of the cluster is the development of novel fuels with tailor-made properties. Thereby, an interdisciplinary approach is followed to identify fuels with improved combustion characteristics that can be produced via effective and sustainable production routes. One of the identified candidate fuels is MEK that shows high knock resistance and increased combustion stability at low engine load in spark ignition engines (Hoppe et al., 2016). Within the TMFB, a conceptual MEK production route starting from lignocellulosic biomass was developed (Penner et al., 2017). Lignocellulosic biomass is pretreated and hydrolyzed and the obtained sugars are converted to 2,3-butanediol via fermentation. After separation from the culture broth, 2,3-butanediol is dehydrated to MEK. Within this thesis, the biotechnological 2,3-butanediol production was investigated in the context of the described TMFB production chain.

Conventionally, 2,3-butanediol is produced via chemical synthesis. Nevertheless, due to ecological as well as political concerns and to decouple the 2,3-butanediol price from fluctuating oil prices, biotechnological 2,3-butandediol production has been the focus of many research activities, which have been summarized in numerous review articles (Bialkowska, 2016; Celinska and Grajek, 2009; Garg and Jain, 1995; Ji et al., 2011; Sabra et al., 2016; Syu,

2001; Zeng and Sabra, 2011). 2,3-Butanediol can be produced from a number of different carbon sources including hexoses, pentoses or glycerol (Syu, 2001). For industrial applications, utilization of cheap and easily available renewable carbon sources is desirable. Lignocellulosic biomass is the most abundant renewable carbon source (Ji et al., 2011). Therefore, lignocellulosic substrates like corn stover (Li et al., 2015a) or wood hydrolysates (Frazer and McCaskey, 1989) have been used for 2,3-butanediol production. However, lignocellulosic biomass usually has to be pretreated by physiochemical or enzymatic methods to make the sugar monomers accessible for biotechnological conversion. In contrast, non-cellulosic waste streams or side products can often be used without physiochemical or enzymatic pretreatment (Bialkowska, 2016). Amongst others, 2,3-butanediol production has been reported from Jerusalem artichoke tubers (Sun et al., 2009), sugarcane molasses (Dai et al., 2015), apple pomace hydrolysate (Bialkowska et al., 2015), whey (Perego et al., 2000) and crude glycerol waste streams of biodiesel production (Cho et al., 2015a).

Under microaerobic conditions, 2,3-butanediol is produced in a mixed acid-2,3-butanediol pathway (Figure 1-3). As some oxygen is available, aerobic pathways like TCA-cycle and respiratory chain are partially active. Additionally, anaerobic pathways are activated to maintain the $NADH/NAD^+$ balance (Zeng and Deckwer, 1996) by formation of glycerol, succinate, ethanol, lactate or 2,3-butanediol. The 2,3-butanediol production pathway starts from pyruvate. Figure 1-3 shows the generation of pyruvate from glucose via glycolysis. When pentoses are used as carbon source, pyruvate is generated via the pentose phosphate pathway (Magee and Kosaric, 1987). Two pyruvate molecules are converted to α-acetolactate and subsequently to acetoin (catalyzed by α-acetolactate synthase and α-acetolactate decarboxylase). During these conversion steps, two carbon dioxide molecules are emitted. Acetoin in finally converted to 2,3-butanediol by 2,3-butanediol dehydrogenases. Depending on the organism, different 2,3-butanediol stereoisomers are formed as different 2,3-butanediol dehydrogenases are present. Figure 1-3 shows the stereoisomer formation mechanism in *Bacillus licheniformis* (Ge et al., 2016). In this case, α-acetolactate is converted to D-acetoin, which is then converted to *meso*- and D-2,3-butanediol. In other organisms, diacetyl is formed either directly from pyruvate, or from α-acetolactate (Ji et al., 2011). Diacetyl is then converted to L-acetoin, which can be converted to *meso*- and L-2,3-butanediol (Chen et al., 2014; Ge et al., 2016; Ji et al., 2011). Due to these pathways, most organisms produce mixtures of *meso*-

2,3-butanediol and either D- or L-2,3-butanediol (Chen et al., 2014). *Bacillus* species usually produce mixtures of *meso*- and D-2,3-butanediol (Ge et al., 2016; Ji et al., 2011; Wang et al., 2012), whereas *Klebsiella* strains produce *meso*- and L-2,3-butanediol (Chen et al., 2014; Ji et al., 2011). But also nearly enantiopure production of *meso*- or D-2,3-butanediol occurs naturally in *Serratia marcescens* (Magee and Kosaric, 1987), or *Paenibacillus polymyxa* (Gao et al., 2010; Nakashimada et al., 1998), respectively.

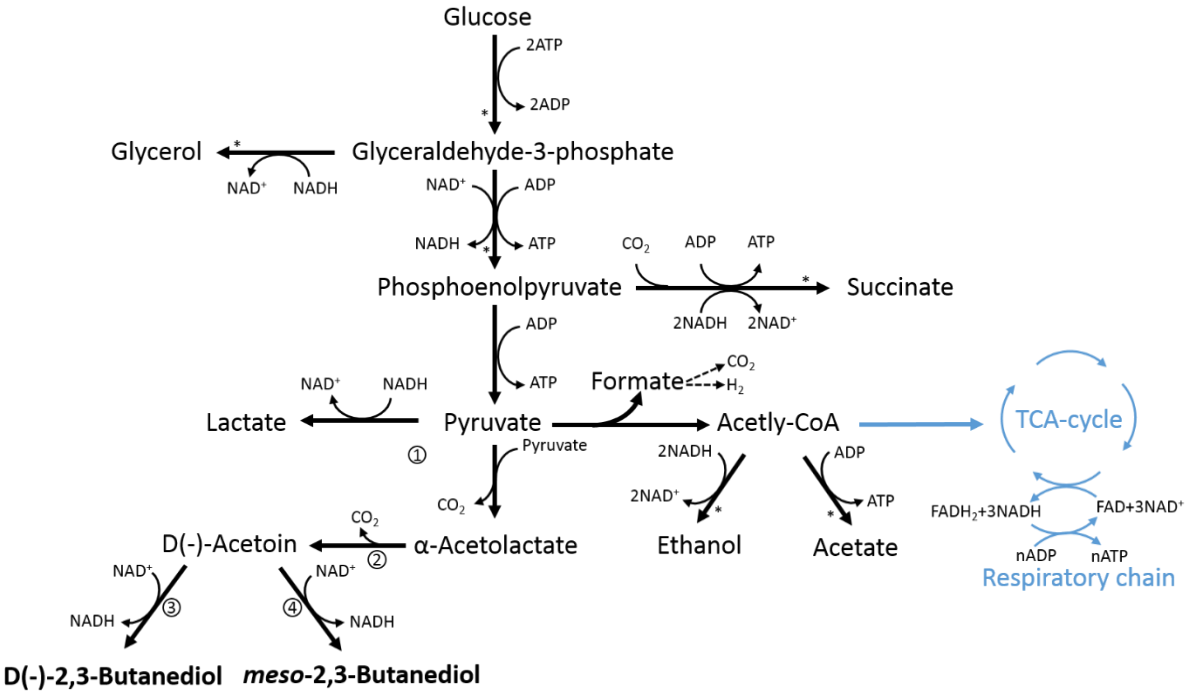

Figure 1-3: Mixed acid-2,3-butanediol production under microaerobic conditions. Aerobic pathways like tricarboxylic acid (TCA) cycle and respiratory chain that are only active in the presence of oxygen are shown in blue. The 2,3-butanediol stereoisomer formation mechanism is shown for *Bacillus licheniformis*. Enzymes in the 2,3-butanediol pathway are indicated by numbers: α-acetolactate synthase (1), α-acetolactate decarboxylase (2), D(-)-2,3-butanediol dehydrogenase (3) and *meso*-2,3-butanediol dehydrogenase (4). Simplified multi step reaction are indicated by * next to the arrowheads. Modified to show the metabolic activity of *Bacillus licheniformis* based on Ge et al. (2016), Ji et al. (2011) and Shariati et al. (1995).

Production of high 2,3-butanediol concentrations up to 150 g/L has been reported especially with pathogenic organisms like *Klebsiella pneumoniae* (Ma et al., 2009), *Klebsiella oxytoca* (Cho et al., 2015b), *Enterobacter cloacae* (Li et al., 2015a), *Enterobacter aerogen*es (Zeng et al., 1991a) and *Serracia marcescens* (Zhang et al., 2010). However, utilization of pathogenic organisms results in higher safety regulations and, therefore, higher costs in industrial

applications. Consequently, non-pathogenic 2,3-butanediol producers are promising candidates for industrial production processes (Jurchescu et al., 2013; Yang et al., 2011). Genetic engineering enables 2,3-butanediol production with well-characterized strains like *Escherichia coli* (Chu et al., 2015; Erian et al., 2018; Hwang et al., 2018; Xu et al., 2014), *Saccharomyces cerevisiae* (Kim et al., 2017; Yamada et al., 2018), *Zymomonas mobilis* (Yang et al., 2016) and *Corynebacterium glutamicum* (Rados et al., 2015; Yang et al., 2015). Furthermore, some *Bacillus* and *Paenibacillus* strains naturally produce 2,3-butanediol (Hässler et al., 2012; Jurchescu et al., 2013). High 2,3-butanediol concentrations of 145 g/L with a space-time yield of 1.14 g/L/h were achieved with the wild type *Bacillus licheniformis* DSM 8785 by additional glucose pulsing (Jurchescu et al., 2013). These performance parameters are in the range of the ones of frequently used pathogenic organisms (Ji et al., 2011). Therefore, *Bacillus licheniformis* DSM 8785 was chosen as production organism in this thesis.

B. licheniformis belongs to the family of the *Bacillaceae* and is a rod-shaped gram-positive bacterium. To endure harsh environmental conditions, *B licheniformis* is capable to produce heat-resistant endospores (Bisset and Street, 1973; Liang et al., 2018). *B. licheniformis* belongs to the *B. subtilis* group (group II) of *Bacillu*s species (Alina et al., 2015). *B. subtilis* is one of the best-studied microorganisms and probably the best-studied gram-positive bacterium (Rey et al., 2004). Therefore, it was used to reveal central characteristics of gram-positive bacteria like gene expression or physiology (Sonenshein et al., 2002). Due to their close relationship, many of the insights gained about *B. subtilis* are also true for *B. licheniformis* (Veith et al., 2004). *B. licheniformis* can utilize a large number of different carbon sources including hexoses, pentoses, glycerol, disaccharides and organic acids (Kallbach et al., 2017). Due to its high growth rate, the capacity to secrete proteins and its GRAS status (generally regarded as safe), it is used as industrial production host (Schallmey et al., 2004). Its industrial products include several enzymes like proteases, α-amylase, penicillinase, pentosanase, cycloglucosyltransferase, β-mannanase and pectinolytic enzymes (Rey et al., 2004). Additionally, other industrially interesting products like poly-γ-glutamic acid (Meissner et al., 2015), surfactants (Horowitz et al., 1990; Yakimov et al., 1995), 2,3-butanediol (Jurchescu et al., 2013) and citric acid (Sardinas, 1973) have been reported.

1.3 Objectives of this thesis

Microaerobic 2,3-butanediol production with *Bacillus licheniformis* DSM 8785 is investigated in this thesis. Thereby, two key objectives are pursued. On the one hand, the role of oxygen supply during 2,3-butanediol production with *B. licheniformis* is characterized in detail in Chapter 3. On the other hand, general methodologies are presented and assessed to provide deeper insights in microaerobic cultivations. In this context, a shake flask methodology is developed for a fast, simple, and precise determination of the impact of the maximum oxygen transfer capacity during microaerobic cultivations (Chapter 3). Additionally, advanced online monitoring approaches for microaerobic cultivations are investigated. In Chapter 4, online monitoring of the respiratory quotient is combined with stoichiometric calculations to reveal distinct metabolic phases during the cultivation. Additionally, redox potential measurements are characterized regarding the influence of dissolved oxygen tension, pH and changing medium composition in Chapter 5. This allows monitoring the dissolved oxygen tension in cultivations without pH control at low levels that cannot be measured directly. Overall, deep insights about 2,3-butanediol production with *B. licheniformis* are gained with the described methodologies. At the same time, this specific bioprocess serves as case study to investigate and validate methodologies that can be transferred to other microaerobic systems to improve the information content of online monitoring.

Chapter 2

Materials and Methods

2.1 Microorganism and medium composition

All biological experiments were performed with *Bacillus licheniformis* DSM 8785. The cells were stored at -80 °C in 150 g/L glycerol. Pre- and main-cultures were performed in a complex medium based on the medium described by Nakashimada et al. (1998). The medium contained 180 g/L glucose, 5 g/L yeast extract (Karl Roth GMBH, Karlsruhe, Germany), 5 g/L tryptone (Karl Roth GMBH, Karlsruhe, Germany), 7 g/L K_2HPO_4, 5.5 g/L KH_2PO_4, 1 g/L $(NH_4)_2SO_4$, 0.25 g/L $MgSO_4 \cdot 7H_2O$, 0.12 g/L $Na_2MoO_4 \cdot 2H_2O$, 0.021 g/L $CaCl_2 \cdot 2H_2O$, 0.029 g/L $Co(NO_3)_2 \cdot 6H_2O$, 0.039 g/L $(NH_4)_2Fe(SO_4)_2 \cdot 6H_2O$, 0.002 g/L nicotinic acid, 0.0002 g/L Na_2SeO_3, 0.00005 g/L $NiCl_2 \cdot 6H_2O$, 0.005 g/L $MnCl_2 \cdot 4H_2O$, 0.001 g/L H_3BO_3, 0.0002 g/L $AlK(SO_4)_2 \cdot 12H_2O$, 0.00001 g/L $CuCl_2 \cdot 2H_2O$, and 0.0055 g/L $Na_2EDTA \cdot 2H_2O$. In shake flask cultivations, 100 mM MES (2-(*N*-morpholino) ethanesulfonic acid) buffer was added to prevent detrimental decreases of the pH. In stirred tank reactor cultivations, pH values above 5.5 were maintained by automated addition of 2 M NaOH. In both reactor types, the initial pH was adjusted to 6.5 by addition of NaOH.

2.2 Shake flask cultivations

Cultivations were performed in unbaffled 250 mL shake flasks on an orbital shaker (Climo shaker ISF1-X, Adolf Kühner AG, Birsfelden, Switzerland), with a shaking diameter of 50 mm at 37 °C. For the pre-culture, 20 mL medium per flask were inoculated with 20 µL from the glycerol stock, cultivated at 350 rpm and harvested in the exponential growth phase that was determined via online monitoring of the oxygen transfer rate (OTR). For the main culture, a master mix was inoculated from the pre culture to an initial optical density (OD_{600}) of 0.1. The master mix was then distributed to the individual shake flasks. At the beginning of the cultivation, a shaking frequency of 350 rpm was adjusted, which was reduced to 100 rpm when an OTR of 20 mmol/L/h was reached. As visualized in Figure 2-1, online monitoring of the respiratory activity was combined with offline sampling.

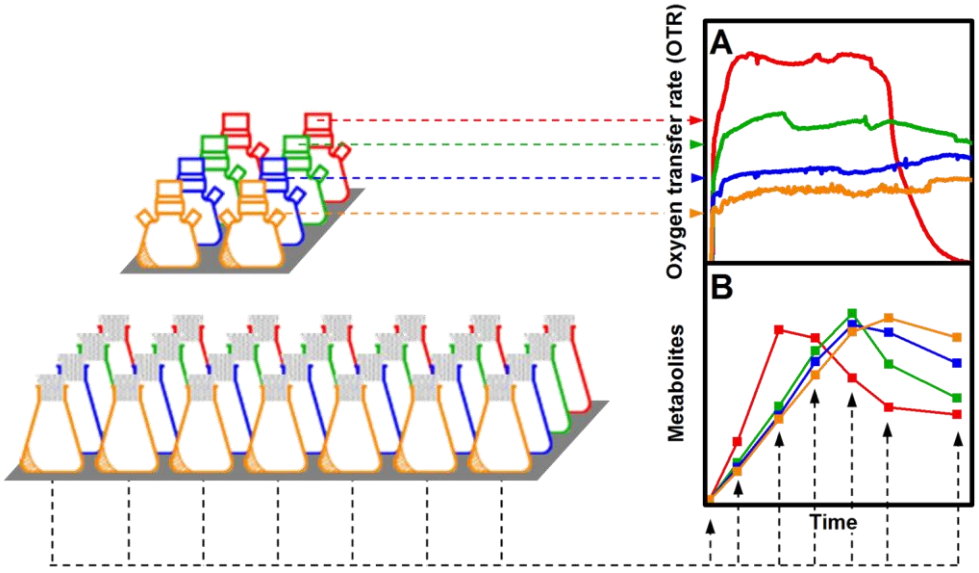

Figure 2-1: Schematic illustration of the experimental setup. Cultivations are performed in multiple individual shake flasks in parallel. As indicated by different colors, four different experimental conditions are investigated in one experiment. Online measurement (A) of oxygen transfer rate (OTR), carbon dioxide transfer rate (CTR) and the respiratory quotient (RQ) is performed as duplicates in a Respiration Activity Monitoring System (RAMOS). Offline samples (B) are taken from individual shake flasks, which are not returned to the shaker after sampling.

All shake flasks were cultivated in parallel under identical conditions. Online monitoring of OTR, carbon dioxide transfer rate (CTR), and respiratory quotient (RQ) (Figure 2-1A) was performed with an in-house fabricated Respiration Activity Monitoring System (RAMOS)

(Anderlei et al., 2004). Commercial versions of the RAMOS device are available from HiTec Zang GMBH (Herzogenrath, Germany) or Adolf Kühner AG (Birsfelden, Switzerland). For offline sampling, conventional 250 mL shake flasks were used (Figure 2-1B). At each sampling point, one flask for each cultivation condition was removed from the shaker, subjected to offline analysis and not returned to the shaker again. Consequently, cultivation data for each experimental condition are derived from multiple individual shake flasks. Therefore, reproducibility of the cultivations is given when a steady course of all offline samples is observed.

2.3 Stirred tank reactor cultivations

A 2 L Autoclavable Bioreactor (Applikon Biotechnology, Foster City, USA) was equipped with three baffles and two Rushton Turbines (6 blades, 45 mm stirrer diameter) and operated with a filling volume of 1.5 L. The reactor was aerated with 0.5 L/min (0.33 vvm) pressurized air via an L-type gas sparger. Dissolved oxygen tension (DOT) (AppliSens pO2 sensor; Applikon Biotechnology, Foster City, USA), pH (AppliSens pH Sensor; Applikon Biotechnology, Foster City, USA) and redox potential (Redox Probe Pt 4805-DPAS-SC-S8/225; Mettler-Toledo, Gießen, Germany) were monitored online during the cultivation. DOT and pH signals were recorded via the control unit of the bioreactor. The redox potential was recorded via an in-house developed LabVIEW program (National Instruments Germany GmbH, München, Germany). The temperature was adjusted to 37 °C using a Pt-100 sensor (Applikon Biotechnology, Foster City, USA) and the integrated cooling jacket. An X-STREAM exhaust gas analyzer (Emerson Process Management GmbH, Wessling, Germany) was used to obtain OTR, CTR and RQ. Plurafac LF 1300 anti-foaming agent (BASF, Ludwigshafen, Germany) was added before inoculation (2 mL) and when foaming was observed during the cultivation (1 mL). 20 mL of an overnight pre-culture (cultivation conditions as described for the shake flask experiments) were used for inoculation. Unless specified otherwise, a high agitation rate was applied at the beginning of the main cultivation to enable oxygen unlimited growth conditions. At a defined OTR of 20 mmol/L/h the agitation rate was reduced to initiate oxygen limitation. The agitation rates of the individual experiments are specified in the respective figure captions.

2.4 Offline analytics

Upon sampling, the remaining liquid volume in the individual shake flasks was determined, resulting in an evaporation rate of 0.04 mL/h. At the point of maximum 2,3-butanediol concentration, between 7 and 20% of the initial filling volume have evaporated (for cultivations with 60 and 10 mL filling volume, respectively). To account for the increase of metabolite concentrations due to this evaporation of water, all concentrations were corrected accordingly and referred to the initial filling volume. In stirred tank reactor cultivations, evaporation was minimized using an exhaust gas cooler and not considered for offline analysis. Cells were separated via centrifugation (5 min at 17,968 g). The cell dry weight was determined gravimetrically in pre-dried and -weighted 2 mL reaction tubes after two washing steps with deionized water. The obtained pellet was dried for at least 48 h at 60 °C. The supernatant of the first centrifugation step was used for further analysis. Metabolite concentrations of the filtered supernatant were determined via high-performance liquid chromatography (HPLC) after 20-fold dilution with deionized water. Metabolites were quantified with a Dionex UltiMate 3000 HPLC system (Dionex, Sunnyvale, USA) at 70 °C using an organic acid-resin (250 · 8 mm, CS-Chromatographie, Langerwehe, Germany) and a Shodex RI-101 detector (Showa Denko, Munich, Germany). As mobile phase 2.5 mM sulfuric acid was chosen with a flow rate of 0.5 mL/min. Unless specified otherwise, 2,3-butanediol concentrations in this work always refer to the sum of all stereoisomers. With the applied method, *meso*-2,3-butanediol was separated from the D- and L-isomer, whereas distinction between the latter was not possible. As only production of meso- and D-2,3-butanediol is described in the literature for *B. licheniformis* (Li et al., 2013; Nilegaonkar et al., 1992), the second peak was considered to be D-2,3-butanediol. The pH was measured with a CyberScan pH 510 (Eutech Instruments, Landsmeer, the Netherlands) pH meter.

2.5 Calculation of metabolite concentrations upon glucose depletion

A combination of offline sampling and online monitoring of the respiratory activity was used to calculate the concentrations of 2,3-butanediol, acetoin and glycerol upon glucose depletion in Chapter 3. The time point of glucose depletion was determined based on the sudden drop of the RQ as mean of duplicate cultivations (t2 in Appendix 1). A decrease of more than 20% between two consecutive measurement points was chosen as cut-off value. The corresponding concentration was calculated from a linear correlation derived from offline samples that were taken during the oxygen-limited phase and before the point of glucose depletion. Only samples with concentrations >0 g/L of the respective metabolite were considered.

2.6 RQ calculations and stoichiometry

The theoretical RQ during different phases of the cultivation was calculated based on partial reaction stoichiometries in Chapter 4. In the metabolic network, these reactions are coupled and do not occur separately. In the course of the cultivation, changing combinations of all partial reactions result in the overall metabolic activity. Stoichiometric coefficients of carbon dioxide formation (ν_{CO_2}) and oxygen consumption (ν_{O_2}) were obtained from partial reaction stoichiometries. The theoretical RQ was calculated according to Equation 2-1:

$$RQ = \frac{\nu_{CO_2}}{\nu_{O_2}} \tag{2-1}$$

To setup the stoichiometry of growth on glucose (Equation 2-2), a biomass composition for *B. licheniformis* of $C_1H_{1.6}O_{0.4}N_{0.2}$ was assumed based on biomass compositions of *B. subtilis* that were determined by Dauner et al. (2001) in N- and P-limited chemostat experiments.

$$C_6H_{12}O_6 + 0.75\ O_2 + NH_3 \rightarrow 5\ C_1H_{1.6}O_{0.4}N_{0.2} + \ CO_2 + 3.5\ H_2O \tag{2-2}$$

Complete combustion of glucose via the respiratory chain follows the stoichiometry of Equation 2-3:

$$C_6H_{12}O_6 + 6\ O_2 \rightarrow 6\ CO_2 + 6\ H_2O \quad (2\text{-}3)$$

Equation 2-4 shows the stoichiometry of 2,3-butanediol production from glucose:

$$C_6H_{12}O_6 + 0.5\ O_2 \rightarrow C_4H_{10}O_2 + 2\ CO_2 + H_2O \quad (2\text{-}4)$$

Glycerol formation from glucose is accompanied by the conversion of NADH to NAD^+. Consequently, less NADH is oxidized via the respiratory chain and the RQ increases. Equation 2-5 expresses this as partial reaction stoichiometry:

$$C_6H_{12}O_6 + 2\ H_2O \rightarrow 2\ C_3H_8O_3 + O_2 \quad (2\text{-}5)$$

The conversion of 2,3-butanediol to acetoin after glucose depletion is shown in Equation 2-6:

$$C_4H_{10}O_2 + 0.5\ O_2 \rightarrow C_4H_8O_2 + H_2O \quad (2\text{-}6)$$

Under anaerobic conditions, ethanol is formed from glucose according to Equation 2-7:

$$C_6H_{12}O_6 \rightarrow 2\ C_2H_6O + 2\ CO_2 \quad (2\text{-}7)$$

Lactate combustion follows the stoichiometry shown in Equation 2-8:

$$C_3H_6O_3 + 3\ O_2 \rightarrow 3\ CO_2 + 3\ H_2O \quad (2\text{-}8)$$

Based on Equation 2-1 to 2-8, theoretical RQs were calculated for specific phases during the cultivation based on partial reaction stoichiometries. Additionally, average RQs for cultivations with different OTR_{max} were calculated. Based on the respective carbon mass balances the produced carbon dioxide was calculated considering all metabolites shown in Equation 2-9.

Thereby, only glucose (180 g/L) was considered as carbon source, while the carbon released from undefined components like yeast extract and tryptone (5 g/L each) was neglected.

$$\nu_{Glu}Glucose + \nu_{O_2}O_2 + \nu_{NH_3}NH_3 \rightarrow \nu_{But}2,3\text{-}Butanediol + \nu_{Aceto}Acetoin + \nu_{Gly}Glycerol + \nu_{Eth}Ethanol + \nu_{Aceta}Acetate + \nu_{Lac}Lactate + \nu_{Suc}Succinate + \nu_{CDW}Cell\ dry\ weight + \nu_{CO_2}CO_2 + \nu_{H_2O}H_2O \quad (2\text{-}9)$$

This calculation was performed for the 2,3-butanediol production phase between the initiation of oxygen-limited conditions and glucose depletion as depicted in Appendix 1B. Oxygen-limited conditions are induced by reduction of the shaking frequency. Glucose depletion can be detected online, as it results in a steep decrease of the RQ. The stoichiometric coefficients ν_i were determined from offline samples. The product concentrations upon glucose depletion were determined via linear interpolation as described and validated in Section 2.5 and 3.3 (Heyman et al., 2019). To minimize the experimental error, also the glucose concentration at the initiation of the oxygen limitation was calculated from the glucose consumption rate. To do so, the glucose consumption rate was determined via linear regression from all samples taken during the 2,3-butanediol production phase. Based on the obtained linear equation, the glucose concentration at the initiation of the 2,3-butanediol production phase was calculated. The consumed oxygen during the 2,3-butanediol production phase was calculated by integrating the measured OTR.

2.7 Abiotic investigations of the redox potential

Unless specified otherwise, abiotic investigations of the redox potential in Chapter 5 were performed in the cultivation medium described in Section 2.1 at 37 °C in a BIOSTAT® B plus benchtop fermenter (Satorius, Göttingen, Germany). Similar to the cultivation experiments, 2 mL Plurafac LF 1300 anti-foaming agent (BASF, Ludwigshafen, Germany) were added. To avoid contamination, kanamycin (33 mg/L) and ampicillin (67 mg/L) were added to the medium. The pH was adjusted by titration of NaOH and H_2SO_4. Pressurized air and nitrogen were mixed with the control unit of the bioreactor to adjust the DOT. DOT (Visiferm DO 120;

Hamilton, Reno, USA) and pH (Easyferm Plus K8 200; Hamilton, Reno, USA) were recorded with the digital control unit of the bioreactor. The redox potential was monitored as specified in Section 2.3.

2.8 Calculation of the DOT from the redox potential

The calculation of the DOT from the redox potential is based on a preceding correction of the measured redox potential at each individual time point t_n ($E_{h_{cor,t_n}}$) according to Equation 2-10. Thereby, the influence of the pH on the redox potential was eliminated.

$$E_{h_{cor,t_n}} = E_{h_{measured,t_n}} - \left(pH_{t_n} - pH_{t_0}\right) \cdot \Delta E_{pH,t_n} \tag{2-10}$$

The indices indicate if the corresponding parameter was corrected (*cor*), measured (*measured*), calculated (*calc*) or calibrated (*calib*) and if it refers to the beginning of the cultivation (t_0) or any time point during the cultivation (t_n). The pH dependency of the redox potential for each time point ($\Delta E_{pH_{t_n}}$) was determined depending on the respective measured DOT ($DOT_{measured,t_n}$) based on the results shown in Figure 5-5 according to Equation 2-11.

$$\Delta E_{pH,t_n} = 0.613 \cdot DOT_{measured,t_n} - 87.06 \tag{2-11}$$

The calculated DOT was derived from the logarithmic DOT ($log_{10}(DOT_{calc,t_n})$) calculated for each time point during the cultivation according to Equation 2-12.

$$log_{10}(DOT_{calc,t_n}) = (\Delta \log_{10}(DOT)/\Delta E_h)_{calib} \cdot (E_{h_{cor,t_n}} - E_{h_{cor,t_0}}) + log_{10}(DOT_{calib,t_0}) \tag{2-12}$$

$(\Delta log_{10}(DOT)/\Delta E_h)_{calib}$ is the slope of the correlation between the data shown in Figure 5-7 with the logarithmic DOT on the ordinate and the redox potential on the abscissa (reverted ordinate and abscissa compared to Figure 5-7). $log_{10}(DOT_{calib,t_0})$ is the respective ordinate section. The

calculation of the DOT is based on the change of the corrected redox potential relative to the initial value at the beginning of the cultivation. Thereby, the calculation is also valid for changing initial redox potentials.

Chapter 3

Impact of the oxygen availability on 2,3-butanediol production with *Bacillus licheniformis*

3.1 Introduction

Independent of the selected microorganism, the oxygen availability during the cultivation is generally accepted to be one of the most influential parameters for 2,3-butanediol production, which occurs under oxygen-limited or microaerobic conditions. The 2,3-butanediol yield increases at lower oxygen availability, while cell growth is favored at high oxygen availability, resulting in faster product formation rates (Jansen et al., 1984; Rodriguez et al., 2017). Furthermore, also the production of by-products strongly depends on the availability of oxygen. Accumulation of acetoin is observed at high oxygen availability, whereas glycerol and ethanol are formed at low oxygen availability (Converti et al., 2003; Rebecchi et al., 2018).

Several different process strategies have been developed to improve 2,3-butanediol production depending on the oxygen availability. Zeng et al. (1994) used the respiratory quotient (RQ) as control parameter and Beronio and Tsao (1993) maintained constant biomass specific oxygen uptake rates. The contrarious effects of oxygen availability on growth and product formation have been addressed in various studies by the application of two-stage cultivation strategies to accelerate 2,3-butanediol production (Cho et al., 2015b; Dai et al., 2014; Fages et al., 1986; Ji et al., 2009; Li et al., 2013; Park et al., 2013; Priya et al., 2016; Qiu et al., 2016; Zhang et al., 2010). Hereby, an initial phase of high oxygen availability leads to increased cell growth and

afterwards 2,3-butanediol production is favored at lower oxygen availability. However, most studies defined the oxygen availability solely based on variations of reactor specific parameters like the agitation or aeration rate. Thus, the resulting oxygen availability and the observed effects are highly dependent on the utilized reactor geometry and operation. To establish general cultivation strategies, detailed characterization and quantification of the influence of oxygen availability on 2,3-butanediol production is required. Thereby, scalable parameters like the k_La value or the maximum oxygen transfer capacity (OTR_{max}) should be used to quantify the oxygen availability independently of the utilized reactor type, geometry and operation. Only a limited number of studies investigated the effect of oxygen availability based on these parameters (de Mas et al., 1988; Jansen et al., 1984; Ji et al., 2009; Ramachandran and Goma, 1987; Ramachandran et al., 1990; Rebecchi et al., 2018). The studies based on the k_La value led to contradictory results, as the highest 2,3-butanediol concentration with *Klebsiella oxytoca* was obtained at 18 h^{-1} by Ji et al. (2009) and at 78 h^{-1} by Ramachandran et al. (1990). This contradiction can be attributed either to different optimum oxygen availabilities amongst individual *K. oxytoca* strains, or to the different utilized dynamic methods for k_La determination (Na_2SO_3 method and gassing out method, respectively). The OTR_{max} leading to the highest 2,3-butanediol concentration differs between different organisms. The highest concentrations were reached at about 15 mmol/L/h for *P. polymyxa* and *K. pneumonia* (de Mas et al., 1988; Ramachandran and Goma, 1987) and at 10 mmol/L/h for *B. licheniformis* and *K. oxytoca* (Jansen et al., 1984; Rebecchi et al., 2018). This demonstrates the need for a fast, inexpensive and reliable methodology to identify the influence of the oxygen availability on 2,3-butanediol production. A necessary prerequisite is the reliable quantification of the maximum 2,3-butanediol concentration. However, 2,3-butanediol is consumed by the organism upon substrate depletion (Ji et al., 2011). Consequently, the maximum 2,3-butanediol concentration has to be determined exactly at this point. Otherwise, the difference between the sampling time and the time of substrate depletion hampers the interpretation of the experimental results. Furthermore, the previously mentioned studies on the effect of oxygen availability on 2,3-butanediol production were performed in stirred tank reactor cultivations, which generally require high cultivation volumes, technical effort and long setup times.

The aim of this chapter is the development of a shake flask methodology to increase the experimental throughput and to reduce the experimental effort and costs. Moreover, the gained

results are scalable and transferable to other reactor systems. First, a defined two-stage protocol for the cultivation of *Bacillus licheniformis* DSM 8785 was developed. At the beginning of the cultivation, a high shaking frequency results in oxygen-unlimited conditions and consequently unrestricted biomass formation. At a defined oxygen transfer rate (OTR) different levels of oxygen limitation are initiated in shake flasks with different filling volumes. Afterwards, a procedure to determine the maximum 2,3-butanediol concentration at the time of substrate depletion has been developed. On this basis, the influence of the OTR_{max} on the cultivation was investigated. Thereby, a fast and reliable methodology to select the ideal cultivation conditions based on the overall demand of any individual process is presented. The results presented in this chapter have been published previously (Heyman et al., 2019). Parts of the results were obtained in collaboration with Hannah Tulke (research internship and master's thesis) and Patrick Lichtner (research internship).

3.2 Selection of suitable cultivation conditions

High 2,3-butanediol production with *B. licheniformis* has been demonstrated in cultivations in baffled shake flasks by Jurchescu et al. (2013). As 2,3-butanediol is produced under oxygen-limited conditions, only low OTR_{max} are required that can easily be achieved with unbaffled shake flasks. Furthermore, utilization of unbaffled shake flasks results in more defined flow regimes and reduces the experimental error (Büchs, 2001; McDaniel et al., 1965). Therefore, cultivation of *B. licheniformis* was performed in unbaffled 250 mL shake flasks in this thesis. As visualized in Figure 2-1, parallel cultivations were performed in multiple shake flasks to combine online monitoring of oxygen and carbon dioxide transfer rates (OTR, CTR) and the RQ with offline sampling.

To investigate the effect of oxygen availability during the cultivation, different OTR_{max} can be adjusted by variation of the filling volume in shake flasks. In Figure 3-1 cultivations with filling volumes between 10 and 60 mL are shown, which were performed in the same medium used by Jurchescu et al. (2013). For all filling volumes a steep increase of the OTR after the lag phase is followed by a plateau (Figure 3-1A) indicating oxygen limitation (Anderlei et al., 2004). The

level of the plateau, which corresponds to the respective OTR_{max} (clearly visualized in Appendix 1), increases from 2.5 to 13 mmol/L/h with decreasing filling volume. The transition from unlimited growth to oxygen-limited conditions occurs as soon as the OTR_{max} is reached. Therefore, cultivations with low OTR_{max} (high filling volumes) have a shorter unlimited growth phase compared to cultivations with a high OTR_{max} (low filling volumes) as shown in the magnified inlet of Figure 3-1A.

Further information about the metabolic activity of the cultures can be derived from the RQ (Figure 3-1B). The RQ of the cultivation with 10 mL filling volume slowly increases to values around 2 and then drops together with the OTR after 30 h. For higher filling volumes, higher RQ levels can be observed. During the steep increase of the OTR, RQ values around 1 indicate aerobic cell growth. When oxygen-limited conditions are reached, the RQs increase and stay nearly constant at values between 4 and 6 for 50, 90 and 115 h (20, 40 and 60 mL, respectively). Hereby, lower OTR_{max} (higher filling volumes) result in higher RQs. The course of the RQ can be explained by 2,3-butanediol production (Figure 3-1C), which leads to high RQs, as 2,3-butanediol is more reduced than the substrate glucose. Subsequent consumption of 2,3-butanediol results in RQ values below 1. The course of the pH during the cultivations is shown in Figure 3-1D. At the beginning of the cultivation, the pH decreases due to the formation of organic acids and the consumption of ammonia (Ji et al., 2011; Meissner et al., 2015). In the further course of the cultivation, the organism switches from organic acid to 2,3-butanediol formation to prevent further acidification (Ji et al., 2011) and the pH increases due to organic acid consumption. After 21 h, the lowest pH is observed for the cultivation with 10 mL filling volume. At this condition, the pH further decreases to values below 5 and does not increase as observed for the other cultivations. This stronger acidification explains the deviation to the other cultivations, as it causes the metabolic activity to stop after 30 h (Figure 3-1A and B) resulting in much lower overall 2,3-butanediol production (Figure 3-1C).

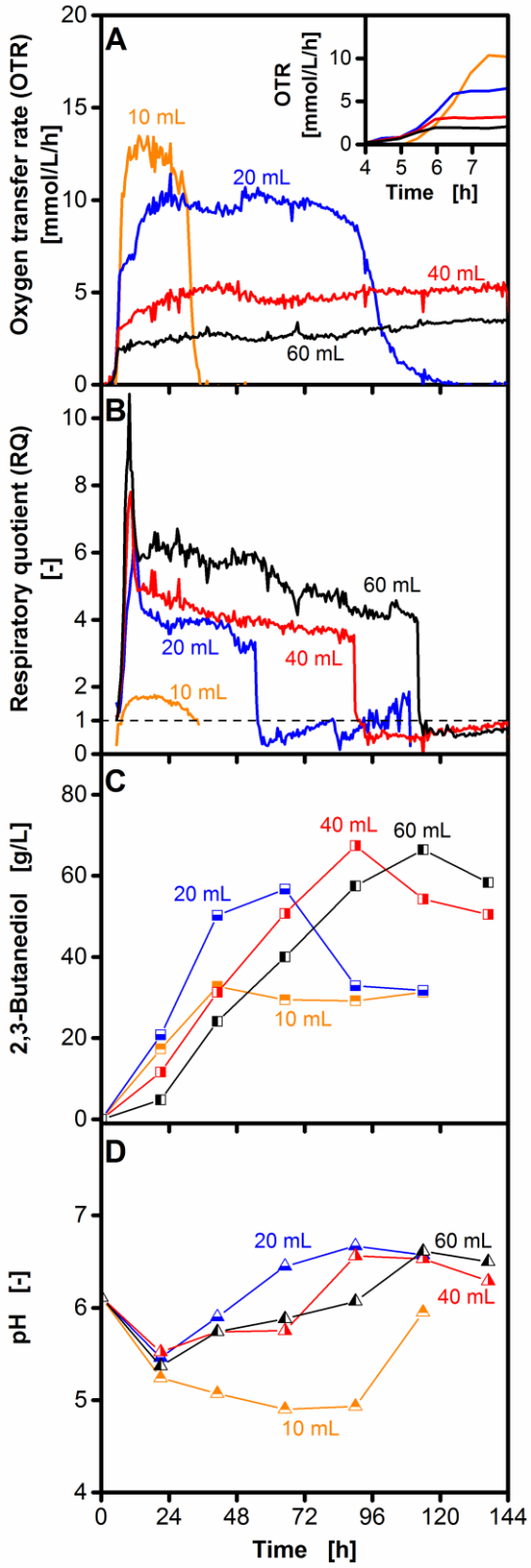

Figure 3-1: Cultivation of *Bacillus licheniformis* DSM 8785 under oxygen-limited conditions. Variation of the filling volume results in different maximum oxygen transfer capacities (OTR_{max}) in shake flask cultivations. Data on oxygen transfer rate (OTR) (A), respiratory quotient (RQ) (B), total 2,3-

butanediol concentration (C) and pH (D) are depicted. 2,3-Butanediol is shown as sum of the stereoisomers. The RQ is only shown for OTR > 1 mmol/L/h. To account for the increase of metabolite concentrations due to evaporation of water, all concentrations were corrected accordingly and referred to the initial filling volume. Cultivation conditions: 250 mL unbaffled shake flasks, temperature: 37 °C, shaking frequency: 100 rpm, shaking diameter: 50 mm, Nakashimada medium without addition of MES buffer.

The results presented in Figure 3-1 reveal three obstacles for a precise assessment of the effects of varied OTR_{max} on 2,3-butanediol production. First, high OTR_{max} cannot be investigated, as the medium is not sufficiently buffered to prevent acidification. Second, the length of the unlimited growth phase at the beginning of the cultivation depends on the target OTR_{max}. Therefore, changes of the OTR_{max} do not solely affect the oxygen availability during the oxygen-limited phase, but also lead to inconsistent growth conditions. Third, 2,3-butanediol is consumed after the maximum concentration is reached. Therefore, a methodology to determine the maximum 2,3-butanediol concentration is required to properly compare different cultivation conditions.

In the used cultivation medium, acidification cannot be prevented as the buffer capacity of the utilized phosphate buffer (with pK_a values of 2, 7.4 and 12.3) is below 10% at the observed pH values during the cultivation. To reduce acidification, an increased initial pH and addition of different MES buffer (pKa = 6.1) concentrations was tested (Appendix 2). The increased initial pH did not prevent acidification and addition of 200 mM MES buffer slightly prolonged the cultivation. Therefore, 100 mM MES buffer was added to reduce the acidification during the cultivation in the following experiments (Figure 3-2). However, tight pH control should be avoided as with decreasing pH the metabolism shifts from organic acid to 2,3-butanediol production (Ji et al., 2011). Furthermore, a defined two-stage cultivation profile was applied in the experiment shown in Figure 3-2.

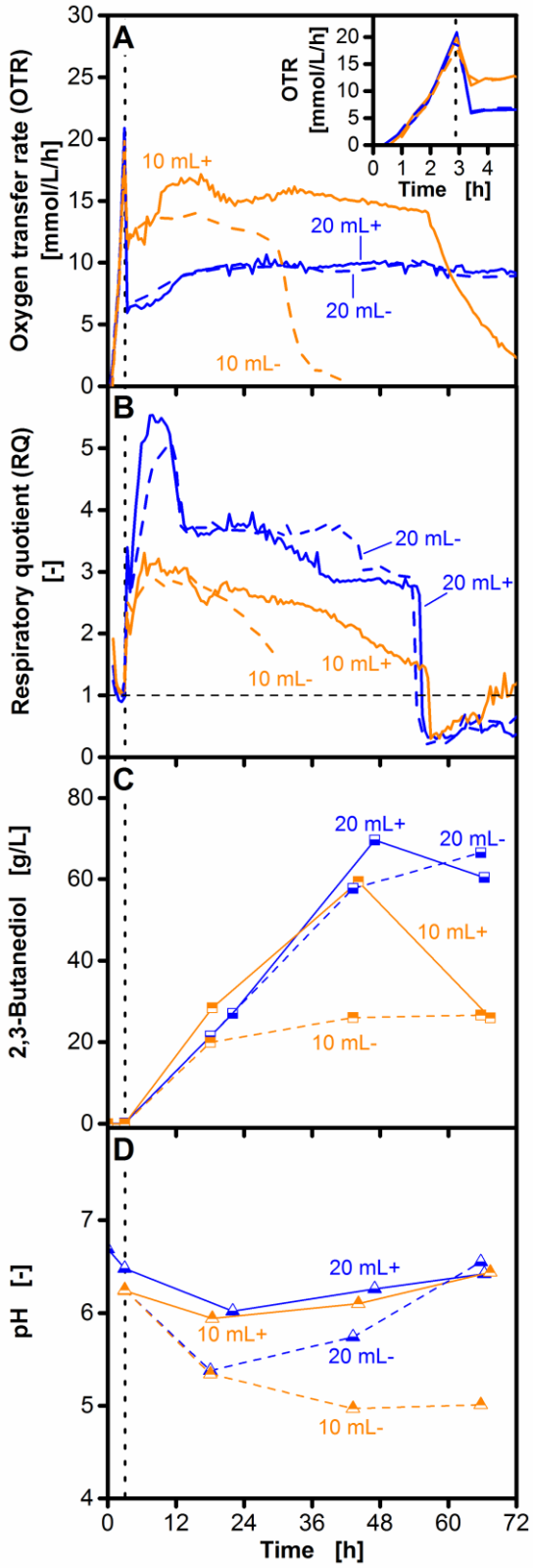

Figure 3-2: Effects of buffering on 2,3-butanediol production with *Bacillus licheniformis* DSM 8785. Cultivations in Nakashimada medium with (+) and without (-) addition of 100 mM MES buffer are compared. Variation of the filling volume results in different maximum oxygen transfer capacities (OTR_{max}) in shake flask cultivations. As indicated by the vertical dotted line, the shaking frequency

was reduced from 350 to 100 rpm after 3 h. Thereby, oxygen-limited conditions are induced at the same time for all cultivations. Data on oxygen transfer rate (OTR) (A), respiratory quotient (RQ) (B), total 2,3-butanediol concentration (C) and pH (D) are depicted. 2,3-Butanediol is shown as sum of the stereoisomers. The RQ is only shown for OTR > 1 mmol/L/h. To account for the increase of metabolite concentrations due to evaporation of water, all concentrations were corrected accordingly and referred to the initial filling volume. Cultivation conditions: 250 mL unbaffled shake flasks, temperature: 37 °C, shaking frequency: 350/100 rpm, shaking diameter: 50 mm.

At the beginning of the cultivation, a shaking frequency of 350 rpm results in oxygen-unlimited conditions for all cultivations (Figure 3-2A). This results in a steeply increasing OTR for all filling volumes. When cultivations reached an oxygen transfer rate of 20 mmol/L/h, the shaking frequency was reduced to 100 rpm to induce oxygen limitation. By this two-stage cultivation profile, defined and comparable cultivation conditions are obtained. The OTR_{max} is the only variation during the second cultivation stage. As soon as the cultures are oxygen-limited, the RQ increases and 2,3-butanediol production is initiated (Figure 3-2B and C). Application of the two stage cultivation profile without MES buffer addition results in the same behavior in terms of OTR, RQ, 2,3-butanediol concentration and pH, compared to the respective cultivations with a constant shaking frequency (cf. Figure 3-1). Consequently, defined cultivation conditions are obtained without changing the general cultivation characteristics.

As depicted in Figure 3-2D, addition of MES buffer prevented acidification of the cultures below pH values of 6 for both filling volumes. Thereby, the early decrease of OTR and RQ for the cultivation with 10 mL filling volume, which was observed without MES buffer addition (Figure 3-1), could be prevented. For the cultivations with 20 mL filling volume, similar courses of OTR, RQ and 2,3-butanediol formation are observed irrespective of MES buffer addition. By the addition of 100 mM MES buffer and application of a two-stage cultivation strategy, defined cultivation conditions were established without changing the general cultivation characteristics. Thereby, the effect of a broad range of different OTR_{max} can be investigated. Consequently, these conditions were applied for all following cultivations.

3.3 Determination of the maximum 2,3-butanediol concentration

To determine the maximum 2,3-butanediol concentration, offline sampling was focused on the time of the dropping RQ (Figure 3-3). At this point glucose is depleted and the maximum 2,3-butanediol concentration is reached (Figure 3-3B). During oxygen limitation, constant glucose consumption and 2,3-butanediol production rates were observed until glucose depletion. For glycerol production a similar trend is visible as for 2,3-butanediol. It is produced at a constant rate, reaches its maximum concentration upon glucose depletion and is consumed afterwards (Figure 3-3C). However, in contrast to 2,3-butanediol, glycerol production does not start as soon as oxygen limitation starts, but is delayed by a few hours. The acetoin concentration slowly increases as long as glucose is present, followed by rapid acetoin accumulation upon glucose depletion.

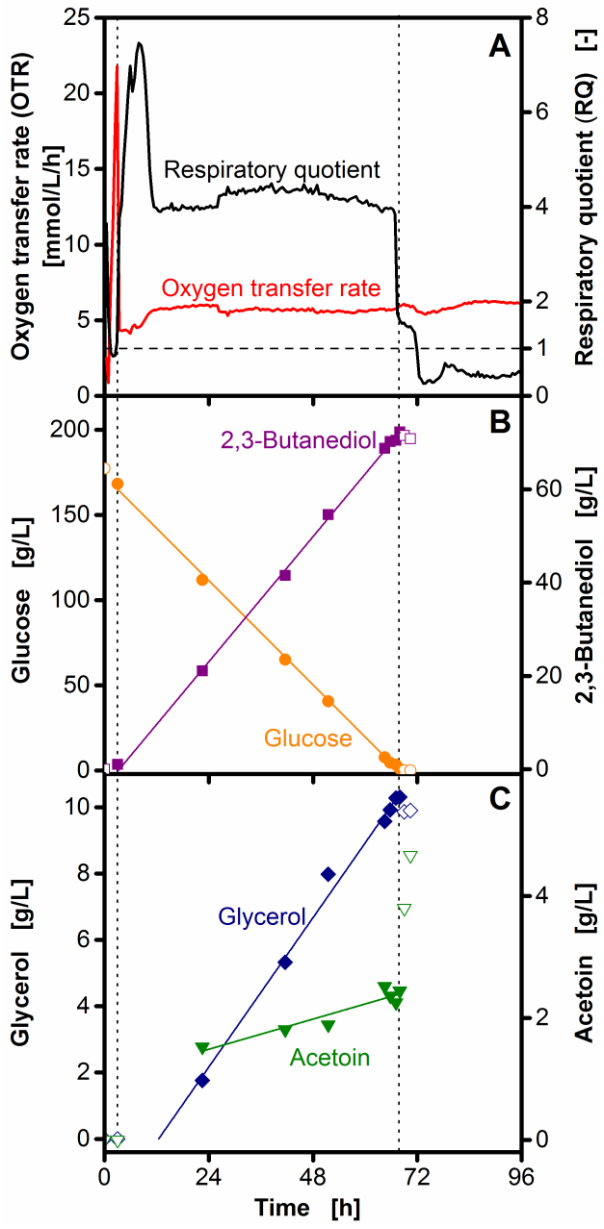

Figure 3-3: Glucose consumption and product formation during the cultivation of *Bacillus licheniformis* DSM 8785. As indicated by the left vertical dotted line, the shaking frequency was reduced from 350 to 100 rpm after 3 h. Data on oxygen transfer rate (OTR) and respiratory quotient (RQ) (A), glucose and total 2,3-butanediol concentration (B) and glycerol and acetoin concentration (C) are depicted. The solid lines represent linear correlations during the 2,3-butanediol production phase (between the dotted vertical lines) with $R^2 \geq 0.99$ for glucose, 2,3-butanediol and glycerol and $R^2 = 0.89$ for acetoin. Filling of symbols represents data points that were (closed symbols) or were not (open symbols) considered for linear correlation. 2,3-Butanediol is shown as sum of the stereoisomers. The RQ is only shown for OTR > 1 mmol/L/h. To account for the increase of metabolite concentrations due to evaporation of water, all concentrations were corrected accordingly and referred to the initial filling volume. Cultivation conditions: 250 mL unbaffled shake flasks, temperature: 37 °C, shaking frequency: 350/100 rpm, shaking diameter: 50 mm, filling volume: 30 mL, Nakashimada medium with 100 mM MES buffer.

Stoichiometric calculations show that high RQs result from consumption of glucose and formation of reduced products (mainly 2,3-butanediol, glycerol; cf. Equations 2-4 and 2-5 in Section 2.6), whereas low RQs result from the oxidation of 2,3-butanediol to acetoin and the consumption of glycerol (cf. Equations 2-5 and 2-6). Therefore, online monitoring of the RQ enables the identification of this metabolic switching point, which is not visible in OTR or dissolved oxygen measurements. Identification of this switching point is crucial to assess the impact of different cultivation conditions as samples have to be taken exactly at this point to correctly determine the maximum 2,3-butanediol concentration. Therefore, without determination of this time point, very close sampling intervals throughout the cultivation would be required. With the aid of online RQ monitoring, fewer samples have to be taken. Still, the requirement to take samples at a distinct time point, which also changes with changing cultivation conditions, makes the experiments very complicated. Therefore, a methodology to determine the maximum 2,3-butanediol concentration was developed combining offline sampling and online monitoring of the RQ. The maximum 2,3-butanediol concentration is calculated from the 2,3-butanediol production rate and the time point of glucose depletion, which is determined from the dropping RQ. The 2,3-butanediol production rate is derived from offline samples taken at arbitrary time points during the 2,3-butanediol production phase. With this methodology, the maximum 2,3-butanediol concentration can be calculated for every experiment without the need of sampling at defined time points. Besides 2,3-butanediol, also the concentrations of glucose, glycerol and acetoin can be calculated with this methodology. To verify the basis for this methodology, constant production rates throughout the oxygen-limited phase were confirmed for different OTR_{max} and initial glucose concentrations (Appendix 3). Thereby, the average deviation between the measured and the calculated 2,3-butanediol concentration of the respective experiment was 3.6%.

3.4 Influence of the maximum oxygen transfer capacity on the cultivation

Based on the described methodology, the influence of different OTR_{max} on the cultivation of *B. licheniformis* DSM 8785 was investigated (Figure 3-4). The courses of OTR and RQ resemble the previous experiments. The application of the two-stage cultivation strategy results in a short

standardized oxygen-unlimited growth phase followed by an oxygen-limited phase with decreasing OTR_{max} for increased filling volumes (Figure 3-4A). A high OTR_{max} leads to higher glucose consumption rates and consequently earlier glucose depletion. This is also reflected in the course of the RQ (Figure 3-4B and C). Measured metabolite concentrations are represented by half-closed symbols and connected with solid lines, whereas the calculated concentrations upon glucose depletion are shown as closed symbols with dotted connection lines (also clearly illustrated in Appendix 4). Increased OTR_{max} result in higher biomass formation with cell dry weights of up to 10 g/L (Figure 3-4D). Fast biomass formation during the first 24 h of cultivation is followed by a phase of slowly increasing biomass. Around the time of glucose depletion, the cell dry weight decreases. From the cell dry weight measurements and the online monitored OTR_{max}, specific oxygen uptake rates can be calculated (Figure 3-4E). With increased OTR_{max}, also the specific oxygen uptake rate increases. However, in contrast to the OTR_{max}, the specific oxygen uptake rates are not constant, but decrease in the course of the cultivation. As observed before, the 2,3-butanediol production rate correlates with the OTR_{max}. However, lower maximum 2,3-butanediol concentrations occur at high OTR_{max} (Figure 3-4F). This finding could only be revealed by calculating the maximum concentration according to the previously described methodology (Section 3.3). As *B. licheniformis* produces two different stereoisomers, D- and meso-2,3-butanediol (Li et al., 2013; Nilegaonkar et al., 1992), Figure 3-4G and H visualize the impact of the OTR_{max} on the 2,3-butanediol composition. As long as glucose is present, both stereoisomers are produced at constant rates, whereby roughly 1.3 times more meso-2,3-butanediol is formed. Upon glucose depletion, only D-2,3-butanediol is oxidized to acetoin, whereas the concentration of meso-2,3-butanediol remains constant. *B. licheniformis* expresses two different 2,3-butanediol dehydrogenases that convert acetoin to 2,3-butanediol resulting in the formation of the two observed stereoisomers (Ge et al., 2016). Consequently, the observed conversion of D-2,3-butanediol indicates that only one of the 2,3-butanediol dehydrogenases catalyzes a reversible reaction.

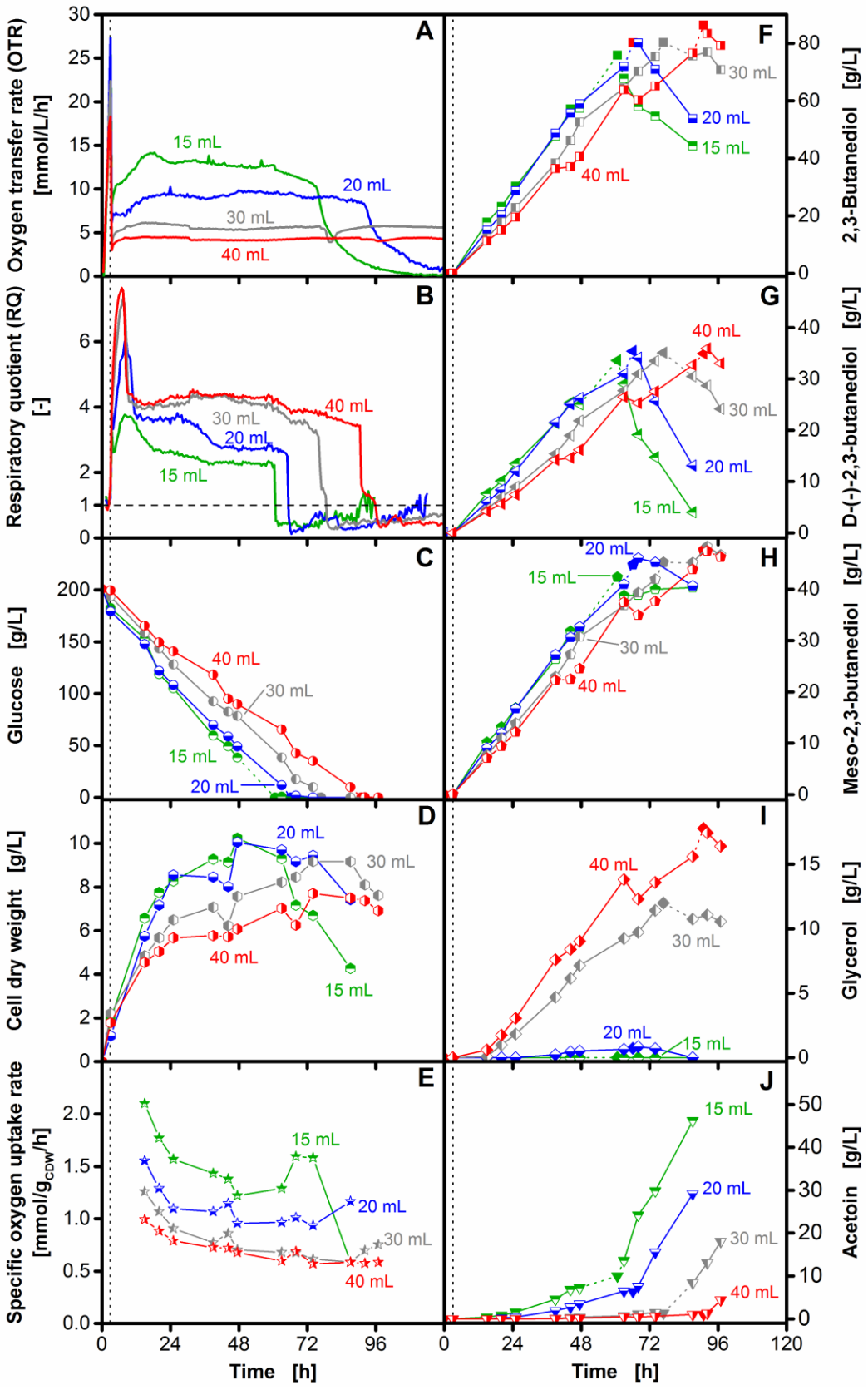

Figure 3-4: Influence of different maximum oxygen transfer capacities on 2,3-butanediol production with *Bacillus licheniformis* DSM 8785. Variation of the filling volume results in different maximum

oxygen transfer capacities (OTR_{max}) in shake flask cultivations. As indicated by the vertical dotted line, the shaking frequency was reduced from 350 to 100 rpm after 3 h. Thereby, oxygen-limited conditions are induced at the same time for all cultivations. Data on oxygen transfer rate (OTR) (A), respiratory quotient (RQ) (B), glucose (C), cell dry weight (D), specific oxygen uptake rate (E), total 2,3-butanediol (F), 2,3-butanediol stereo isomer (G and H), glycerol (I) and acetoin (J) concentrations are depicted. In addition to offline samples (half-closed symbols), the concentrations upon glucose depletion were calculated as described in Figure 3-3 (closed symbols). For clarity, the connection between the measured and calculated values is shown as dotted line. The RQ is only shown for OTR > 1 mmol/L/h. To account for the increase of metabolite concentrations due to evaporation of water, all concentrations were corrected accordingly and referred to the initial filling volume. Cultivation conditions: 250 mL unbaffled shake flasks, temperature: 37 °C, shaking frequency: 350/100 rpm, shaking diameter: 50 mm, Nakashimada medium with 100 mM MES buffer.

Both, the glycerol formation rate as well as the maximum concentration increase with decreasing OTR_{max} (Figure 3-4I). Up to 18 g/L glycerol are formed at the lowest OTR_{max} (40 mL filling volume), whereas glycerol formation is completely prevented for the cultivation with the highest OTR_{max} (15 mL filling volume). In contrast to that, higher OTR_{max} result in higher acetoin concentrations (Figure 3-4J). Whereas acetoin only accumulates after glucose depletion for cultivations with low OTR_{max} (30 and 40 mL filling volume), higher OTR_{max} result in increasing acetoin concentrations throughout the cultivation (15 and 20 mL filling volume). Upon glucose depletion, oxidation of D-2,3-butanediol results in acetoin accumulation.

As the course of the acetoin concentration drastically changes upon glucose depletion, this aspect was investigated in detail in Figure 3-5. Here, the time axis is shifted to the point of glucose depletion (shown as 0 h for all cultivations). At this point, increasing OTR_{max} lead to increased acetoin concentrations ranging from 2 to 28 g/L for 4 and 16 mmol/L/h, respectively. As long as glucose is present, the acetoin concentration steadily increases for cultivations with OTR_{max} above 10 mmol/L/h (filling volumes lower than 20 mL). For lower OTR_{max}, the acetoin concentration remains constantly low as long as glucose is present. As soon as glucose is depleted, fast acetoin accumulation is observed for all cultivations as explained in the description of Figure 3-4**.**

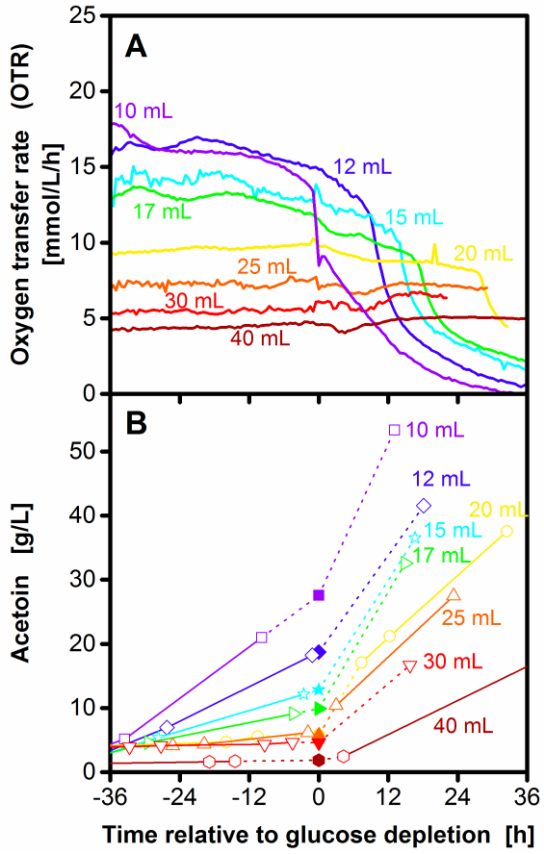

Figure 3-5: Influence of different maximum oxygen transfer capacities on acetoin formation with *Bacillus licheniformis* DSM 8785. Variation of the filling volume results in different maximum oxygen transfer capacities (OTR_{max}) in shake flask cultivations. The shaking frequency was reduced from 350 to 100 rpm after 3 h. Thereby, oxygen-limited conditions are induced at the same time for all cultivations. Oxygen transfer rates (OTR) (A) and acetoin concentrations (B) are depicted. The time on the abscissa is presented relative to the time of glucose depletion (0 h). In addition to offline samples (open symbols), the concentrations upon glucose depletion were calculated as described in Figure 3-3 (closed symbols). For clarity, the connection between the measured and calculated values is shown as dotted line. The time of glucose depletion is derived from the sudden drop of the respiratory quotient (RQ), as illustrated in Figure 3-3. To account for the increase of metabolite concentrations due to evaporation of water, all concentrations were corrected accordingly and referred to the initial filling volume. Cultivation conditions: 250 mL unbaffled shake flasks, temperature: 37 °C, shaking frequency: 350/100 rpm, shaking diameter: 50 mm, Nakashimada medium with 100 mM MES buffer.

To analyze the influence of the OTR_{max} in more detail, Figure 3-6 shows the calculated metabolite concentrations upon glucose depletion from 28 individual experiments plotted as function of the respective OTR_{max}. Thereby, the observed results can be applied independent of the utilized reactor system and scale. When the OTR_{max} is increased from 4 to 16 mmol/L/h, the maximum 2,3-butanediol concentration linearly decreases from 80 to 65 g/L (Figure 3-6A). Consequently, the molar yield also decreases from 0.9 to 0.7, as 180 g/L glucose was used as

substrate in all cultivations. This accounts for up to 90% of the stoichiometrically possible yield, neglecting that carbon is also utilized for cell growth or maintenance. The glycerol concentration decreases linearly with increasing OTR_{max}. Glycerol is not formed at all for OTR_{max} higher than 10 mmol/L/h (Figure 3-6B). In contrast to that, the acetoin concentration increases with increasing OTR_{max} (Figure 3-6C). For OTR_{max} between 4 and 13 mmol/L/h, a moderate increase from 2 to 12 g/L acetoin is observed. However, higher OTR_{max} result in a stronger increase and much higher acetoin concentrations of up to 28 g/L at 16 mmol/L/h. The sum of glycerol and acetoin concentrations is shown in Figure 3-6D. A minimum by-product concentration is observed for an OTR_{max} of 10 mmol/L/h, resulting from the lowest acetoin concentration without glycerol formation. Consequently, the by-product concentration increases with higher OTR_{max} due to increased acetoin formation. At lower OTR_{max}, higher by-product concentrations result from glycerol formation, which has a stronger impact than the reduced acetoin formation under these conditions.

The influence of the OTR_{max} on the product and by-product spectrum of *B. licheniformis* can be explained based on the NADH/NAD^+ balance of the organism (cf. Figure 1-3). During oxygen limitation, only small amounts of NADH can be oxidized in the electron transport chain. Therefore, glycolysis becomes a major source of the organism's ATP production. There are two options to oxidize the herein produced NADH to NAD^+, which is crucial to maintain ATP production via glycolysis. One option is the production of reduced overflow metabolites like 2,3-butanediol or glycerol. Additionally, oxidation via the electron transport chain occurs in accordance with the available amount of oxygen. Consequently, increasing amounts of NADH have to be oxidized by overflow metabolite production with decreasing OTR_{max}. For the production of 1 mole 2,3-butanediol from 1 mole of glucose, 2 moles of NADH are obtained during glycolysis, whereas only 1 mole of NADH is oxidized to NAD^+ during the reduction of acetoin to 2,3-butanediol (Ji et al., 2011). For high OTR_{max}, acetoin accumulates, as enough oxygen is available to oxidize more than 1 mole of NADH via the electron transport chain. For low OTR_{max}, the NADH oxidation in the electron transport chain decreases leading to almost complete acetoin reduction to 2,3-butanediol. Moreover, increasing amounts of glycerol are formed. For glycerol formation from glucose, 1 molar equivalent of NADH is oxidized to NAD^+ without NADH generation. Therefore, glycerol formation can balance out the NAD^+ deficiency during 2,3-butanediol production at low OTR_{max}.

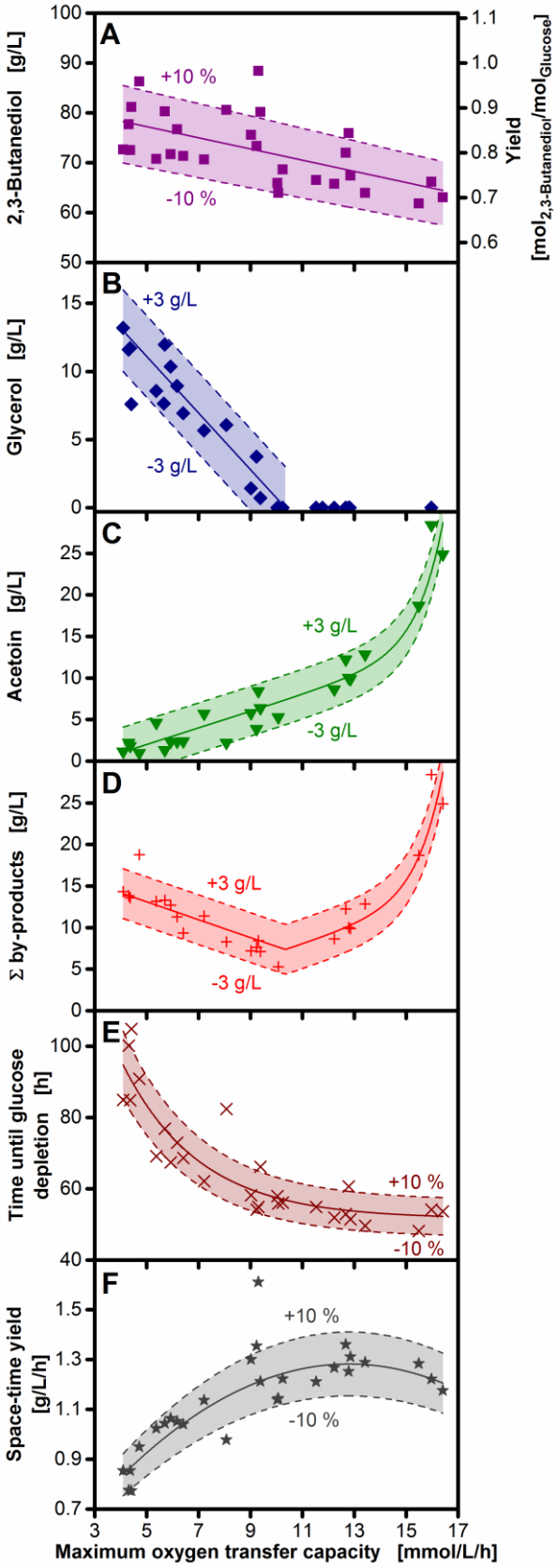

Figure 3-6: Influence of the maximum oxygen transfer capacity on 2,3-butanediol production with *Bacillus licheniformis* DSM 8785. Calculated maximum total 2,3-butanediol (A), glycerol (B) and acetoin

concentrations (C), the sum of accumulated by-products (D), the time until glucose was depleted (E) and the space-time yield (F) are shown in dependency of the maximum oxygen transfer capacity (OTR_{max}) during the 2,3-butanediol production phase. Each data point is derived from one of 28 individual experiments and refers to the time point of glucose depletion. 2,3-Butanediol is shown as sum of the stereoisomers. The time of glucose depletion is determined from the sudden drop of the respiratory quotient, which was measured in biological duplicates. Acetoin, 2,3-butanediol and glycerol concentrations at this time were calculated from offline samples as illustrated in Figure 3-3. The space-time yield was calculated from the time of glucose depletion and the maximum 2,3-butanediol concentration. The solid lines represent the fitted linear (A and B), exponential (C and E) or cubic (F) correlations. The solid line in E was calculated as sum of the fitted lines from B and C. Error margins (10% for A, D and E; 3 g/L for B, C and D) are represented by dashed lines. To account for the increase of metabolite concentrations due to evaporation of water, all concentrations were corrected accordingly and referred to the initial filling volume.

Apart from product and by-product formation, the overall cultivation time also has a significant impact on the selection of suitable cultivation conditions. For industrial 2,3-butanediol production, cultivations should be terminated as soon as glucose is depleted to achieve the maximum 2,3-butanediol concentration, complete substrate utilization and to avoid acetoin accumulation. Therefore, the influence of the OTR_{max} on the time until glucose is depleted is analyzed in Figure 3-6E. Low OTR_{max} of 4 mmol/L/h result in long cultivation times of nearly 100 h. The cultivation time decreases, when the OTR_{max} is increased. Increasing the OTR_{max} above 11 mmol/L/h has only minor effects on the cultivation time. From the cultivation time and the 2,3-butanediol concentration, the space-time yield was calculated (Figure 3-6F). The maximum space-time yield of 1.3 g/L/h is reached at an OTR_{max} of 13 mmol/L/h. At higher OTR_{max}, the space-time yield decreases due to lower 2,3-butanediol concentrations. In contrast, lower OTR_{max} lead to decreased space-time yields due to increased cultivation times.

Overall, the results presented in Figure 3-6 clearly show that there is not one defined optimum condition for 2,3-butanediol production with *B. licheniformis*. Different parameters become more or less important depending on the overall production chain and economics. The concentrations of 2,3-butanediol, acetoin and glycerol are especially important with regard to the chosen downstream processing. Depending on the demands, either high 2,3-butanediol concentrations, or low by-product concentrations are most beneficial. It is also important to consider, whether efficient separation of acetoin or glycerol from 2,3-butanediol is possible. For example, via distillation acetoin (boiling point at 148 °C) can be separated from 2,3-butanediol (boiling point at 183 °C) together with the process water. However, for glycerol separation (boiling point at 290 °C), a second distillation step would be necessary. Qureshi et

al. (1994) investigated vacuum membrane distillation for 2,3-butanediol resulting in constantly decreasing 2,3-butanediol to acetoin ratios. Using different solvents for 2,3-butanediol extraction, Anvari et al. (2009) did not observe co-extraction of acetoin. Also during anionic extraction of 2,3-butanediol via phenylboronic acid, no acetoin is co-extracted, whereas co-extraction of glycerol was observed (Drabo et al., 2017). In these cases, avoiding glycerol formation by selection of OTR_{max} above 10 mmol/L/h will most likely be beneficial. Even though the selection of suitable OTR_{max} strongly depends on the specific process demands, some general conclusions can be drawn. OTR_{max} above 13 mmol/L/h should be avoided. In that case, 2,3-butanediol concentration and space-time yield decrease, while the acetoin concentration severely increases. Also very low OTR_{max} should not be selected, as this only leads to small increases in the 2,3-butanediol concentration at the expense of severely prolonged cultivation times and higher glycerol formation. Selection of an OTR_{max} between 11 and 13 mmol/L/h will be beneficial for most processes. This results in high space-time yields at low by-product formation and completely avoids glycerol formation.

3.5 Comparison between shake flask and stirred tank reactor cultivations

To verify that the results obtained in Figure 3-6 can be transferred between different bioreactor systems, a shake flask and a stirred tank reactor cultivation are compared in Figure 3-7. As shown in Figure 3-7A and D, the same OTR_{max} of 7 mmol/L/h was adjusted in both scales after reduction of the shaking frequency and agitation rate, respectively. This results in comparable process performance as demonstrated by the similar courses of glucose and 2,3-butanediol concentrations (Figure 3-7B and E). The courses of the RQ are comparable (Figure 3-7A and D), however, in the stirred tank reactor a higher RQ results from increased glycerol formation compared to the shake flask cultivation (Figure 3-7C and F). The cell dry weight increases to 5 g/L during the first 24 h of cultivation in both bioreactor systems, stays constant until glucose is depleted and decreases afterwards (Figure 3-7C and F). The previously described rapid accumulation of acetoin upon glucose depletion is also observed in both bioreactors (Figure

3-7C and F). This comparison shows that the OTR_{max} is a suitable parameter to achieve comparable process performance in shake flasks and lab-scale stirred tank reactors.

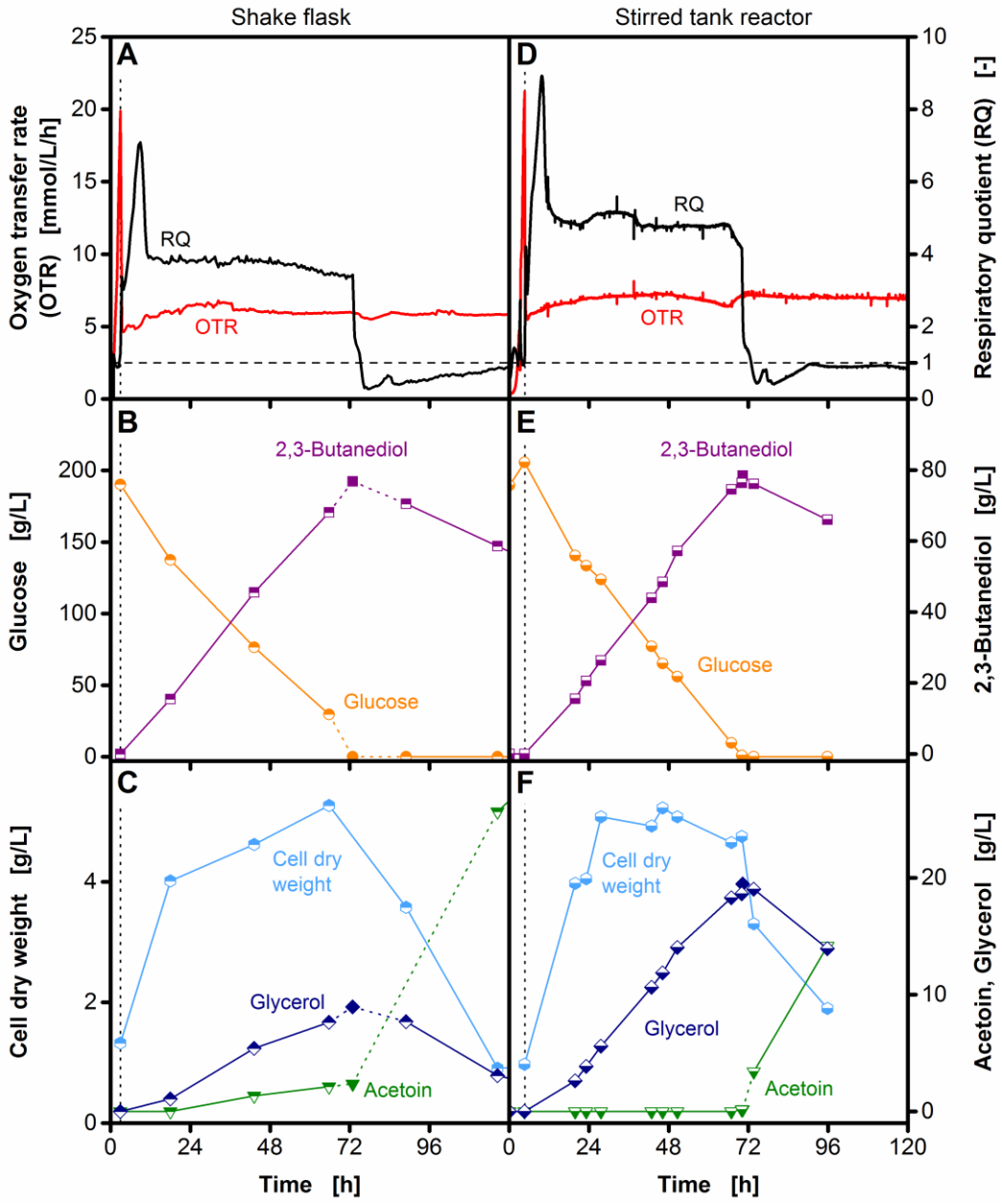

Figure 3-7: Comparison of shake flask and stirred tank reactor cultivations of *Bacillus licheniformis* DSM 8785. As indicated by the vertical dotted lines, the shaking frequency of the shake flask cultivation (A-C) and the agitation rate of the stirred tank reactor cultivation (D-F) were reduced from 350 to 100 and from 1000 to 500 rpm after 4.5 and 3 h, respectively. The courses of oxygen transfer rates (OTR) and respiratory quotients (RQ) (A and D), glucose and total 2,3-butanediol concentrations (B and E), as well as cell dry weight, acetoin and glycerol concentrations (C and F) are shown. In addition to offline samples (half-closed symbols), the concentrations upon glucose depletion were calculated as described in Figure 3-3 (closed symbols). For clarity, the connections between the measured and calculated values are shown as dotted lines. 2,3-Butanediol is shown as sum of the

stereoisomers. The RQ is only shown for OTR > 1 mmol/L/h. To account for the increase of metabolite concentrations due to evaporation of water, concentrations of the shake flask cultivation were corrected accordingly and referred to the initial filling volume. Cultivation conditions: Temperature: 37 °C; shake flask cultivation: 250 mL unbaffled shake flasks, filling volume: 30 mL, shaking frequency: 350/100 rpm, shaking diameter: 50 mm; Nakashimada medium with 100 mM MES buffer. Stirred tank reactor cultivation: 2 L stirred tank reactor, filling volume: 1.5 L, aeration rate: 0.5 L/min (0.33 vvm), agitation rate: 1000/500 rpm, Nakashimada medium without MES buffer addition.

In addition to the direct comparison between shake flask and stirred tank reactor cultivations (Figure 3-7**)**, the impact of the OTR_{max} on the cultivation (cf. Figure 3-6) is comparable to the results Rebecchi et al. (2018) generated in a stirred tank reactor with the same organism. The same maximum 2,3-butanediol yields of 0.9 mol/mol (0.45 g/g) were observed in both studies. However, a linear dependency between OTR_{max} and 2,3-butanediol yield was observed in Figure 3-6, whereas Rebecchi et al. (2018) observed reduced yields between 2 and 7 mmol/L/h. This probably results from missing offline samples at the time of maximum 2,3-butanediol concentration. In this thesis, this problem is avoided by the described method to quantify the maximum 2,3-butanediol concentration. The highest space-time yield was observed at OTR_{max} slightly above 10 mmol/L/h in both studies. However, in this thesis a higher space-time yield was reached (1.3 instead of 1.0 g/L/h), which probably results from the utilization of different cultivation media. In both studies, exactly the same OTR_{max} of at least 10 mmol/L/h completely prevented glycerol formation.

3.6 Conclusion

Even though the impact of the oxygen availability on 2,3-butanediol production is widely discussed in the literature, only few studies focused on this effect on the basis of scalable parameters (de Mas et al., 1988; Jansen et al., 1984; Ji et al., 2009; Ramachandran and Goma, 1987; Ramachandran et al., 1990; Rebecchi et al., 2018). However, this is necessary to transfer the obtained results to other bioreactor setups and, thus, make them available to other research groups. Therefore, the OTR_{max} was selected to quantify the effects of oxygen availability in this chapter. The above-mentioned studies revealed different optimum oxygen availabilities for different microorganisms. Therefore, a fast and simple, but reliable methodology to investigate

this effect was presented in this chapter. In contrast to the above-mentioned studies, this chapter presents a shake flask methodology to reduce the technical and experimental effort.

Two concepts were applied to increase the precision of the experimental results compared to existing studies (de Mas et al., 1988; Jansen et al., 1984; Ji et al., 2009; Ramachandran and Goma, 1987; Ramachandran et al., 1990; Rebecchi et al., 2018). First, online monitoring of the RQ was combined with offline sampling to determine metabolite concentrations exactly at the point of glucose depletion. This prevents misinterpretation of results due to inadequate sampling time points, as 2,3-butanediol and glycerol are consumed and acetoin accumulates after glucose depletion (Figure 3-3). To the author's knowledge, this effect has not yet been considered in the existing literature. Second, a defined two-stage cultivation profile was applied. Two-stage cultivation strategies have already been described in the literature to accelerate 2,3-butanediol formation (Cho et al., 2015b; Dai et al., 2014; Fages et al., 1986; Ji et al., 2009; Li et al., 2013; Park et al., 2013; Priya et al., 2016; Qiu et al., 2016; Zhang et al., 2010). In contrast, the here applied two-stage cultivation profile aimed at providing defined cultivation conditions instead of accelerating product formation. This strategy synchronizes the initiation of oxygen limitation between different cultivations and, thus, allows for the isolated determination of the influence of the OTR_{max}.

Optimum cultivation conditions for *Bacillus licheniformis* DSM 8785 were identified at OTR_{max} between 11 and 13 mmol/L/h. Under these conditions, high product and space-time yields are achieved, while glycerol formation is completely prevented and only small amounts of acetoin accumulate. Moreover, selection of suitable OTR_{max} slightly improves 2,3-butanediol production compared to the so far best reported results from batch experiments with the same organism (73 g/L 2,3-butanediol at a space-time yield of 0.86 g/L/h) (Jurchescu et al., 2013). In this thesis, the same space-time yield was achieved at an OTR_{max} of 4.3 mmol/L/h, resulting in an increased 2,3-butanediol concentration of 77 g/L. A maximum value of 73 g/L 2,3-butanediol was observed at an OTR_{max} of 8.3 mmol/L/h at an increased space-time yield of 1.27 g/L/h. Generally, the shake flask-based results in this chapter are in good agreement with own and external stirred tank reactor cultivations (Rebecchi et al., 2018). This demonstrates that the presented approach is suitable to investigate the impact of the OTR_{max} on 2,3-butanediol production and can probably be transferred to other organisms.

Chapter 4

Potential of online respiratory quotient monitoring during microaerobic cultivations

4.1 Introduction

Biotechnological 2,3-butanediol production is a much studied example for microaerobic cultivation processes. As explained in detail in Section 1.2, 2,3-butanediol is produced in a mixed acid-2,3-butanediol fermentation pathway (Kallbach et al., 2017). Depending on the oxygen availability, different by-products like acetoin, glycerol, ethanol and organic acids are formed (Converti et al., 2003; Heyman et al., 2019; Ji et al., 2011; Rebecchi et al., 2018). This results in reduced product yields, as well as more challenging downstream processing (Qureshi et al., 1994; Xiu and Zeng, 2008). Consequently, online monitoring of the production process to understand and control the underlying mechanisms of by-product formation is an essential step towards commercially feasible 2,3-butanediol production.

As discussed in Section 1.1, online monitoring during microaerobic cultivations is challenging as the dissolved oxygen tension (DOT) cannot be measured and the information content from oxygen transfer rate (OTR) measurements is limited. In contrast, the respiratory quotient (RQ) has been successfully applied for process monitoring and control during microaerobic cultivations (Brandberg et al., 2007; Chen et al., 2003; Franzén, 2003; Franzén et al., 1996; Xiu et al., 2007; Zhang et al., 2010). Furthermore, Zeng et al. (1994) used the RQ to control the oxygen supply for 2,3-butanediol production and to monitor the viable biomass during the

cultivation (Zeng et al., 1991b). The RQ is the quotient of carbon dioxide formation and oxygen consumption and provides additional information about the metabolic activity of the organism. Different RQs are observed depending on the utilized carbon source, biomass formation and the formation of overflow metabolites. Generally, an RQ of 1 results when substrate and product have the same degree of reduction. The RQ is above 1 when the product is more reduced than the substrate and below 1 in the opposite case. For a given reaction stoichiometry, a theoretical RQ can be calculated based on oxygen consumption and carbon dioxide formation.

Despite the above-mentioned benefits, there is not much literature about RQ monitoring of microaerobic cultivations. Most of these studies either focused on process control and scale-up strategies (Franzén et al., 1996; Rebecchi et al., 2018; Zeng et al., 1994; Zhang et al., 2010) or investigated the formation of ethanol, (Brandberg et al., 2007; Franzén, 2003) and 1,3-propanediol (Chen et al., 2003; Xiu et al., 2007). Therefore, the aim of this chapter is to understand the metabolic activity in different cultivation phases of the mixed acid-2,3-butanediol production and to improve the explanatory power of online RQ monitoring. Therefore, microaerobic cultivations of *Bacillus licheniformis* DSM 8785 were investigated, both in shake flasks and in a stirred tank reactor. Consequently, the obtained results are independent of the utilized bioreactor system and scale. According to the measured RQ, partial reaction stoichiometries were set up for each metabolic phase. Thereby, the respective predominant metabolic activity was identified and confirmed by offline sampling. Finally, the average RQ was correlated to the maximum oxygen transfer capacity (OTR_{max}) of different cultivations, reflecting the metabolic response to changing oxygen availability. Most results presented in this chapter have been published previously (Heyman et al., 2020). Parts of these results have been obtained in collaboration with Hannah Tulke (research internship and master's thesis) and Damarice Wandji (master's thesis).

4.2 Cultivation of *Bacillus licheniformis* DSM 8785

In this chapter, cultivations were performed in unbaffled 250 mL shake flasks and a 2 L stirred tank reactor. All shake flask cultivations were performed in at least 7 shake flasks in parallel

and the respiration activity was monitored online with the Respiration Activity Monitoring System (RAMOS) (Anderlei et al., 2004) as visualized in Figure 2-1.

The cultivation of *B. licheniformis* under microaerobic conditions follows three distinct phases (Figure 4-1). An unlimited growth phase (until the first dotted line) is followed by the 2,3-butanediol production phase (between the dotted lines) and finally 2,3-butanediol is converted to acetoin (after the second dotted line). Figure 4-1A depicts the courses of OTR and carbon dioxide transfer rate (CTR) in 250 mL shake flasks. A two-stage cultivation profile was applied in all cultivations to enable defined microaerobic cultivation conditions as described in detail in Section 3.3. At the beginning of the cultivation, a shaking frequency of 350 rpm resulted in oxygen unlimited growth as shown by the steep increase of the OTR. When the OTR reached values around 20 mmol/L/h, the shaking frequency was decreased to 100 rpm. Thereby, oxygen limitation was initiated, resulting in an OTR plateau at the level of the OTR_{max} of 5 mmol/L/h (cf. Appendix 1A). The CTR peaks at 30 mmol/L/h at the beginning of the oxygen-limited 2,3-butanediol production phase and then remains constant at 20 mmol/L/h until 60 h. Between 60 and 90 h the CTR slowly declines. Afterwards, a sharp decrease of the CTR to a shoulder at 6 mmol/L/h is followed by a second sharp decrease to 2 mmol/L/h at 96 h. Figure 4-1B shows the course of the RQ. A theoretical RQ can be calculated for a given reaction stoichiometry based on oxygen consumption and carbon dioxide formation (Equation 2-1 in Section 2.6). Thus, monitoring of the RQ can be combined with stoichiometric considerations to understand the metabolic activity during the cultivation. During the oxygen unlimited phase in the first 3 h of the cultivation, the RQ is around 1 indicating growth on glucose. Due to the high lipid content in the membrane, biomass is more reduced than glucose, resulting in a calculated RQ of 1.3 during biomass formation (Equation 2-2). However, this calculation does not include maintenance or other energy requiring processes. Thus, a slightly lower RQ can be expected, when a combination of growth and glucose combustion is assumed during the first 3 h of cultivation (Figure 4-1B). Afterwards, the course of the RQ resembles the course of the CTR, as the OTR stays constant due to oxygen limitation. The general course of the RQ can be explained by the courses of glucose, 2,3-butanediol (Figure 4-1C), glycerol and acetoin (Figure 4-1D). The RQ of 4 between 9 and 90 h mainly results from glucose consumption and 2,3-butanediol production, as the calculated RQ for this reaction is 4 (Equation 2-4). Additionally, glycerol and biomass are formed at that time (Figure 4-1D). Compared to 2,3-butanediol

production, biomass formation reduces the RQ (Equation 2-2 and 2-4), whereas glycerol formation increases the RQ (Equation 2-5). Upon glucose depletion, 2,3-butanediol is consumed and converted to acetoin (clearly visible in Figure 3-4). This conversion provides protons that can be oxidized in the respiratory chain (Equation 2-6) resulting in RQ values below 1. The above-mentioned RQ course has been investigated and discussed in detail in Chapter 3. However, the peak after 7 h, the slow decline between 60 and 90 h and the shoulder between 90 and 96 h (highlighted as I, II and III in Figure 4-1B) cannot be explained by the above mentioned mechanisms and were investigated in this chapter.

For a comprehensive and universal investigation of these phenomena, shake flask and stirred tank reactor cultivations were combined. Thereby, the benefits of both systems can be utilized. Shake flasks provide high experimental throughput and parallelization, whereas stirred tank reactors provide high reaction volumes and a technical setup that is closer to industrial production processes. The scalability of the investigated 2,3-butanediol production process between shake flasks and stirred tank reactor was already demonstrated in Section 3.5 (Figure 3-7). However, different oxygen transfer mechanisms are relevant in the different bioreactor systems. In unbaffled shake flasks, oxygen transfer from the gas to the liquid phase takes place at the liquid surface. The shape of the rotating bulk liquid in shake flasks only depends on the operation conditions and not on the physiochemical properties of the culture liquid. Thus, the mass transfer area is very defined and constant (Klöckner and Büchs, 2012; Maier and Büchs, 2001). In contrast, oxygen transfer in stirred tank reactors occurs at the interface between gas bubbles and the liquid. Thus, complex phenomena like bubble dispersion and coalescence or foaming affect the oxygen transfer (Devi and Kumar, 2017; Karimi et al., 2013; Martinov et al., 2008; Schaepe et al., 2013; Takesono et al., 2001). Consequently, combination of both systems guarantees that biological effects can be investigated under microaerobic conditions, independent of bioreactor-specific oxygen transfer phenomena.

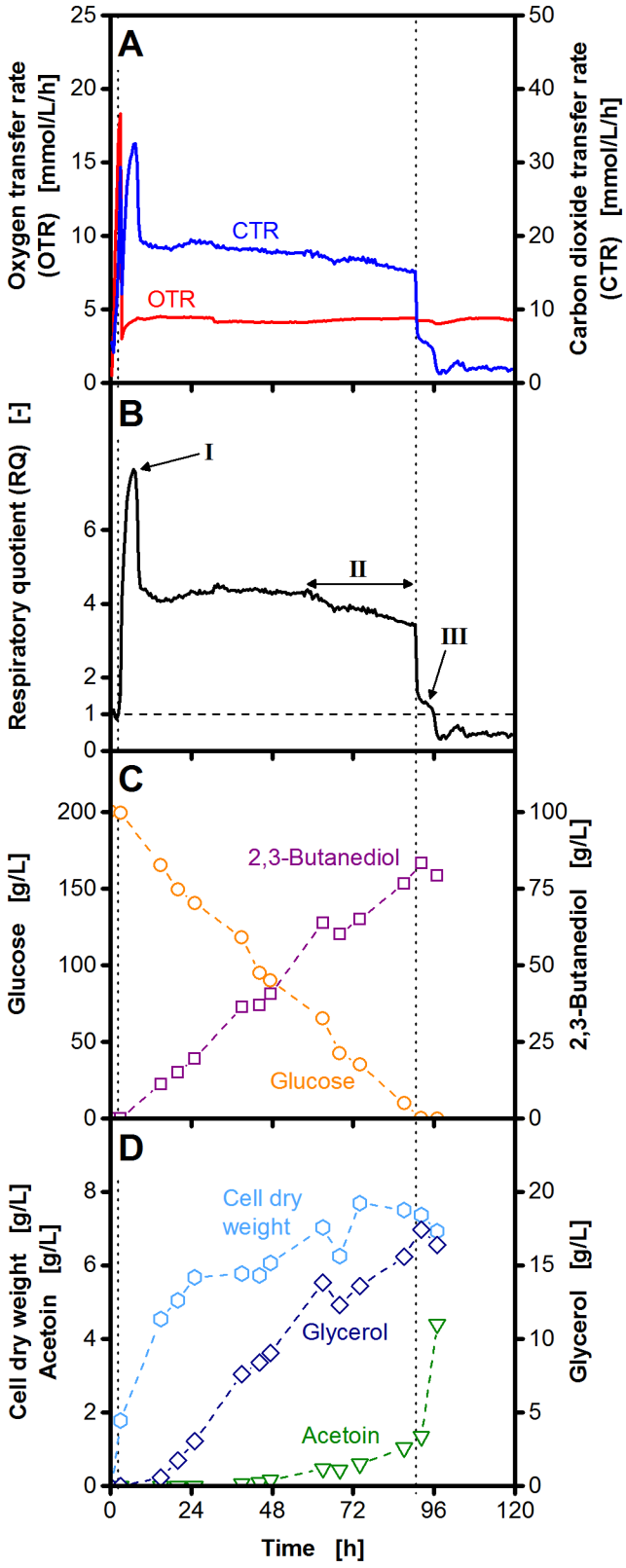

Figure 4-1: Shake flask cultivation of *Bacillus licheniformis* DSM 8785 under microaerobic conditions. The courses of oxygen (OTR) and carbon dioxide transfer rates (CTR) (A), the respiratory quotient (RQ) (B), as well as glucose, 2,3-butanediol (C), acetoin, glycerol and cell dry weight (D) are shown. The

shaking frequency was reduced from 350 to 100 rpm after 3 h (left vertical dotted line). As visualized by the vertical dotted lines, an oxygen unlimited growth phase is followed by the 2,3-butanediol production phase and subsequent 2,3-butanediol consumption. The peak (I), the slow decline (II) and the shoulder (III) of the RQ course (B) are investigated in this chapter. Cultivation conditions: 250 mL unbaffled shake flasks, temperature: 37 °C, filling volume: 40 mL, shaking frequency: 350/100 rpm, shaking diameter: 50 mm, Nakashimada medium with 100 mM MES buffer.

4.3 Investigation of the peak in the respiratory quotient

The metabolic causes for the RQ peak at the beginning of the 2,3-butanediol production phase (marked as I in Figure 4-1B) were investigated. As described above, the RQ provides information on the degree of reduction of the utilized carbon source and the produced metabolites. Consumption of glucose and formation of 2,3-butanediol result in RQs around 4 (Equation 2-4). The RQ peak can have two different metabolic causes: Either, the production of a by-product that is more reduced than 2,3-butanediol, or the consumption of a substrate that is more oxidized than glucose. As the OTR is constant during the period of the RQ peak, it originates from a CTR peak (cf. Figure 4-1A). Thus, also non-metabolic effects that cause additional carbon dioxide release could be an explanation for the observed peak. When the pH decreases during the cultivation in the range of the pK_a value of the bicarbonate buffer (6.1), previously dissolved carbon dioxide can be released from the culture broth. This carbon dioxide will then be detected in the gas phase and result in an overestimation of the CTR.

To investigate the cause of the RQ peak, two shake flask cultivations with different filling volumes and a stirred tank reactor cultivation are compared in Figure 4-2. The filling volume of shake flask cultivations determines the OTR_{max} (Appendix 1) and, thus, severely influences the formation of by-products (Heyman et al., 2019; Rebecchi et al., 2018). Figure 4-2A-C depict the CTRs and RQs during the first 30 h of cultivation, forming the previously observed peaks. For all cultivation conditions, the pH decreases from 6.6 to 6 during the first hours of cultivation before the RQ peak occurs (Figure 4-2D-F). During the RQ peak, the pH slightly increases and decreases after the peak. Consequently, the course of the pH cannot explain the RQ peak. Equilibrium changes of the bicarbonate buffer only cause carbon dioxide release from the

culture broth at decreasing pH values. Thus, with the observed pH profile the measured CTR would rather be decreased than increased.

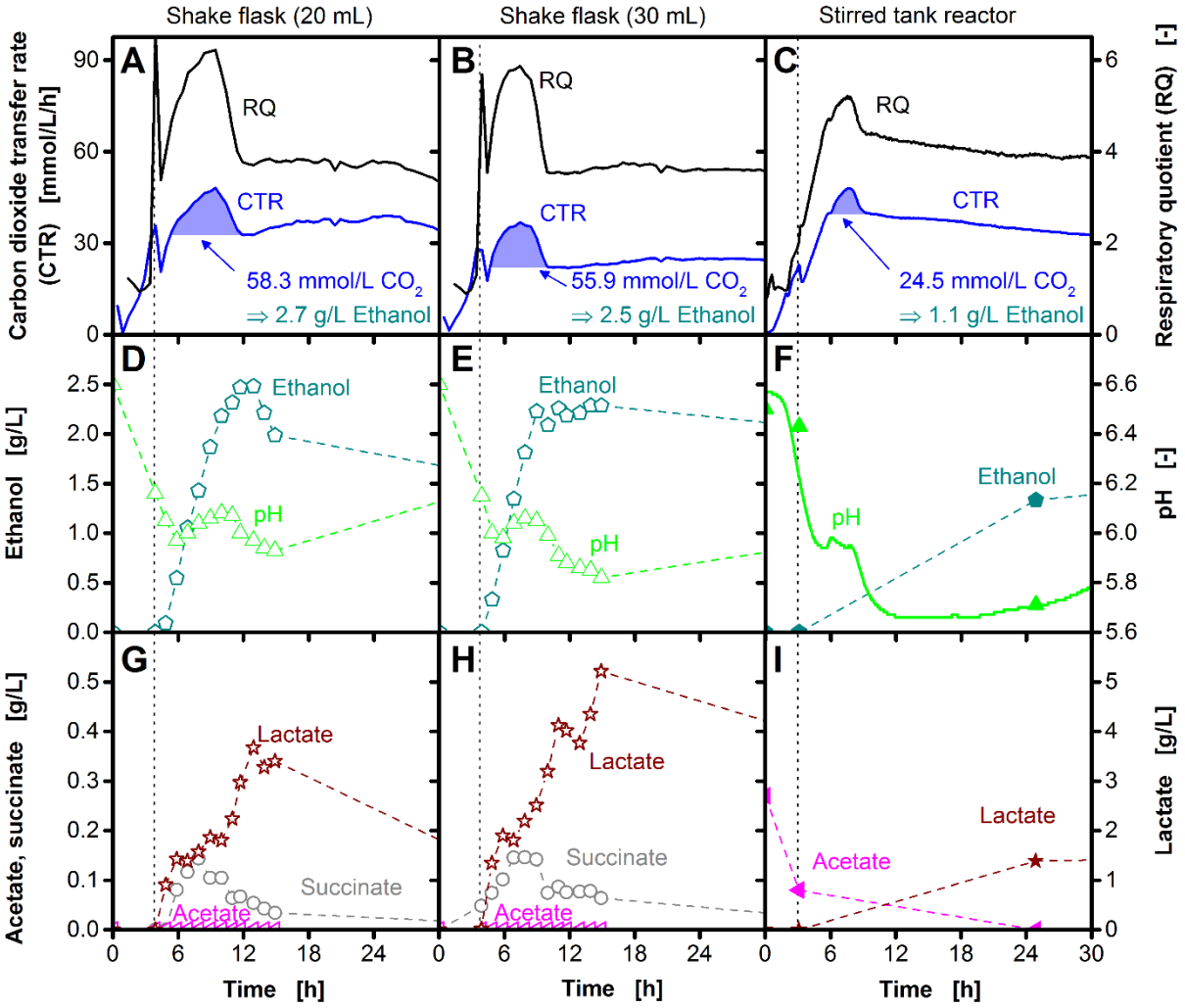

Figure 4-2: Investigation of the peak in the respiratory quotient. The formation of the peak (marked as I in Figure 4-1B) is investigated in shake flask (A, B, D, E, G, H) and stirred tank reactor (C, F, I) cultivations. Carbon dioxide transfer rates (CTR) and respiratory quotients (RQ) (A-C), ethanol concentrations and pH values (D-F) as well as organic acid concentrations (G-I) are shown. In the stirred tank reactor, the pH was measured online (line) and offline (symbols). Ethanol formation under microaerobic conditions results in equimolar carbon dioxide formation (blue colored areas under the CTR peak in A-C). The shaking frequency and the agitation rate were reduced from 350 to 100 rpm and from 1000 to 500 rpm after 3 and 4 h, respectively (vertical dotted lines). Cultivation conditions: Temperature: 37 °C; shake flask cultivation: 250 mL unbaffled shake flasks, shaking frequency: 350/100 rpm, shaking diameter: 50 mm, Nakashimada medium with 100 mM MES buffer. Stirred tank reactor cultivation: 2 L stirred tank reactor, filling volume: 1.5 L, aeration rate: 0.5 L/min (0.33 vvm), agitation rate: 1000/500 rpm, Nakashimada medium without MES buffer addition.

Ethanol, a highly reduced by-product is formed during the RQ peak (Figure 4-2D-F). Under microaerobic cultivation conditions, ethanol formation results in equimolar carbon dioxide formation (Equation 2-7). The excess carbon dioxide formation during the period of the peak time (blue colored areas in Figure 4-2A-C) was calculated to 58, 56 and 25 mmol/L/h, which correlates to the formation of 2.7, 2.5 and 1.1 g/L ethanol for the shake flasks with 20 and 30 mL and the stirred tank reactor cultivation, respectively. This is in good agreement with the offline measured ethanol concentrations (Figure 4-2D-F) and indicates that ethanol formation causes the peak in the RQ at about 7 h. Furthermore, Zeng et al. (1994) concluded that increased RQs can be expected upon ethanol formation, which further substantiates this result.

Under microaerobic conditions, 2,3-butanediol production is initiated as response to previous organic acid formation (Ji et al., 2011). As some organic acids (e.g. succinate) are more oxidized than glucose, organic acid formation during the period of the RQ peak was investigated. Concentrations of succinate, acetate and lactate are shown in Figure 4-2 G-I. In addition to these organic acids, formate formation is reported in the literature (Ji et al., 2011), which could not be detected in the conducted experiments. Only consumption of acetate (probably carried over from the pre-culture) could be observed during the RQ peak in the stirred tank reactor cultivation. No organic acid consumption was observed in the shake flask experiments at this time. As acetate has the same degree of reduction as glucose, acetate formation cannot cause the RQ peak. Up to 0.2 g/L succinate, which is more oxidized than glucose, was formed during the period of the RQ peak. As succinate production leads to a decreased RQ, this is also not the cause of the RQ peak. As neither pH-changes (Figure 4-2D-F), nor organic acid consumption (Figure 4-2G-I) can explain the RQ peak, this confirms that the RQ peak results from ethanol formation (Figure 4-2D-F).

4.4 Investigation of the slowly declining respiratory quotient

At the end of the 2,3-butanediol production phase, a slow decline of the RQ is observed (marked as II in Figure 4-1B), before the RQ drops sharply upon glucose depletion. During 2,3-

butanediol production with *Enterobacter aerogenes*, Zeng et al. (1991b) also observed a slow decline of the RQ. They reported that this decline originates from a decrease of the viable cell mass that could not be detected via cell dry weight measurements. The oxygen supply to the culture broth stays constant during the cultivation, as the OTR_{max} does not change. When the amount of viable and actively breathing cells decreases, the ratio of available oxygen per cell increases. Thereby, the amount of glucose that is completely oxidized via the respiratory chain increases. According to Equation 2-3, complete utilization of glucose in this pathway would result in an RQ of 1. Consequently, an increased oxidative utilization of glucose decreases the RQ during the 2,3-butanediol production phase, as Equation 2-3 and 2-4 have to be combined to describe the predominant metabolic activity.

To test if decreasing viable cell mass explains the observed slow decline of the RQ during cultivations of *B. licheniformis*, the shaking frequency was steadily reduced during shake flask experiments (Figure 4-3). Thereby, the OTR_{max} is reduced to counteract the decreasing viable cell mass. A reference cultivation with constant shaking frequency during the 2,3-butanediol production phase is compared to two cultivations with different shaking frequency reduction rates in Figure 4-3A. Due to the reduction of the shaking frequency, the OTR decreases (Figure 4-3B), reflecting the reduction of the OTR_{max}. In the reference cultivation, the RQ slowly declines between 30 and 65 h (Figure 4-3C). In contrast, the RQ stays constant at values slightly above 4 during this time at both reduction rates of the shaking frequency.

As shown in Figure 4-3, the slow decline of the RQ can be prevented by reduction of the shaking frequency. This supports the hypothesis that this decline is caused by decreasing viable cell mass as observed by Zeng et al. (1991b). Furthermore, this conclusion is in good agreement with redox potential measurements performed in stirred tank reactor cultivations (Section 5.7). These redox potential measurements revealed that the DOT increases during the cultivation. In a similar experiment to the one shown in Figure 4-3, reduction of the agitation rate resulted in a constantly low DOT during the 2,3-butanediol production phase (cf. Figure 5-11). These matching results of redox potential and RQ measurements in shake flask and stirred tank reactor cultivations are a strong evidence that the observed slow decline of the RQ results from decreasing viable cell mass.

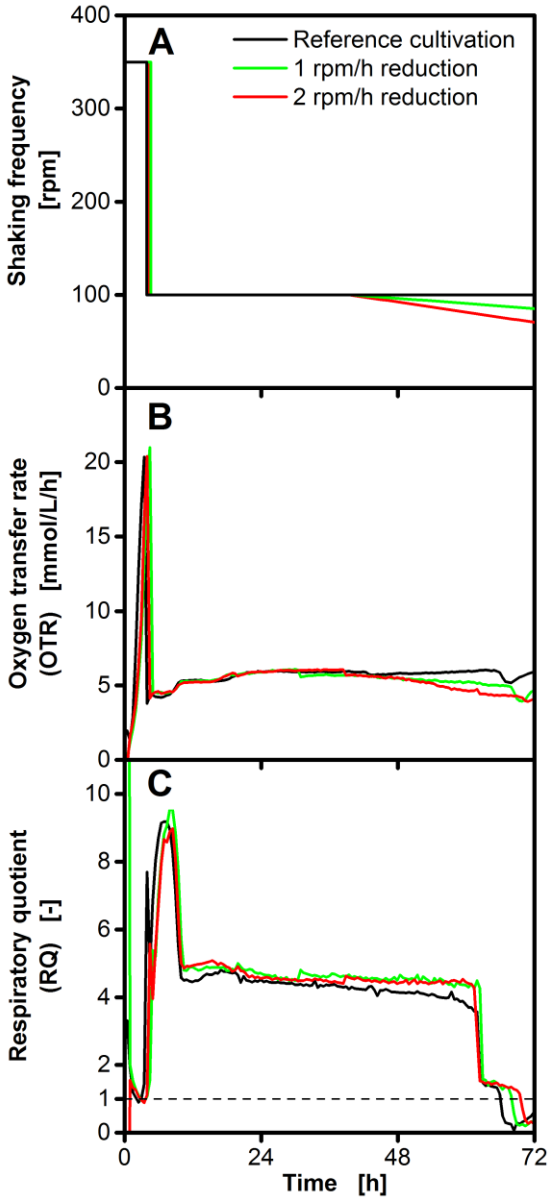

Figure 4-3: Investigation of the slowly declining respiratory quotient. The course of the respiratory quotient (RQ) at the end of the 2,3-butanediol production phase (marked as II in Figure 4-1B) was manipulated by reduction of the shaking frequency in shake flask cultivations. Courses of the shaking frequency (A), the oxygen transfer rate (OTR) (B) and the RQ (C) are shown for three cultivations. After 3.5 h the shaking frequency was reduced from 350 to 100 rpm to induce oxygen limitation. The following steady reduction of the agitation rate (reduction rate is indicated in the figure legend) was predefined using a shaker control software (ISIS-Software; Adolf Kühner AG, Birsfelden, Switzerland). Cultivation conditions: Temperature: 37 °C; 250 mL unbaffled shake flasks, filling volume: 30 mL, shaking diameter: 50 mm, Nakashimada medium with 100 mM MES buffer.

4.5 Investigation of the shoulder in the respiratory quotient

The sharp drop of the RQ at the end of the 2,3-butanediol production phase is caused by glucose depletion. The formation of a shoulder (marked as III in Figure 4-1B) during this drop is only observed for strong oxygen limitations at low OTR_{max} (Appendix 1). With increasing OTR_{max}, the shoulder becomes smaller and finally disappears completely. To investigate the RQ shoulder, a shake flask and a stirred tank reactor cultivation are compared in Figure 4-4. The shake flask cultivation (Figure 4-4A) has a slightly lower OTR_{max} resulting in a longer RQ shoulder compared to the stirred tank reactor cultivation (Figure 4-4B). The formation of the RQ shoulder is accompanied by a rapidly decreasing lactate concentration, resulting in a simultaneous increase of the pH (Figure 4-4C and D). As specified by Equation 2-8, combustion of lactate results in a theoretical RQ of 1. The measured RQ during the shoulder is slightly above 1 (at 90 and 72 h in Figure 4-4A and B, respectively). However, also other factors like the consumption of non-detected by-products most likely have an effect on the level of the RQ during this time. Therefore, lactate combustion is not the only, but the major factor causing the shoulder in the RQ.

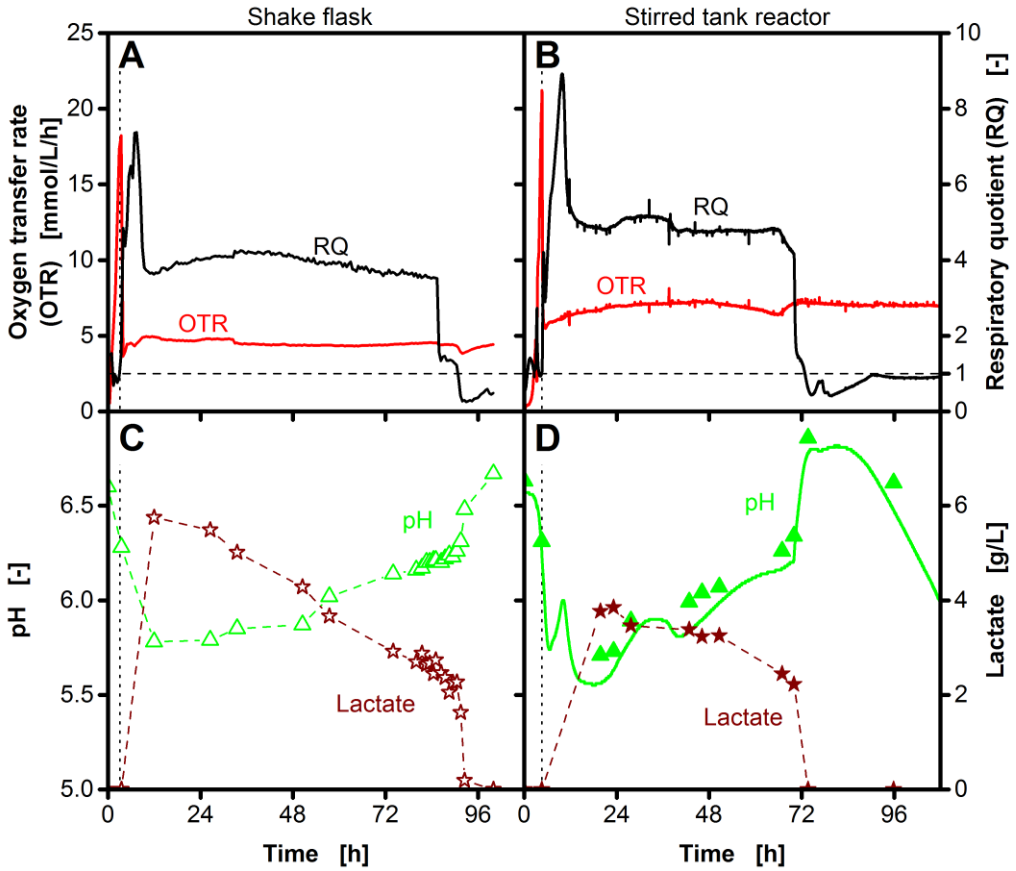

Figure 4-4: Investigation of the shoulder in the respiratory quotient. The formation of the shoulder (marked as III in Figure 4-1B) is investigated in shake flask (A, C) and stirred tank reactor (B, D) cultivations. Oxygen transfer rates (OTR) and respiratory quotients (RQ) (A, B) and the pH and lactate concentrations (C, D) are shown. In the stirred tank reactor, the pH was measured online (line) and offline (symbols). The shaking frequency and the agitation rate were reduced from 350 to 100 rpm and from 1000 to 500 rpm after 4.5 and 3.5 h, respectively (vertical dotted lines). Cultivation conditions: Temperature: 37 °C; shake flask cultivation: 250 mL unbaffled shake flasks, filling volume: 40 mL, shaking frequency: 350/100 rpm, shaking diameter: 50 mm, Nakashimada medium with 100 mM MES buffer. Stirred tank reactor cultivation: 2 L stirred tank reactor, filling volume: 1.5 L, aeration rate: 0.5 L/min (0.33 vvm), agitation rate: 1000/500 rpm, Nakashimada medium without MES buffer addition.

4.6 Correlation between average RQ and maximum oxygen transfer capacity

In the previously described results, the RQ was used to understand the metabolic activity during specific phases of the cultivation. In addition to these learnings, the average RQ during a longer

cultivation period provides information on the overall stoichiometry of the cultivation. Therefore, the average RQ during the 2,3-butanediol production phase was determined. In shake flasks, the 2,3-butanediol production phase is initiated by the reduction of the shaking frequency to induce oxygen limitation and ends when the RQ sharply drops upon glucose depletion (visualized in Appendix 1). The average RQ was determined by two different approaches. For the conventional determination, the online measured carbon dioxide formation and oxygen consumption are divided according to Equation 2-1. Additionally, carbon mass balancing (Equation 2-9; Appendix 5) based on measured metabolite and cell dry weight concentrations was used to calculate the carbon dioxide formation, which was then divided by the online measured oxygen consumption. Figure 4-5 shows the correlation between the average RQ and the OTR_{max} for 19 individual experiments.

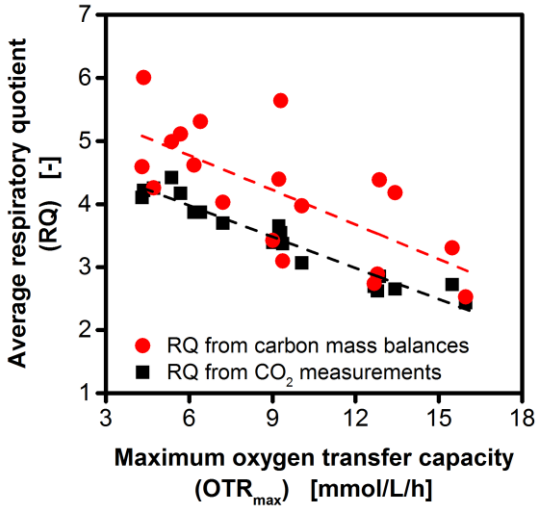

Figure 4-5: Correlation between average respiratory quotient and maximum oxygen transfer capacity. Average respiratory quotients (RQ) from 19 individual shake flask cultivations at varied maximum oxygen transfer capacities (OTR_{max}) are shown. The OTR_{max} was derived from the course of the OTR (cf. Appendix 1). To calculate the RQ, carbon dioxide formation during 2,3-butanediol production was either measured online, or derived from carbon balances of offline samples (cf. Appendix 1, Equation 2-9). The metabolite and cell dry weight formation during the 2,3-butanediol production phase is summarized in Appendix 5. The consumed oxygen for RQ calculations was derived from measured oxygen transfer rates. Cultivation conditions: 250 mL unbaffled shake flasks, temperature: 37 °C, shaking frequency: 350/100 rpm, shaking diameter: 50 mm, Nakashimada medium with 100 mM MES buffer.

The OTR_{max} is one of the most influential parameters during microaerobic cultivations and strongly determines the product and by-product spectrum (Heyman et al., 2019; Rebecchi et al., 2018). With increasing OTR_{max}, the average RQ from online carbon dioxide measurement

(black symbols) decreases linearly from 4 to 2.5. The average RQ from carbon mass balances (red symbols) decreases from 5 to 3 with increasing OTR_{max}. Even though generally higher RQs were derived from mass balancing, the overall trend matches the results obtained from carbon dioxide measurements. This confirms that the dependency of the average RQ of the OTR_{max} reflects the adaption of the metabolism to changing oxygen availability. With decreasing OTR_{max}, the amount of energy that can be obtained by oxidation in the respiratory chain decreases (Zeng et al., 1994). Consequently, more energy has to be generated via glycolysis. To regenerate NADH and to maintain glycolysis, more reduced overflow metabolites have to be formed (Appendix 5) resulting in an increased average RQ.

Rebecchi et al. (2018) also observed decreasing RQs for cultivations with increasing OTR_{max}. However, it is not clear if this refers to average RQs or to RQs measured at a specific time during the cultivation. In this thesis, calculation of the average RQ based on carbon mass balances from offline samples yielded generally higher RQs and shows a higher variation compared to RQs derived from online carbon dioxide measurements. The cultivations were performed in a complex medium in the presence of undefined components like yeast extract and tryptone. Their contribution to the carbon balance was neglected. Consequently, exact calculation of the RQ could not be expected. Still the overall trend matches the measured RQs. This clearly indicates that the observed correlation reflects the organism's metabolic response to varied oxygen availability as already explained in detail in Section 3.4.

4.7 Conclusion

Based on the course of the RQ, the cultivation can be divided into different metabolic phases. With the initiation of oxygen-limited conditions, the 2,3-butanediol production phase starts (Figure 4-1). At the beginning of this phase, additional ethanol formation results in an RQ peak (cf. Figure 4-2). Afterwards, an RQ plateau is observed, but due to decreasing viable cell mass, the RQ slowly declines towards the end of the 2,3-butanediol production phase (cf. Figure 4-3). Upon glucose depletion, the RQ rapidly drops to values below 1. In cultivations with low OTR_{max}, utilization of the previously formed lactate results in a formation of a shoulder during

this drop (cf. Figure 4-4). Finally, 2,3-butanediol is converted to acetoin after glucose depletion. A very similar course of the RQ was observed for the cultivation of *Bacillus vallismortis* (Kallbach, 2018). However, to the author's knowledge, the metabolic reasons for the observed peak and shoulder have not yet been described in the literature.

In this chapter, two approaches were presented to utilize online monitoring of the RQ to gain deeper insights into the metabolic activity of a culture under microaerobic cultivation conditions. Based on the course of the RQ, different metabolic phases during the cultivation were identified. Combined with partial reaction stoichiometries, the predominant metabolic activities in these phases were revealed. Additionally, the average RQs in the 2,3-butanediol production phase of 19 individual cultivations at varied OTR_{max} reflect the organism's metabolic adaption to varied oxygen availability. The combination of online RQ monitoring with stoichiometric considerations is generally applicable to other microorganism and products. Thus, the presented approaches increase the potential of online process monitoring and characterization tools for microaerobic cultivations.

Chapter 5

Redox potential measurement as online dissolved oxygen monitoring tool for microaerobic cultivations

5.1 Introduction

In a reduction-oxidation (redox) reaction, electrons are transferred from one compound to another. One compound (*Ox*) transfers *n* electrons (e^-) to the other compound (*Red*) as shown in Equation 5-1.

$$Ox + n \cdot \mathrm{e}^- \rightleftarrows Red \tag{5-1}$$

With the help of the Nernst Equation (Equation 5-2), the redox potential E_h can be calculated for any redox reaction (Kjaergaard, 1977).

$$E_h = E^0 + \frac{RT}{nF} \cdot ln \frac{activity\ of\ Ox}{activity\ of\ Red} \tag{5-2}$$

In this equation, E^0 is the standard potential referred to the normal hydrogen electrode. *R* and *F* are the gas and Faraday constants, respectively and *T* is the absolute temperature.

The redox potential, also called oxidation-reduction potential (ORP), or reduction potential describes the affinity of a redox pair to electrons. Thereby, high (positive) redox potentials

indicate high electron affinity and vice versa. The redox potential can be calculated easily for simple reactions as shown in Equation 5-1 and 5-2. In contrast, precise calculations in biological systems are problematic due to the large number of (often unknown) involved redox reactions (Kjaergaard, 1977). However, measurement of the redox potential in biological systems provides valuable information about the metabolic activity. In general two principles of redox potential measurement in biological systems can be distinguished, measurement of intracellular or extracellular redox potential (Liu et al., 2013).

The intracellular redox potential can be measured optically, using fluorescent sensor proteins (Gutscher et al., 2008; Hung et al., 2011; Schwarzländer et al., 2016) or Raman spectroscopy-based nanosensors (Auchinvole et al., 2012). Measurement of the redox potential in the individual organelles of a cell provides valuable insights on the cellular activity and viability. Consequently, measurement and manipulation of the intracellular redox potential are promising approaches in the development of medical therapies and strain engineering (Auchinvole et al., 2012; Liu et al., 2013). The intracellular redox potential is highly regulated and dysregulation is associated with several cardiovascular and neurodegenerative diseases and cancer (Dewhirst et al., 2008; Wright et al., 2010). Furthermore, the intracellular redox potential is crucially involved in inflammation, apoptosis, toxicity, protein interactions, signaling, cell cycle and differentiation (D'Autreaux and Toledano, 2007; Liu et al., 2009; Menon and Goswami, 2007; Paulsen and Carroll, 2010; Rybicka et al., 2010). The intracellular redox potential can be manipulated to redirect the electron flow in the cell and alter metabolic pathways (Liu et al., 2013). Following this strategy, genetic engineering approaches have been used to improve the production of butanol (Shen et al., 2011) or lactic acid (Liu et al., 2011).

Theoretically, there are two principles for the measurement of the extracellular redox potential. Measurement via electrochemical redox probes or via redox dyes (Kjaergaard, 1977). However, measurement via redox dyes is only semi quantitative and the dyes may be inhibitory or toxic for the cells (Hill, 1973). Consequently, the extracellular redox potential is usually measured with electrochemical redox probes during a cultivation. The extracellular redox potential influences the intracellular redox potential via electrons or substances that cross the cell membrane (de Graef et al., 1999; Liu et al., 2013). Therefore, the extracellular redox potential can be altered to manipulate the intracellular redox potential. By addition of reducing agents, the production of reduced compounds like 2,3-butanediol (Dai et al., 2014) or 1,3-propanediol

(Zhang et al., 2005) and even oxidized compounds like succinate (Park and Zeikus, 1999) can be improved. Additionally, application of electrical current in bioelectrical reactors resulted in increased succinate (Park and Zeikus, 1999) and ethanol (Jeon and Park, 2010) production.

This chapter focuses on the measurement of the extracellular redox potential. Therefore, unless specified otherwise, the term redox potential will be used to refer to the extracellular redox potential from here on. The temperature influences the redox potential of each redox pair (cf. Equation 5-2). However, as cultivations are usually performed at a constant temperature, the redox potential is not influenced by temperature changes. In temperature controlled aerobic cultivations, the observed changes of the redox potential ΔE_h result from the influences of changing chemical composition of the medium (ΔE_{medium}), the dissolved oxygen tension (ΔE_{DOT}) and the pH (ΔE_{pH}) on the redox potential (Ishizaki et al., 1974; Kjaergaard, 1977) as expressed in Equation 5-3.

$$\Delta E_h = \Delta E_{medium} + \Delta E_{DOT} + \Delta E_{pH} \tag{5-3}$$

Depending on the cultivation conditions, different conclusions can be drawn from redox potential measurements. During anaerobic or DOT-controlled cultivations, ΔE_{DOT} is zero. The same applies for ΔE_{pH} at pH-controlled conditions. Therefore, in pH controlled cultivations, the redox potential provides direct information about changing medium composition under anaerobic (Liu et al., 2013) or DOT-controlled (Ishizaki et al., 1974) conditions.

The redox potential is often measured to determine low DOTs in pH-controlled cultivations. In this case, the redox potential is influenced by DOT and medium composition changes (Equation 5-3). The major redox pairs involved in biological systems have standard redox potentials between H^+/H (-420 mV) and O_2/H_2O (+820 mV) (Liu et al., 2013). Therefore, oxygen is the prior acceptor for transferred electrons. Consequently, oxygen has a stronger effect on the redox potential than other involved metabolites even at low DOTs (Pham et al., 2008). The influence of changing DOT on the redox potential (ΔE_{DOT}) is expressed by the Nernst Equation as function of the oxygen activity a_{O2} (Equation 5-4) (Ishizaki et al., 1974; Kjaergaard, 1977). This shows that the redox potential decreases with decreasing DOT.

However, the amount of the redox potential change depends on the total amount of transferred electrons (*n*) and the amount of oxygen that serves as electron acceptor (*j*).

$$\Delta E_{DOT} = \frac{2.3jRT}{nF} \cdot \Delta\log\left(a_{O_2}\right) \tag{5-4}$$

Kjaergaard (1977) calculated a redox potential decrease of 14.8 mV upon reduction of the DOT by a factor of 10. This is in good agreement with measured values (15 mV) in phosphate buffer (Ishizaki et al., 1974). However, during cultivations of *Bacillus subtilis* (40 mV) (Shibai et al., 1974) *Brevibacterium lactofermentum* (40 mV) (Akashi et al., 1978) *Bacillus megaterium* (100 mV) (Ishizaki et al., 1974) and *Brevibacterium flavum* (115 mV) (Ishizaki et al., 1974) different correlations between redox potential and logarithmic DOT were observed. This deviation highlights the difficulties to calculate the redox potential in biological systems. The difference between the calculated and measured values are most likely attributed to the different medium compositions that change the ratio of transferred electrons and oxygen as electron acceptor in Equation 5-4. Nevertheless, redox potential measurements to monitor traces of oxygen in microaerobic cultivations were successfully applied to enhance the formation of numerous products. Amongst others, this includes leucine production with *Brevibacterium lactofermentum* (Akashi et al., 1978), xylitol production with *Candida tropicalis* (Kastner et al., 2003) or *Candida parapsilosis* (Oh et al., 1997), acetic acid production with *Bacillus licheniformis* (Kjaergaard, 1976), ethanol production with *Saccharomyces cerevisiae* (Liu et al., 2016) and xylanase, amylase and protease production with *Bacillus amyloliquefaciens* (Memmert and Wandrey, 1987).

In this chapter, redox potential measurements are used to investigate 2,3-butanediol production with *Bacillus licheniformis* DSM 8785 in microaerobic cultivations with uncontrolled pH. Therefore, the redox potential is not only affected by DOT and medium changes, but also by pH changes (Equation 5-3). Similar to the influence of the DOT, the influence of the pH on the redox potential ΔE_{pH} can be expressed by the Nernst Equation (Ishizaki et al., 1974; Kjaergaard, 1977) depending on the amount of transferred protons (*m*) and electrons (*n*) (Equation 5-5).

$$\Delta E_{pH} = -\frac{2.3mRT}{nF} \cdot \Delta pH \tag{5-5}$$

To quantify the influences of DOT and pH on the redox potential, abiotic experiments were performed. The results were then used to calculate the DOT during the cultivation of *B. licheniformis*. Parts of the results presented in this chapter have been obtained in collaboration with Hannah Tulke (master's thesis), Damarice Wandji (master's thesis) and Katja Rohr (research internship).

5.2 Redox potential measurement during cultivations of *Bacillus licheniformis* DSM 8785

To investigate the feasibility of redox potential measurements as online monitoring tool during microaerobic cultivations, a stirred tank reactor cultivation of *B. licheniformis* is shown in Figure 5-1. The two-stage cultivation profile explained in Section 3.2 was not applied here. Nevertheless, the courses of oxygen transfer rate (OTR) and respiratory quotient (RQ) (Figure 5-1A) follow the same trends as described before (cf. Section 3.2 and 4.2). The sudden increase of the OTR and the corresponding response of the RQ after 18 h result from an adjustment of the agitation rate as specified in the figure caption. The peak in the OTR after 96 h probably results from an elevated gas liquid mass transfer due to foam formation upon cell lysis. Also the courses of offline measured glucose and 2,3-butanediol concentrations, as well as the final 2,3-butanediol concentration of 80 g/L (Figure 5-1C) are in good agreement with the previously discussed shake flask results at the same maximum oxygen transfer capacity (OTR_{max}; cf. Figure 3-6). The online monitored courses of pH, DOT and the redox potential are shown in Figure 5-1B. As the cultivation was performed without pH control, the previously observed course of the pH is visible (cf. Figure 3-1 and Figure 4-4). During the first hours of cultivation, the pH decreases to 5.5 followed by a fluctuating increase to values around 6.5 until the end of the cultivation. The DOT decreases from 100 to 0% within the first 2 h and stays at this level. The redox potential follows the decreasing DOT, however, the minimum of -200 mV is reached after 7 instead of 2 h. In the following course of the cultivation, the redox potential increases slowly. Similar to the increase of the pH, there is no constant, but a fluctuating increase. However, a thorough comparison of the courses of pH and redox potential reveals a reversed trend between the two signals. During phases of slightly decreasing pH values (e.g. after 48 and

90 h) the redox potential increases. When the pH increases (e.g. after 72 h), a nearly constant redox potential is observed. As already described in the literature (Ishizaki et al., 1974; Kjaergaard, 1977), this demonstrates that the redox potential is not only affected by the DOT, but also by the pH (Equation 5-3).

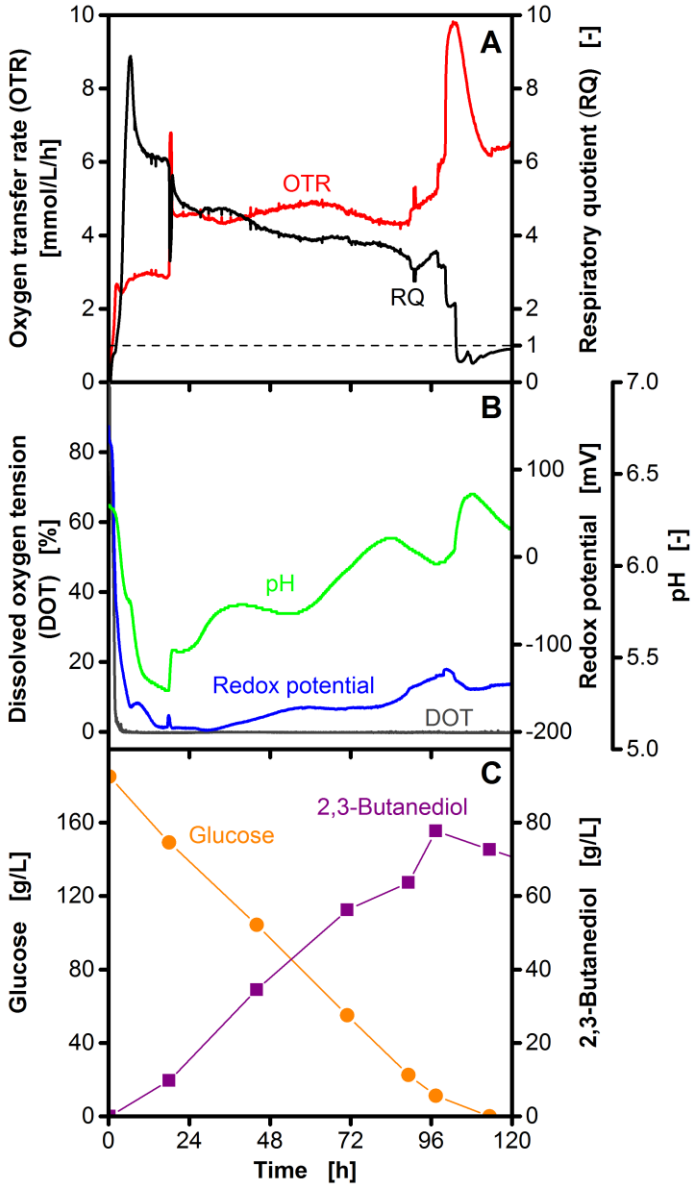

Figure 5-1: Redox potential measurement during a cultivation of *Bacillus licheniformis* DSM 8785 at uncontrolled pH. The courses of oxygen transfer rate (OTR) and respiratory quotient (RQ) (A), dissolved oxygen tension (DOT), pH and redox potential (B), as well as glucose and total 2,3-butanediol concentrations (C) are shown. 2,3-Butanediol is shown as sum of the stereoisomers. At the beginning of the cultivation, an agitation rate of 400 rpm was applied. At 18 h, the agitation rate was shortly adjusted to 500 rpm for 0.5 h and then reduced to 450 rpm for the rest of the cultivation. Cultivation conditions: Temperature: 37 °C, 2 L stirred tank reactor, filling volume: 1.5 L, aeration rate: 0.5 L/min (0.33 vvm), Nakashimada medium without MES buffer addition.

To exclude the influence of changing pH values on the course of the redox potential, cultivations with pH control were conducted (Figure 5-2). To investigate the influence of pH control on the cultivation, two different pH set points were chosen. Both cultivations were controlled at low pH values, as acidification of the culture broth triggers 2,3-butanediol production (Ji et al., 2011). Raspoet et al. (1991) conducted pH controlled cultivations with *B. licheniformis* and observed the best 2,3-butanediol production at the lowest tested pH of 6. Therefore, two cultivations with different pH set points of 6 and 5.5 were investigated (Figure 5-2**)**. The pH set-point of 5.5 (Figure 5-2A-C) is the minimum observed value in the cultivation without pH control (Figure 5-1) and was found to be close to the minimum tolerable pH of the organism (cf. Figure 3-1). To promote biomass formation, the cultivation was started at a pH of 6.5. The pH control was activated as soon as the set point was reached by the organism's natural acidification of the culture broth.

The OTR reaches values around 5 mmol/L/h after 3 h (Figure 5-2A). However, in contrast to the cultivation without pH control (Figure 5-1A), the OTR does not stay constant, but oscillates between 4 and 7 mmol/L/h until the end of the cultivation. This oscillation might be caused by switching metabolic activity as the mixed acid-2,3-butanediol fermentation is amongst others regulated by the course of the pH (Ji et al., 2011). Therefore, a forced constant pH might interfere with this regulation. A comparable behavior of *B. licheniformis* has been observed in pH controlled fed-batch cultivations in the literature (Giesecke et al., 1991; Mao et al., 1992). Even though the authors did not show OTR data, the agitation rate fluctuates during phases of controlled and constant DOT. This indicates similar switching metabolic activity as observed from the oscillating OTR at constant agitation in Figure 5-1A. Furthermore, the course of the RQ shows an oscillating trend that can probably be attributed to the same effects. Consequently, local minima of the OTR correspond with local maxima of the RQ and vice versa. During the first 70 h of cultivation, the RQ decreases to 1.5, followed by a steep increase to 6. After 115 h the typical steep decrease to values below 1 occurs indicating complete glucose consumption.

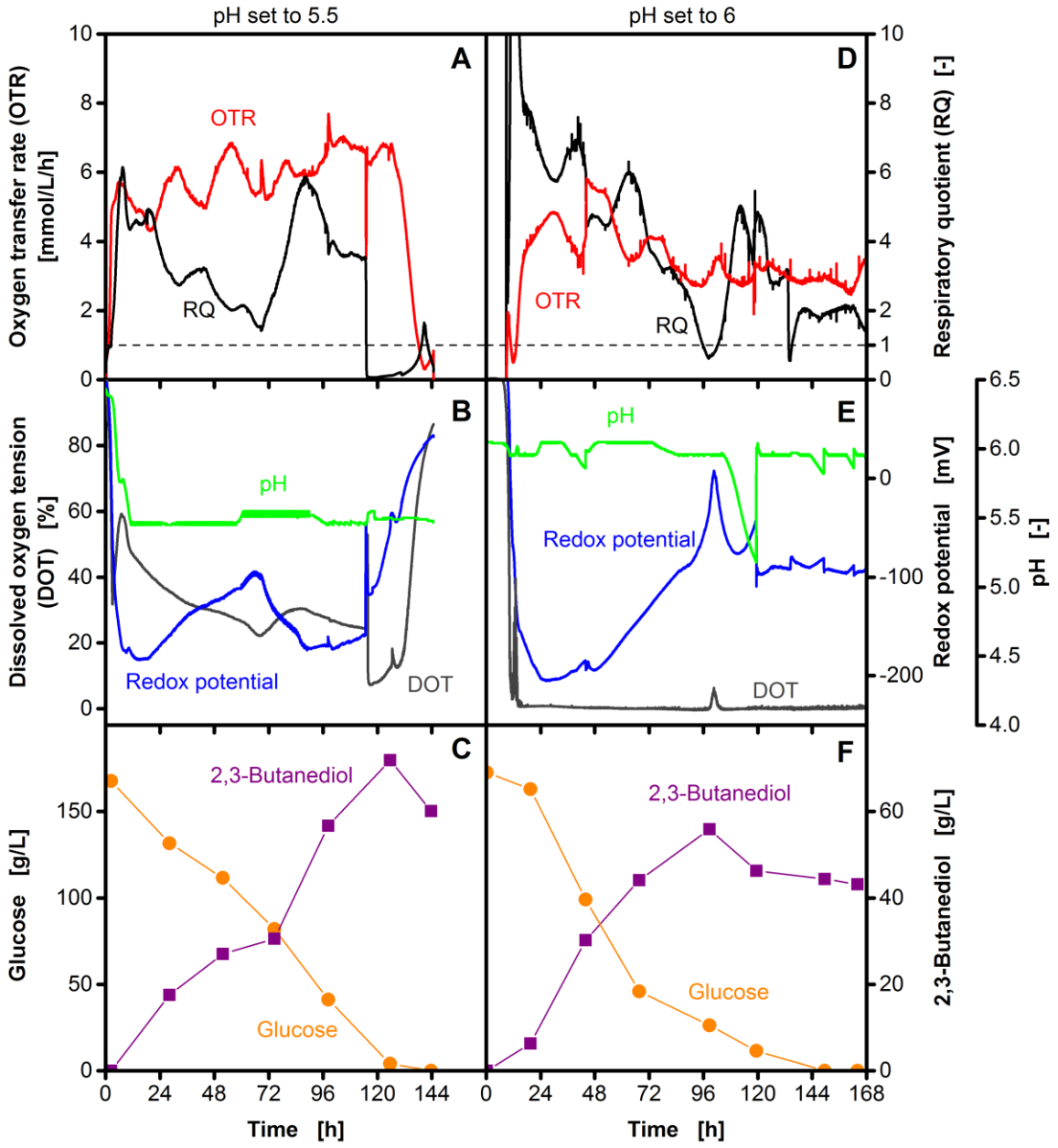

Figure 5-2: Redox potential measurement during pH controlled cultivations of *Bacillus licheniformis* DSM 8785. Two cultivations with different pH set points of 5.5 (A-C) and 6 (D-F) are compared. The courses of oxygen transfer rate (OTR) and respiratory quotient (RQ) (A, D), dissolved oxygen tension (DOT), pH and redox potential (B, E), as well as glucose and total 2,3-butanediol concentrations (C, F) are shown. 2,3-Butanediol is shown as sum of the stereoisomers. In the cultivation with a pH set point of 5.5, pH control was started as soon as the set point was reached by natural acidification of the organism. In the cultivation with a pH set point of 6, pH control was started at the beginning of the cultivation. Due to a leakage in the tubing, no pH control was active between 105 and 120 h (decreased pH in E). Cultivation conditions: Temperature: 37 °C, 2 L stirred tank reactor, filling volume: 1.5 L, aeration rate: 0.5 L/min (0.33 vvm), agitation rate: 450 rpm, Nakashimada medium without MES buffer addition.

As the same agitation rate was chosen as in the experiment without pH control (Figure 5-1), oxygen-limited conditions were expected. However, the DOT does not fall below 20% as long as glucose is present (Figure 5-2B). Interestingly, the DOT follows a similar trend as the RQ with a minimum after 70 h. Gassing with nitrogen after the cultivation confirmed that the DOT probe worked properly as it reached 0% (not shown here). Remarkably, more than 70 g/L 2,3-butanediol were produced (Figure 5-2C), which usually requires oxygen-limited conditions (Ji et al., 2011). The pH set point of 5.5 was reached after 5 h due to acidification of the organism and afterwards the pH was controlled (Figure 5-2B). Between 5 and 60 h the pH was controlled at the lower boundary of the set point range (± 0.05 pH units), indicating that acidification was prevented. Between 60 and 90 h, this changed to the upper boundary as an increase of the pH was prevented. In contrast, increasing pH values were observed from 24 h onwards in the cultivation without pH control (Figure 5-1**)**.

In the second pH-controlled cultivation, the pH was set to 6 to provide milder conditions (Figure 5-2D-F). The pH control was activated at the beginning of the cultivation, resulting in a prolonged lag phase of 8 h. OTR and RQ (Figure 5-2D) show comparable trends to the cultivation with a pH set point of 5.5 (Figure 5-2A). Both values oscillate and after 96 h, the RQ decreases below 1 even though glucose is not depleted. At this point also a peak in the DOT is visible (Figure 5-2E). However, in contrast to the cultivation controlled at a pH of 5.5, the DOT stays at 0% during the rest of the cultivation. At around 100 h, the pH shortly decreases to nearly 5, as a leakage in the pumping tubes occurred (Figure 5-2E). Even though this did not negatively affect the glucose consumption rate, the 2,3-butanediol concentration decreased from that time on. Interestingly, the glucose consumption rate was not constant during this cultivation. At around 72 h, the glucose consumption rate decreased. At this point, the pH control still worked properly. This effect has not been observed in any other cultivation.

The cultivations with pH regulation have been performed to analyze the redox potential without the influence of pH effects. In both cultivations, the redox potential decreased at the beginning of the cultivation together with the DOT (Figure 5-2B and E). Afterwards, a steady increase was observed resulting in a maximum at the same time, when the RQ reached its minimum. At this time, also the DOT increased in the cultivation controlled at a pH of 6 (Figure 5-2E**)**. After the described maximum, the redox potential decreased in both cultivations as the RQ increased again. In the cultivation controlled at a pH of 6, the previously observed and expected positive

correlation between redox potential and DOT was visible (Figure 5-2E**)**. However, in the cultivation controlled at pH 5.5, the redox potential shows the inverse behavior compared to the DOT.

The results presented in Figure 5-2 demonstrate that cultivation of *Bacillus licheniformis* DSM 8785 at controlled pH has several disadvantages. Instead of improved process monitoring from an easily interpretable redox potential, the information content gained from online monitoring is reduced. Several phenomena like the oscillating trends of OTR and RQ do not follow the trends of uncontrolled cultivations that were investigated in detail in Chapter 3 and 4 and are well understood. Therefore, the metabolic activity can no longer be monitored precisely. Furthermore, pH control leads to increased cultivation times and consequently reduced space-time yields. Consequently, pH controlled cultivations are not applicable for 2,3-butanediol production with *Bacillus licheniformis* DSM 8785.

5.3 Characterization of the redox potential in abiotic experiments

To investigate the applicability of redox potential measurements for process monitoring in cultivations without pH control, the influence of pH and DOT on the redox potential were investigated. To minimize any influencing factors related to microbial activity and the resulting changes of the medium composition, these investigations were performed in abiotic experiments. Figure 5-3 shows redox potential, pH and DOT measurements in the sterile cultivation medium. Gassing with nitrogen and pressurized air was used to change the DOT. The pH was varied by addition of NaOH and H_2SO_4.

Low aeration and agitation rates were chosen to obtain a low gas liquid mass transfer and a slowly changing DOT (Figure 5-3A**)**. Thereby, multiple data points could be recorded during dynamically changing DOT levels to investigate the influence of the DOT on the redox potential. Starting from nitrogen-saturated conditions, aeration with pressurized air during the first 0.5 h, results in an increase of both, DOT and redox potential (Figure 5-3B**).** Titration of

the pH at a constant DOT between 0.5 and 1 h revealed a negative correlation between pH and DOT. When the reactor was gassed with nitrogen at a constant pH between 1.2 and 2.5 h, the redox potential constantly decreased, even when the DOT reached a constant level. The results presented in Figure 5-3 clearly demonstrate that dynamically changing conditions are not well suited to quantify the correlation between the redox potential and pH or DOT.

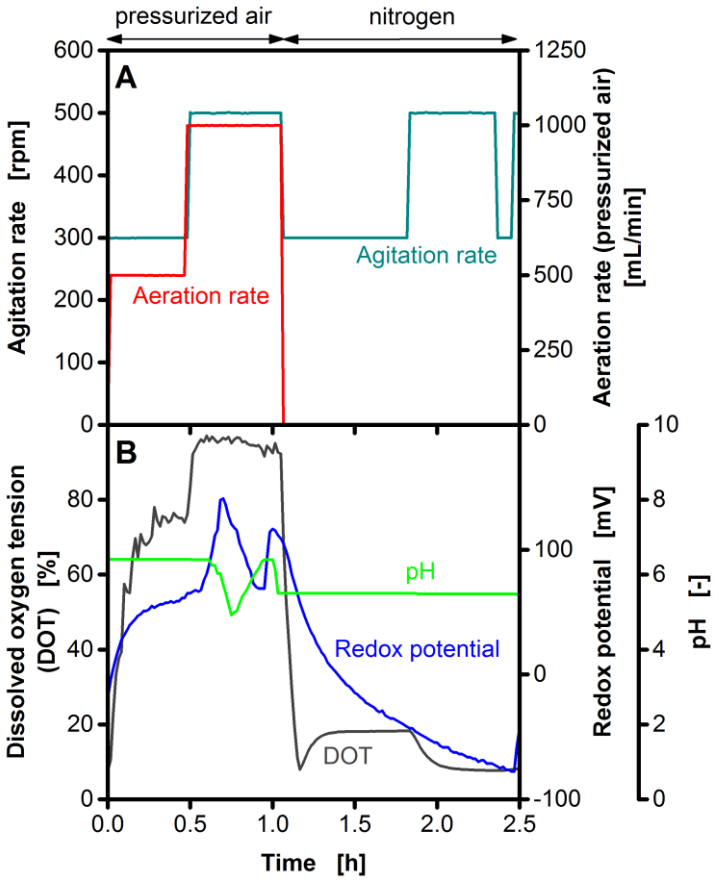

Figure 5-3: Abiotic redox potential measurement under dynamic conditions. To exclude any effects of microbial growth, sterile cultivation medium was used to investigate the redox potential. By changing the aeration and agitation rate (A) and switching between pressurized air and nitrogen gassing, the dissolved oxygen tension (DOT) was changed. Pressurized air was supplied via the control unit of the bioreactor and monitored online. Nitrogen was supplied directly to the stirred tank reactor and not monitored. Redox potential, DOT and pH were monitored online (B). The pH was adjusted by titration with H_2SO_4 and NaOH. Experimental setup: Temperature: 37 °C, 2 L stirred tank reactor, filling volume: 1.5 L, Nakashimada medium without MES buffer addition.

5.4 Correlation between pH and redox potential

To quantify the correlation between pH and redox potential, the pH was adjusted at a constant DOT in abiotic experiments. When steady state conditions were achieved, redox potential and pH values were recorded to set up the correlation. Figure 5-4 shows the response of the redox potential to changing pH values between 5 and 7.5 at constant nitrogen gassing resulting in a DOT of 0%. Thereby, the whole pH range that occurs during pH-uncontrolled cultivations of *B. licheniformis* is covered (cf. Figure 5-1). As observed before, the redox potential decreases with increasing pH in a range from -100 to -300 mV. Steady state conditions were achieved within a few minutes after pH titration.

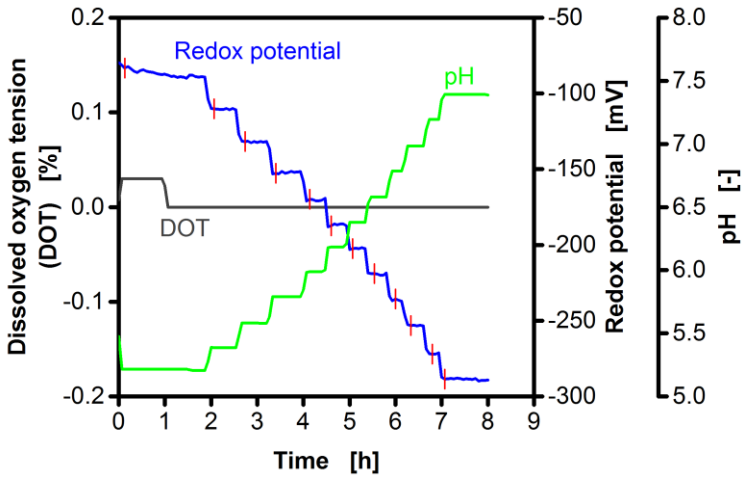

Figure 5-4: Influence of the pH on the redox potential. To exclude any effects of microbial growth, sterile cultivation medium was used to investigate the redox potential. The reactor was constantly gassed with nitrogen and the pH was adjusted by NaOH titration. Data pairs of pH and redox potential were determined as indicated by the red marks and used to set up the correlation presented in Figure 5-5. Experimental setup: Temperature: 37 °C, 2 L stirred tank reactor, filling volume: 1.5 L, Nakashimada medium without MES buffer addition.

From similar experiments, the correlation between redox potential and pH at different constant DOT levels was derived (Figure 5-5A**)**. The absolute values of the redox potential vary greatly due to the different DOT levels (Appendix 6). As the absolute redox potential is influenced by a variety of different factors, the shift of the redox potential due to pH changes is more interesting than the absolute value. To clearly visualize the changes caused by the pH, the redox potential shift is shown in Figure 5-5A. To calculate this shift, the redox potential at a pH of 5 was subtracted from each value measured at a different pH.

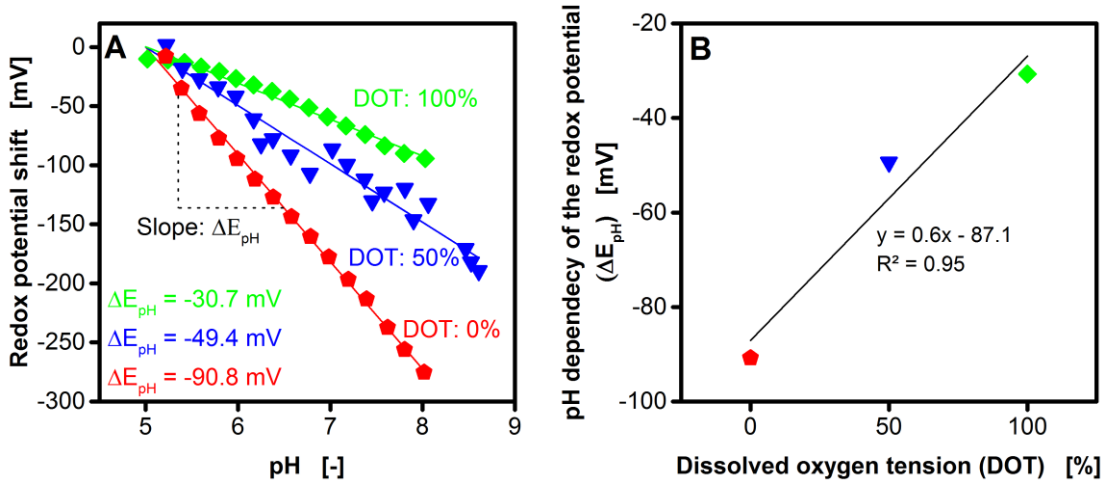

Figure 5-5: Correlation between pH and redox potential. Correlations between pH and redox potential shift (A) were derived from three abiotic experiments similar to the one shown in Figure 5-4. The redox potential was shifted by subtracting the redox potential at a pH of 5 from each data point. The pH dependency of the redox potential (ΔE_{pH}) shown in (B) is defined as the slope of the linear correlation between redox potential and pH in (A). Data points in (B) represent the slope of the linear correlation of the respective dataset in (A) measured at the constant dissolved oxygen tension (DOT) that is shown on the abscissa. The coefficients of determination for the correlations (R^2) in (A) were 0.99, 0.95 and 0.98 in order of increasing DOT. Experimental setup: Temperature: 37 °C, 2 L stirred tank reactor, filling volume: 1.5 L, Nakashimada medium without MES buffer addition.

A linear dependency between redox potential and pH is observed for all DOT levels. In addition to the shown DOT levels, experiments were conducted to determine the correlation between redox potential and pH at DOTs below 5%. However, in this range, the DOT could not be adjusted to a constant level (Appendix 7). Due to the constantly changing DOT, these experiments could not be evaluated, as the redox potential was influenced by two changing factors.

The pH dependency of the redox potential (ΔE_{pH}; the slope of the linear correlation between redox potential shift and pH) changes from -31 mV at a DOT of 100% to -50 and -91 mV at DOT levels of 50 and 0%, respectively (Figure 5-5A**)**. ΔE_{pH} is plotted in Figure 5-5B as function of the DOT. The data points correspond to the respective slopes of the linear correlations shown in Figure 5-5A and reveal a linear correlation to the DOT themselves. This shows that ΔE_{pH} changes at different DOT levels.

The observed negative correlation between redox potential and pH is also predicted by Equation 5-5. The dependency of ΔE_{pH} from the DOT might be attributed to decreasing amounts

of transferred electrons (*n* in Equation 5-5), when less oxygen is available as electron acceptor. Ishizaki et al. (1974) determined a correlation between redox potential and pH of -33 mV during a cultivation of *Bacillus megaterium*. The exact DOT is not mentioned, but the DOT was kept constant at non-limiting conditions. Therefore, the correlation between redox potential and pH is at least in the same order of magnitude as observed in this chapter.

5.5 Correlation between dissolved oxygen tension and redox potential

To investigate the influence of the DOT on the redox potential, abiotic experiments at constant pH values were performed in the cultivation medium. Defined DOTs were adjusted by gassing with mixtures of pressurized air and nitrogen. When the gas composition was changed, the DOT changed rapidly and a constant DOT level was achieved within minutes. In contrast, the redox potential did not reach constant values even when the DOT remained constant for several hours. Data of two exemplary experiments are shown in Figure 5-6 to demonstrate typical problems that occurred during these measurements. In the experiment shown in Figure 5-6A, the redox potential decreased constantly, even when the DOT stayed constant for 70 h. Additionally, also oscillating courses of the redox potential were observed (Figure 5-6B), resulting in a repeated 24 h cycle of increasing and decreasing redox potential. To exclude medium specific reasons for the observed phenomena, comparable experiments were conducted in pure phosphate buffer, revealing similar effects (Appendix 8) as in the cultivation medium. In addition, temperature related effects can be excluded, as the experiments were performed at controlled temperature in a stirred tank reactor. Interestingly, these phenomena only occurred in abiotic experiments and not during cultivations of *B. licheniformis*. A substantial difference between biotic and abiotic experiments is the addition of nitrogen in the gas mixture during abiotic experiments. In Figure 5-6B, the high peaks on the redox potential only occured during gassing with a mixture of nitrogen and pressurized air. However, also during gassing with pure pressurized air during the first 30 h an oscillating signal was observed. In the experiments to investigate the influence of the pH on the redox potential (Figure 5-5**)** the above described problems were not observed. This might be explained by the different experiment length of

several hours for the pH experiments compared to several days for the DOT experiments (cf. Figure 5-4**,** Figure 5-6).

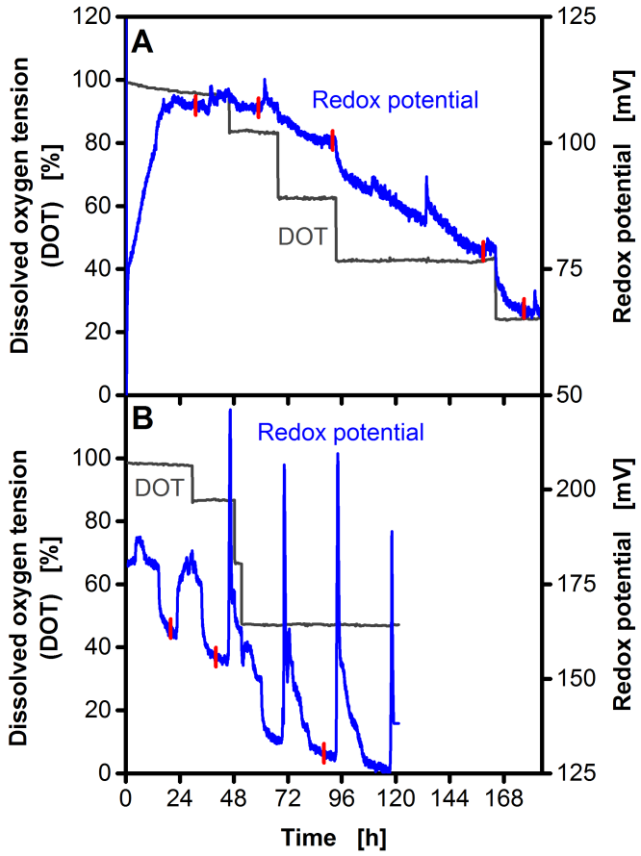

Figure 5-6: Influence of the dissolved oxygen tension on the redox potential. To exclude any effects of microbial growth, sterile cultivation medium was used to investigate the redox potential. The pH was kept at constant levels (7.5 in (A) and 5.5 in (B)) and the dissolved oxygen tension (DOT) was adjusted by gassing with mixtures of pressurized air and nitrogen. The figure shows exemplary data sets that highlight two observed obstacles for the data acquisition to investigate the correlation between redox potential and DOT. The redox potential either decreased at constant DOTs (A) or oscillated in 24 h cycles (B). Data pairs of DOT and redox potential were determined as indicated by the red marks and used to set up the correlation presented in Figure 5-7. Experimental setup: Temperature: 37 °C, 2 L stirred tank reactor, filling volume: 1.5 L, Nakashimada medium without MES buffer addition.

Even though the problems described above could neither be explained nor solved, corresponding redox potentials to each DOT level were determined as best as possible (highlighted by the red marks in Figure 5-6). The resulting correlation between redox potential and DOT is shown in Figure 5-7. Figure 5-7A combines data from six experiments at three different pH values as indicated in the figure legend. No significant difference could be observed amongst the experiments conducted at different pH values. With increasing DOT, the

redox potential increases, resulting in a linear correlation between the logarithmic DOT and the redox potential with a slope of ΔE_{DOT} = 79 mV.

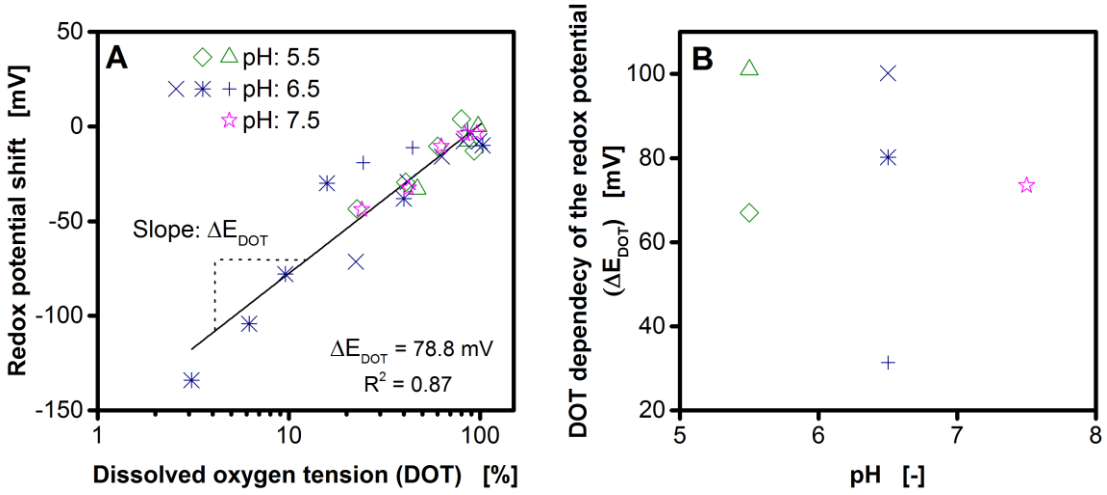

Figure 5-7: Correlation between dissolved oxygen tension and redox potential. A correlation between dissolved oxygen tension (DOT) and redox potential shift (A) was derived from six abiotic experiments similar to the one shown in Figure 5-6. The redox potential was shifted by subtracting the redox potential at a DOT of 100% from each data point. The DOT dependency of the redox potential (ΔE_{DOT}) shown in (B) is defined as the slope of the linear correlation between redox potential and logarithmic DOT in (A). Data points in (B) represent the slope of the linear correlation of the respective dataset in (A) measured at the constant pH that is shown on the abscissa. Experimental setup: Temperature: 37 °C, 2 L stirred tank reactor, filling volume: 1.5 L, Nakashimada medium without MES buffer addition.

For each of the six conducted experiments, the slope of the correlation between redox potential and the logarithmic DOT (ΔE_{DOT}) was calculated separately (Figure 5-7B). Even though there is a high variation between the resulting slopes, the pH does not seem to influence ΔE_{DOT}. The high variation between the observed slopes in the individual experiments probably results from the unsteady courses of the redox potential during data acquisition (cf. Figure 5-6) resulting in error prone data analysis. This is also reflected in the mediocre coefficient of determination (R^2 = 0.87) of the correlation between redox potential and logarithmic DOT in Figure 5-7A. Furthermore, it has to be noted that only three data points at DOT below 10% were considered for the correlation. Compared to all other data points, these data points at low DOT have a disproportionately high impact on the slope of the linear correlation. Moreover, these three data point were all taken from the same experiment. Due to the described experimental difficulties, this was not possible in the other experiments. Other authors determined ΔE_{DOT} during the cultivation and not in abiotic steady state conditions (Akashi et al., 1978; Ishizaki et al., 1974;

Shibai et al., 1974). In contrast, Schuldiner et al. (1966) designed a special gas tight reactor to investigate abiotic steady state redox potentials. Thereby, small amounts of oxygen leaking into the system were prevented. Nevertheless, the authors concluded that especially at low oxygen partial pressures long time periods (up to a month) are needed to obtain true steady state conditions.

Overall, the results shown in Figure 5-7 confirm that there is a linear correlation between redox potential and the logarithmic DOT as already described in the literature (Kjaergaard, 1977) (Equation 5-4). However, due to experimental difficulties during data acquisition, a considerable error on the slope of this correlation can be expected. Nevertheless, the obtained value for ΔE_{DOT} = 79 mV is in good agreement with literature values. During cultivation of different *Bacillus* and *Brevibacterium* strains ΔE_{DOT} values between 40 and 115 mV were observed in different cultivation media (Akashi et al., 1978; Ishizaki et al., 1974; Shibai et al., 1974).

5.6 Influence of media components on the redox potential

In the above-described abiotic experiments, changes of the culture medium that occur during the cultivation of microorganisms were not considered. Therefore, the influence of glucose and 2,3-butanediol concentration on the redox potential was investigated. During the cultivation of *B. licheniformis*, the glucose concentration decreases from 180 to 0 g/L, while 2,3-butanediol increases from 0 to 80 g/L. These are by far the strongest changes of the medium composition. Consequently, their influence on the redox potential helps to estimate the impact of changing medium composition on the redox potential.

Figure 5-8 shows an abiotic experiment with changing glucose and 2,3-butanediol concentrations in the cultivation medium. With increasing glucose concentration, the redox potential increases linearly with a slope of 0.06 mV/(g/L) (Figure 5-8A). In contrast, the redox potential decreases with increasing 2,3-butanediol concentration with a slope of -0.13 mV/(g/L) (Figure 5-8B) independent of the present glucose concentration. Consequently, during a

cultivation, consumption of 180 g/L glucose and production of 80 g/L 2,3-butanediol results in a decrease of the redox potential by 20 mV. Of course, this only gives a first impression of the impact of changing medium composition as no other products and substrates were considered. Especially, as a complex cultivation medium is used, changes in the undefined components like yeast extract and tryptone will affect the redox potential.

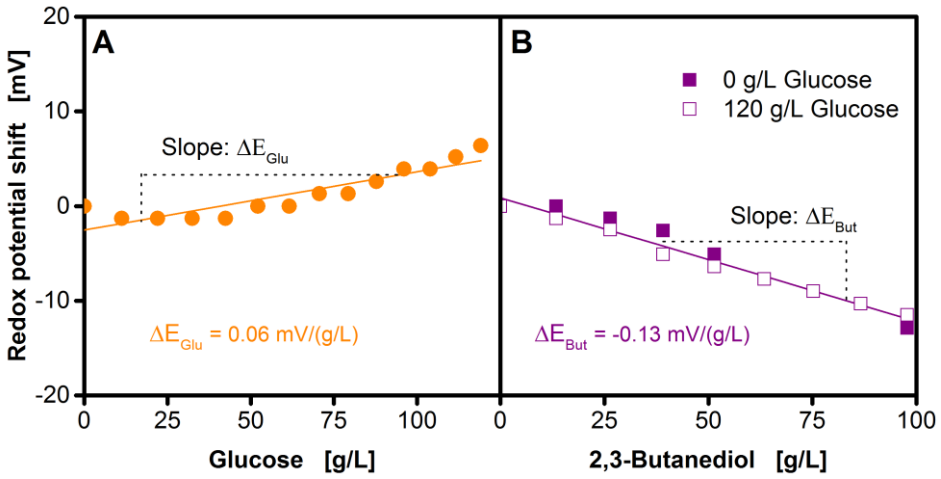

Figure 5-8: Influence of glucose and 2,3-butanediol concentration on the redox potential. Correlations between glucose and redox potential shift (A) and 2,3-butanediol and redox potential shift (B) are shown. The influence of 2,3-butanediol was tested in the presence and absence of glucose. The redox potential was shifted by subtracting the redox potential at a concentration of 0 g/L from each data point. The dependency of the redox potential (ΔE_{Glu} and ΔE_{But}) on both substances is defined as the slope of the linear correlation between redox potential and the concentration of the respective substance. Experimental setup: Sterile Nakashimada medium (without MES buffer addition) was mixed in a beaker glass with a magnetic stirrer at room temperature and glucose or 2,3-butanediol solutions were added gradually. Data pairs were recorded when the redox potential reached constant values. A negative control with water addition confirmed that the observed effects do not originate from the dilution of the cultivation medium (Appendix 9).

In Figure 5-9 the same data as in Figure 5-5, Figure 5-7 and Figure 5-8 are shown. However, in Figure 5-9 the dependency of the redox potential on pH, DOT, glucose and 2,3-butanediol is compared with the same scaling of the ordinate. This demonstrates that compared to the influence of DOT and pH on the redox potential, the observed effects of changing medium composition can be neglected. As oxygen is the primary electron acceptor in biological systems, the influence of media components on the redox potential will always be smaller when oxygen is available (Pham et al., 2008).

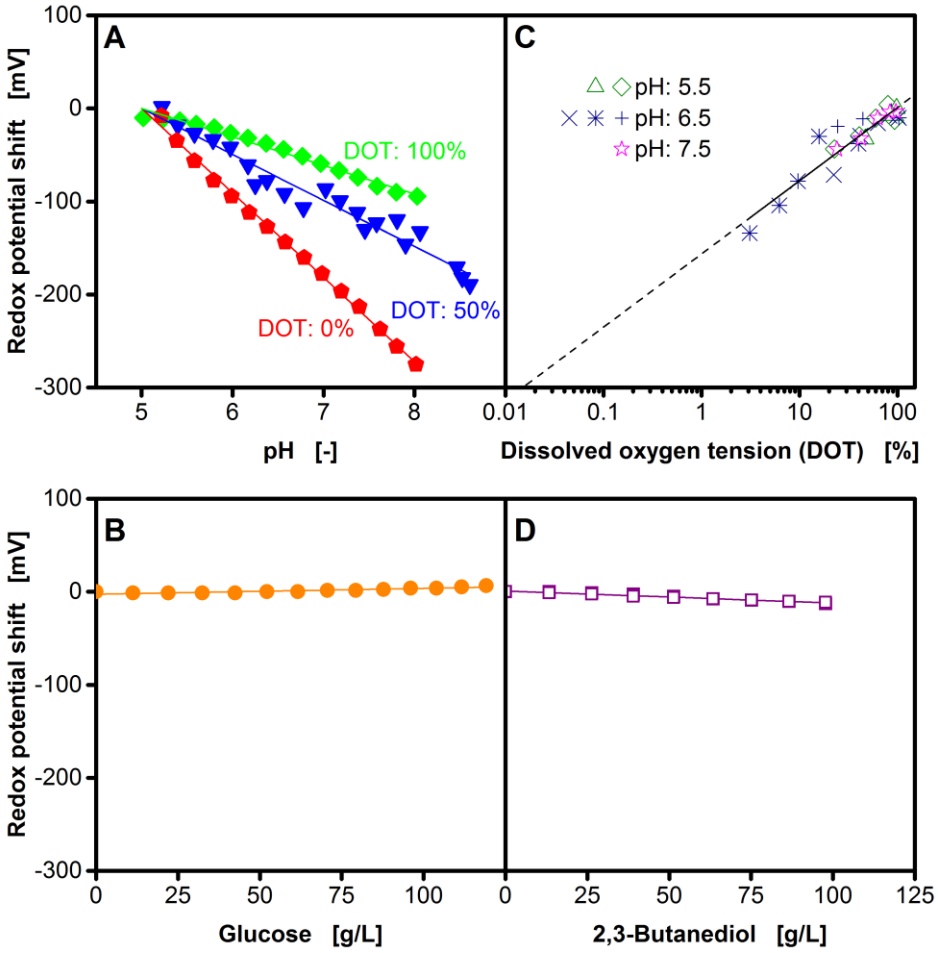

Figure 5-9: Comparison of different influences on the redox potential. The influence of pH (A), dissolved oxygen tension (DOT) (C), glucose (B) and 2,3-butanediol (D) on the redox potential is compared. The same data as in Figure 5-5, Figure 5-7 and Figure 5-8 are shown, but the ordinate showing the redox potential shift is scaled identically for easy comparison. The absolute measurement values of the redox potential are shown in Appendix 6. Solid lines represent linear correlations in the range of the measured data. The dashed line in (C) visualizes the approach to interpolate the correlation to determine low DOTs via redox potential measurements.

5.7 Calculation of the dissolved oxygen tension from redox potential measurements

Figure 5-9C shows the dependency of the redox potential on the logarithmic DOT and demonstrates the underlying approach of redox potential measurements to monitor low DOTs during a cultivation (Akashi et al., 1978). The correlation between redox potential and

logarithmic DOT is established at DOTs that can be measured with conventional DOT probes (solid line). Then this correlation is extrapolated to lower DOTs (dashed lines).

Figure 5-10 shows data from the cultivation of *B. licheniformis* without pH control that is also depicted in Figure 5-1**.** The measured DOT (Figure 5-10B) decreases to 0% at the beginning of the cultivation and stays at this level. As discussed above, the measured redox potential (Figure 5-10B) mainly depends on the DOT and the pH. Therefore, the online measured pH was used to correct the redox potential according to the correlations described in Figure 5-5 (the calculation is explained in detail in Section 2.8). The course of the resulting corrected redox potential (Figure 5-10C) shows the response of the redox potential to changing DOT independent of the pH. The corrected redox potential decreases to a minimum of -280 mV within the first 20 h of the cultivation. Afterwards the corrected redox potential increases steadily to -150 mV at the point of glucose depletion (when the RQ steeply decreases after 100 h). As the course of the redox potential is predominantly influenced by the DOT, this indicates an increasing DOT during the cultivation, which cannot be detected by the DOT probe.

The corrected redox potential was then used to calculate the DOT according to the correlation set up in Figure 5-7 (explained in detail in Section 2.8). The calculated DOT (Figure 5-10C) decreases to 0.00% within 20 h. Afterwards, the calculated DOT increases up to a maximum of 0.05% upon glucose depletion after 100 h. It has to be noted that the absolute values of the calculated DOT are not necessarily precise. Due to the linear correlation between redox potential and logarithmic DOT, high signal changes in the redox potential occur at low changes of the DOT. Nevertheless, due to the high degree of extrapolation, potential inaccuracies in the underlying linear equation can sum up to substantial inaccuracies in DOT quantification. Consequently, relative changes of the DOT can be monitored precisely via redox potential measurements. However, the exact quantification of the DOT will be error prone, especially regarding the discussed problems during data acquisition (cf. Figure 5-6). This leads to significant differences in the slopes of the linear correlation between redox potential and logarithmic DOT between six individual experiments as shown in Figure 5-7B. To assess the error range of DOT quantification via the redox potential, the slopes of the linear correlations derived from each of the six individual experiments (ΔE_{DOT}) were used to calculate the DOT during the cultivation (Appendix 10). With one exception, the absolute calculated DOT values

vary between 0.01 and 0.1% at the point of glucose depletion. The relative trend of slowly increasing DOT in the course of the cultivation is consistent in all calculations. Furthermore, the calculated increase of the DOT in the course of the cultivation matches the observations of the slowly decreasing RQ as discussed in Section 4.4.

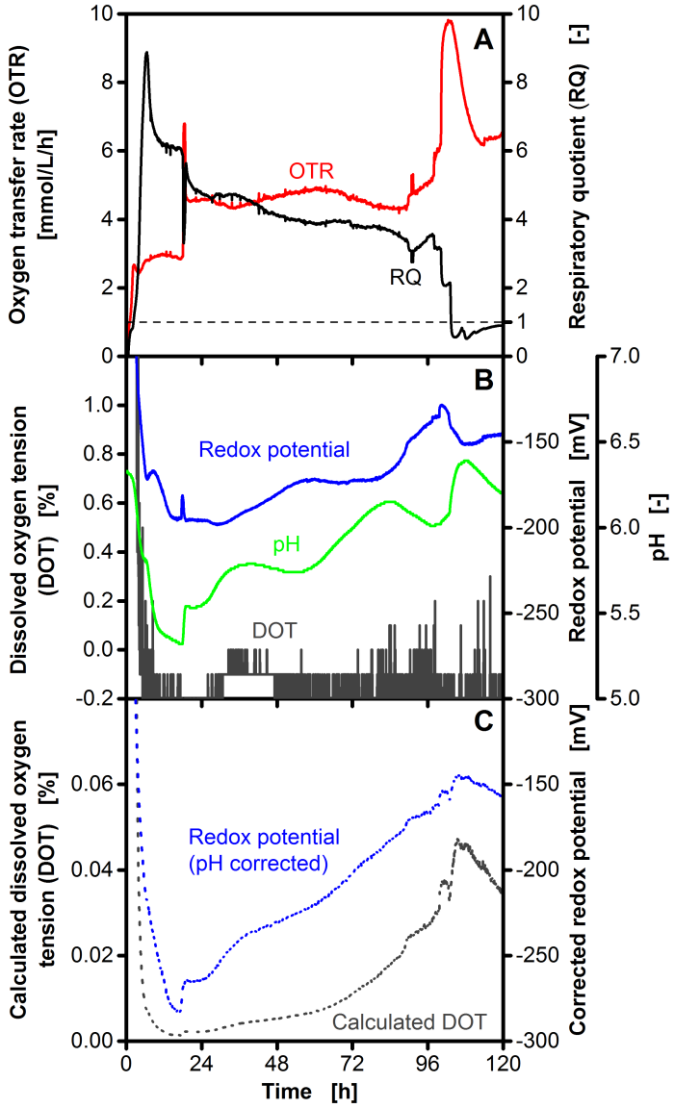

Figure 5-10: Calculation of the dissolved oxygen tension via redox potential measurement during the cultivation of *Bacillus licheniformis* DSM 8785. The courses of oxygen transfer rate (OTR) and respiratory quotient (RQ) (A), dissolved oxygen tension (DOT), pH and redox potential (B) are shown. Additionally, the measured redox potential was corrected by the influence of the pH based on the correlations set up in Figure 5-5 (C). From this corrected redox potential the DOT was calculated according to the correlation set up in Figure 5-7A (C). At the beginning of the cultivation, an agitation rate of 400 rpm was applied. At 18 h, the agitation rate was shortly adjusted to 500 rpm for 0.5 h and then reduced to 450 rpm for the rest of the cultivation. Cultivation conditions: Temperature: 37 °C, 2 L stirred tank reactor, filling volume: 1.5 L, aeration rate: 0.5 L/min (0.33 vvm), Nakashimada medium without MES buffer addition.

To validate the calculation of the DOT based on the redox potential, the agitation rate was slowly decreased during a cultivation of *B. licheniformis*. Thereby, the observed increase of the calculated DOT was counteracted by reduction of the maximum oxygen transfer capacity (OTR_{max}). Figure 5-11 shows two cultivations of *B. licheniformis* without pH control. A two-stage cultivation profile as explained in Section 3.2 was applied in both cultivations. In the reference cultivation, the agitation rate was kept constant at 500 rpm after the initial reduction at 4.5 h (Figure 5-11A). In contrast, the agitation rate was steadily decreased after 19 h in the other cultivation (Figure 5-11E). OTR, RQ (Figure 5-11B), pH and DOT (Figure 5-11C) of the reference cultivation show the same courses as observed before (Figure 3-7, Figure 5-1). As expected, the reduction of the agitation rate in the other cultivation resulted in a steadily decreasing OTR, as the OTR_{max} decreased (Figure 5-11F). This also resulted in an increase of the RQ, which is in good agreement with the trends observed in Figure 4-5. The sharp decrease of the RQ indicating glucose depletion (cf. Figure 3-3) is slightly delayed in the cultivation with decreased agitation rate. However, this delay is comparable to the variations observed between different experiments with the same cultivation conditions (cf. Figure 3-6). Furthermore, biomass formation and 2,3-butanediol yields are comparable between both cultivations (Appendix 11). In contrast, acetoin and glycerol yields reflect the reduced OTR_{max} with decreases agitation rate. However, as for the time of glucose depletion no significant variation can be proven.

While the redox potential stayed nearly constant in the reference cultivation (Figure 5-11C), it slightly decreased with the reduction of the shaking frequency (Figure 5-11G). Interestingly, the measured DOT in the cultivation with steady reduction of the shaking frequency decreases from 5 to 0% between 4 and 50 h. As the OTR indicates oxygen limitation during this time (Figure 5-11F), this might be attributed to an inaccurate calibration of the DOT probe.

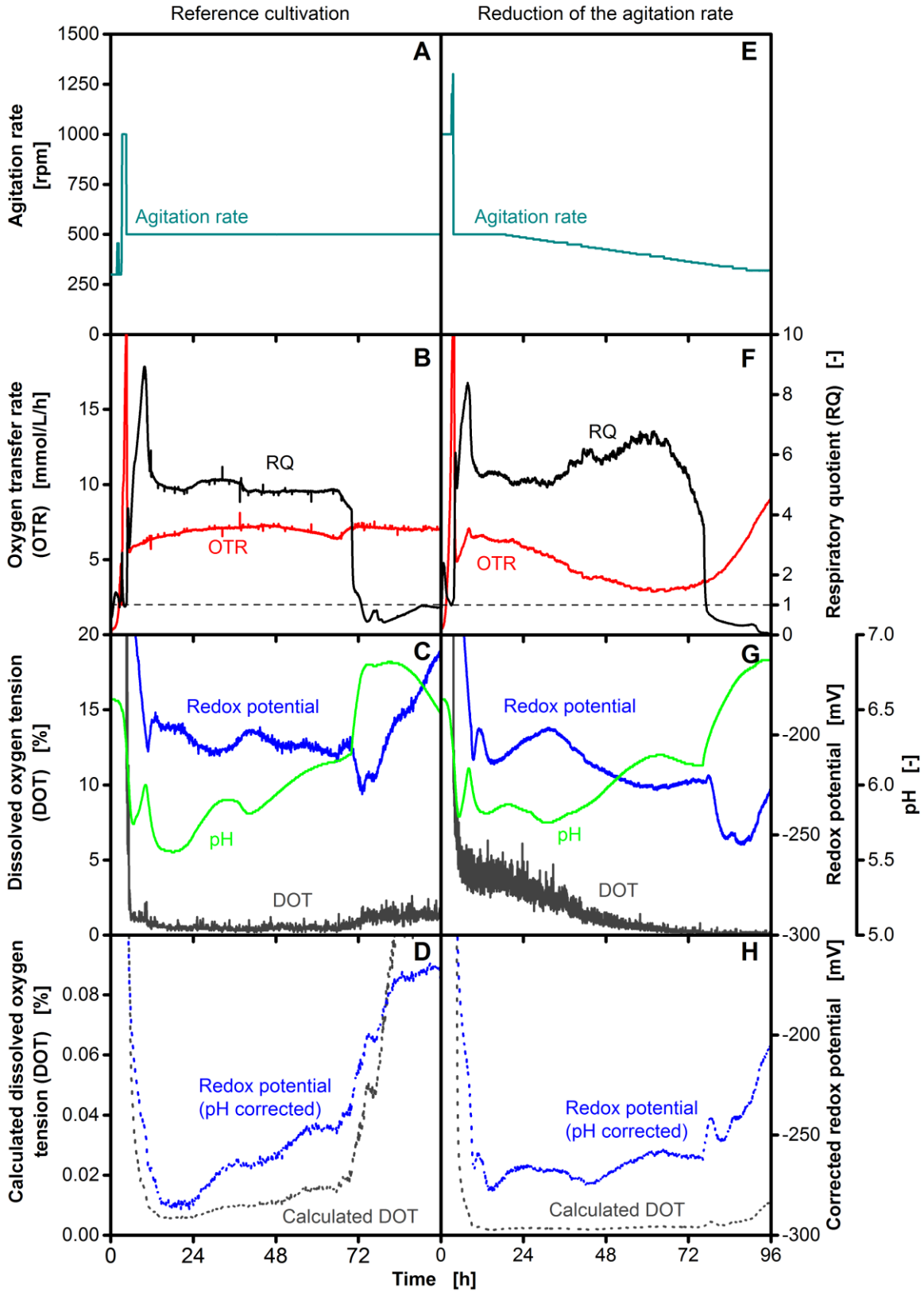

Figure 5-11: Reduction of the agitation rate during the cultivation of *Bacillus licheniformis* DSM 8785. A reference cultivation (A-D) and a cultivation with steadily decreased agitation rate (E-F). The courses of the agitation rate (A, E), oxygen transfer rate (OTR) and respiratory quotient (RQ) (B, F),

dissolved oxygen tension (DOT), pH and redox potential (C, G) are shown. Additionally, the measured redox potential was corrected by the influence of the pH based on the correlations set up in Figure 5-5 (D, H). From this corrected redox potential, the DOT was calculated according to the correlation set up in Figure 5-7A (D, H). At the beginning of the cultivation, oxygen unlimited growth conditions were assured using an agitation rate control (DOT≥30%) (A) or a manually adjusted high agitation rate (E). To induce oxygen-limited conditions the agitation rate was then reduced to 500 rpm. After 19 h the agitation rate was steadily decreased to counteract the increasing DOT in E. Cultivation conditions: Temperature: 37 °C, 2 L stirred tank reactor, filling volume: 1.5 L, aeration rate: 0.5 L/min (0.33 vvm), Nakashimada medium without MES buffer addition.

Similar to Figure 5-10C, the effect of the pH on the redox potential was corrected and the DOT was calculated from the corrected redox potential (Figure 5-11D and H). In the reference cultivation, the corrected redox potential and the calculated DOT increase during the course of the cultivation, as previously observed in Figure 5-10C. Moreover, the range of the calculated DOT is comparable in both experiments. This indicates that a relative comparison of calculated DOTs between experiments with a comparable setup is possible. In the experiment with steady reduction of the agitation rate, the corrected redox potential stays nearly constant until the RQ decreases due to glucose depletion (Figure 5-11H). Consequently, the calculated DOT also stays constant at 0.00%. This matches the expectations, as the reduction of the agitation rate results in a constantly decreasing OTR_{max} and consequently reduced oxygen supply. Therefore, an increase of the DOT during the cultivation is prevented. Overall, the results presented in Figure 5-11 show that the calculation of the DOT from the redox potential is a suitable approach to investigate small changes of the DOT during the cultivation that cannot be revealed with conventional DOT probes.

5.8 Conclusion

Microaerobic cultivation conditions are operated at DOT levels that cannot be measured with conventional DOT probes (Liu et al., 2013). Therefore, the redox potential was investigated in this chapter with the aim to monitor minor changes of the DOT close to 0%. Apart from the DOT, also the pH has a significant influence on the redox potential. The commonly described approach to eliminate pH effects on the redox potential is pH regulation during the cultivation (Akashi et al., 1978; Kastner et al., 2003; Kjaergaard, 1976; Memmert and Wandrey, 1987).

However, during the cultivation of *Bacillus licheniformis* DSM 8785, pH regulation results in decreased 2,3-butanediol production (cf. Figure 5-1 and Figure 5-2). Additionally, oscillating courses of OTR and RQ were observed. Therefore, pH control is not a suitable approach as it decreases both, the information content from online monitoring and product formation.

To utilize the redox potential during cultivations without pH control, the influence of pH, DOT and changing concentrations of glucose and 2,3-butanediol was investigated in abiotic experiments. In comparison to the strong effects of changing pH and DOT, the influence of glucose consumption and 2,3-butanediol production on the redox potential can be neglected (Figure 5-9). A linear correlation between pH and redox potential was observed at constant DOTs. However, the slope of this correlation changed depending on the DOT (Figure 5-5). Consequently, the influence of the pH on the redox potential also depends on the present DOT. Additionally, a linear correlation between redox potential and the logarithmic DOT was determined at constant pH values (Figure 5-7). However, experimental difficulties during data acquisition hindered the precise quantification of this correlation. Therefore, it could not be clarified with certainty if the correlation between redox potential and logarithmic DOT is pH dependent or not.

Based on the correlation between redox potential and pH, the measured redox potential during the cultivation was corrected to be independent of pH changes. Subsequently, the resulting corrected redox potential was used to calculate the DOT during the cultivation. This procedure revealed a steady increase of the calculated DOT even before glucose was depleted (Figure 5-10). The observed trend of the calculated DOT was validated in a cultivation experiment with steadily decreased OTR_{max}, resulting in a constant calculated DOT as response to the decreased oxygen supply (Figure 5-11).

The results presented in this chapter clearly demonstrate that online measurement of the redox potential can be used to monitor minor DOT changes during cultivations without pH control. While the qualitative trend of the DOT is reliable, the absolute values of the calculated DOT could not be quantified precisely. However, a qualitative trend of the DOT already provides valuable information about the cultivation. Moreover, for a constant experimental setup, the obtained DOT levels from different cultivations can probably be compared. However, to

develop quantitative DOT monitoring during microaerobic cultivations without pH control, a more precise correlation between redox potential and DOT is required.

Chapter 6

Conclusion and Outlook

Production of 2,3-butanediol from renewable resources is a promising measure to decrease the consumption of fossil resources in the chemical industry. As precursor for the production of high volume products like 1,3-butadiene or methyl-ethyl-ketone (MEK) it is a versatile platform chemical that can be utilized in diverse chemical production processes to substitute oil-based intermediates (Bialkowska, 2016). One of the most influential process parameters on biotechnological 2,3-butanediol production is the oxygen availability during the cultivation. As 2,3-butanediol is produced under microaerobic process conditions, a well-controlled oxygen supply is the key parameter to control biomass, 2,3-butanediol and by-product formation. As biomass is on the one hand not the final product, but on the other hand the essential biocatalyst, the optimal compromise between biomass formation and 2,3-butanediol production has to be defined. Therefore, a fast and simple shake flask methodology to determine suitable oxygen supply conditions during the cultivation was developed in this thesis. It was applied to characterize the influence of oxygen availability during 2,3-butanediol production with *Bacillus licheniformis* DSM 8785. Furthermore, online monitoring of the respiratory quotient (RQ) and the redox potential was studied to improve the information content of online monitoring during microaerobic cultivations.

Suitable cultivation conditions for *Bacillus licheniformis* DSM 8785 were selected to investigate the influence of the maximum oxygen transfer capacity (OTR_{max}) on 2,3-butanediol production in Chapter 3. In shake flask cultivations, the OTR_{max} can be adjusted by variations

of the filling volume. At the beginning of the cultivation, oxygen-unlimited conditions are present due to the low biomass concentration. As soon as the organism's oxygen demand exceeds the OTR_{max}, oxygen-limited conditions are initiated. This results in inconsistent cultivation conditions, as the duration of the oxygen-unlimited growth phase depends on the OTR_{max}. Therefore, a defined two-stage cultivation strategy was introduced and oxygen limitation was induced by reduction of the shaking frequency at a defined oxygen transfer rate (OTR) of 20 mmol/L/h. This enabled the investigation of the metabolic response to different defined OTR_{max} at equal initial growth conditions. The RQ was measured online to determine the point of glucose depletion, as 2,3-butanediol is consumed afterwards. At this point, the maximum product concentration is reached. By a combination of online RQ monitoring and offline sampling at arbitrary time points, the maximum 2,3-butanediol concentration was calculated for 28 independent cultivations. On this basis, the influence of the OTR_{max} on 2,3-butanediol and by-product formation and the space-time yield was determined. The highest space-time yield (1.3 g/L/h) and a 2,3-butanediol concentration of 68 g/L combined with low acetoin concentrations and avoided glycerol formation were achieved at an OTR_{max} of 13 mmol/L/h. The highest overall 2,3-butanediol concentration of 78 g/L was observed at an OTR_{max} of 4 mmol/L/h. With the OTR_{max}, a scalable parameter that is independent of the chosen bioreactor type and scale was chosen to quantify the oxygen availability. Consequently, the shake flask cultivations could be transferred to a stirred tank reactor by adjustment of the OTR_{max}. Furthermore, the observed impact of the OTR_{max} on the cultivation is consistent with results obtained by Rebecchi et al. (2018) in stirred tank reactor cultivations of the same organism.

To date, all profound investigations on the impact of oxygen availability on 2,3-butanediol production were performed in stirred tank reactor cultivations (de Mas et al., 1988; Jansen et al., 1984; Ji et al., 2009; Ramachandran and Goma, 1987; Ramachandran et al., 1990; Rebecchi et al., 2018). As described above, the shake flask methodology developed in Chapter 3 provides comparable results to stirred tank reactor cultivations. Therefore, this methodology allows for precise investigations at a reduced technical and experimental effort with reduced material consumption and costs. This methodology is independent of the utilized microorganism and can easily be adapted to investigate and optimize 2,3-butanediol production with other organisms. Furthermore, the principle approach of combining online monitoring of the

respiratory activity in shake flasks with offline sampling can be adapted to other microaerobic cultivations.

In Chapter 4, online monitoring of the RQ was used to investigate the metabolic activity of *Bacillus licheniformis* DSM 8785 during 2,3-butanediol production in more detail. Thereby, the RQ provides valuable information about different metabolic phases during the cultivation. In addition to RQ monitoring, partial reaction stoichiometries were set up to reveal the metabolic activity in each phase of the cultivation. The cultivation can be divided in three distinct phases. After an oxygen unlimited growth phase at an RQ around 1, the 2,3-butanediol production phase is initiated upon oxygen limitation. In this phase, constant glucose consumption and 2,3-butanediol and glycerol formation is observed, resulting in RQs between 2.5 and 6. As soon as glucose is depleted, 2,3-butanediol is converted to acetoin and glycerol is consumed at an RQ below 1. However, especially during the 2,3-butanediol production phase the metabolic activity gradually changes as indicated by the roman numbers in Figure 4-1. Shortly after the initiation of oxygen limitation, ethanol formation results in a peak in the RQ (I). Towards the end of the 2,3-butanediol production phase, the RQ slowly declines (II) as the viable cell mass decreases. Finally, lactate consumption upon glucose depletion results in the formation of a shoulder in the RQ (III), before the RQ finally drops to values below 1. This demonstrates that the metabolic activity is directly reflected in the course of the RQ.

In addition to the specific RQ, which provides details about the metabolic activity during the individual cultivation phases, the average RQ throughout the cultivation was investigated. The average RQ negatively correlates with the OTR_{max} during the cultivation. Carbon mass balancing revealed that this reflects the increased formation of reduced metabolites like 2,3-butanediol and glycerol with decreasing OTR_{max}. This observation is in good agreement with the impact of the OTR_{max} on the cultivation that was investigated in detail in Chapter 3. Overall, the combination of online RQ monitoring and stoichiometric calculations provides detailed insights in the metabolic activity during specific phases of the cultivation. This approach is generally applicable to different microaerobic cultivations, as the stoichiometry is independent of the utilized microorganism. Consequently, it can be applied to reveal the formation of by-products under microaerobic conditions and to adapt the cultivation process accordingly.

The applicability of redox potential measurements to monitor trace levels of oxygen (DOT < 1%) during microaerobic cultivations was investigated in Chapter 5. The most commonly described approach to monitor low dissolved oxygen tensions (DOT) is the reduction of other parameters that influence the redox potential. Usually, this is achieved in temperature- and pH-controlled cultivations (Akashi et al., 1978; Kastner et al., 2003; Kjaergaard, 1976; Memmert and Wandrey, 1987). However, pH-control results in impaired 2,3-butanediol production with *Bacillus licheniformis* DSM 8785. Therefore, DOT monitoring via redox potential measurement in cultivations without pH control was envisaged in Chapter 5.

The influence of pH, DOT and changing glucose and 2,3-butanediol concentrations on the redox potential was investigated separately in abiotic experiments. Thereby, changes of 2,3-butanediol and glucose concentration in the ranges that occur during the cultivation only have a minor impact on the redox potential. In contrast, pH changes have significant impact on the redox potential. Therefore, the redox potential was corrected to exclude the influence of the pH. Subsequently, the course of the DOT was calculated from this corrected redox potential. This revealed a steady increase of the DOT during the oxygen-limited 2,3-butanediol production phase. By steady reduction of the agitation rate during the cultivation, the increasing calculated DOT could be prevented, demonstrating the qualitative feasibility of the presented calculations. In contrast, the absolute DOT could not be calculated precisely, as experimental difficulties resulted in a considerable uncertainty of the correlation between redox potential and DOT. Experimental methods to obtain more reliable data on the impact of DOT changes on the redox potential are required to improve the quantitative monitoring of low DOT levels. The utilization of special gas tight reactors might be necessary to obtain these data, as Schuldiner et al. (1966) observed leakage of oxygen into a glass reactor that could be prevented by operating the whole reactor in a controlled nitrogen atmosphere. Nevertheless, the obtained qualitative DOT trends provide additional information about the cultivation that would not be available without redox potential measurements. Similar to the RQ monitoring approaches investigated in Chapter 4, the presented redox potential-based DOT monitoring can easily be transferred to microaerobic cultivations with different microorganisms and products.

In the literature, high 2,3-butanediol concentrations are generally achieved by additional glucose supplementation during the cultivation (Cho et al., 2015b; Hässler et al., 2012; Jurchescu et al., 2013; Ma et al., 2009). Thereby, the 2,3-butanediol production phase is

prolonged by maintaining high glucose concentrations. However, this thesis aimed at the characterization of basic process parameters and the development of transferrable methodologies and not on optimized 2,3-butanediol production. Thus, a batch operation mode was chosen to minimize the experimental complexity. Nevertheless, reasonable production conditions were applied as a high initial glucose concentration of 180 g/L was chosen. This results in high maximum 2,3-butanediol concentrations up to 80 g/L, which is amongst the highest reported concentrations from batch experiments (Jurchescu et al., 2013).

The online monitoring-based approaches presented in this thesis can be utilized to develop and improve microaerobic cultivation processes. Based on the methodology presented in Chapter 3, the optimal OTR_{max} can be selected for any individual 2,3-butanediol production process. While this is one of the key parameters for microaerobic cultivations, also other factors are important for industrially relevant production processes. To increase the final 2,3-butanediol concentration, additional glucose supplementation during the cultivation is essential (Jurchescu et al., 2013; Ma et al., 2009). Additionally, genetic engineering to decrease by-product formation and to enable production of optically pure 2,3-butanediol will be beneficial (Lee et al., 2015; Li et al., 2015a; Wang et al., 2012). Furthermore, the cultivation medium has to be optimized with respect to utilization of cheaper carbon sources and media components (Bialkowska et al., 2015; Erian et al., 2018; Pflügl et al., 2014; Rebecchi et al., 2018; Yang et al., 2016). In this context, especially utilization of renewable carbon sources derived from organic waste streams, or lignocellulosic biomass is a challenging, but necessary precondition to supply 2,3-butanediol as environmentally friendly and economically feasible alternative for industrial applications.

In this thesis, 2,3-butanediol production with *Bacillus licheniformis* DSM 8785 was used as model bioprocess to develop online monitoring-based methodologies to understand and assess microaerobic cultivations. A shake flask methodology was presented to investigate the impact of the OTR_{max} on 2,3-butanediol production. Furthermore, improved approaches to utilize online RQ and redox potential monitoring were presented. Finally, application of these methodologies increased the understanding of microaerobic 2,3-butanediol production with *Bacillus licheniformis* DSM 8785. This can directly be applied for the improvement of 2,3-butanediol production processes with regard to the oxygen availability, contributing to the industrial application of bio-based 2,3-butanediol. Additionally, the presented methodologies

can be transferred to other microaerobic bioprocesses to facilitate the development of further biotechnological production processes.

Bibliography

1. Akashi, K., Ikeda, S., Shibai, H., Kobayashi, K., Hirose, Y. **1978**. Determination of redox potential levels critical for cell respiration and suitable for L-leucine production. *Biotech Bioeng*, 20, 21-41.

2. Alina, S.O., Constantinescu, F., Petruta, C.C. **2015**. Biodiversity of *Bacillus subtilis* group and beneficial traits of *Bacillus* species useful in plant protection. *Rom Biotech Lett*, 20(5).

3. Anderlei, T., Büchs, J. **2001**. Device for sterile online measurement of the oxygen transfer rate in shake flasks. *Biochem Eng J*, 7, 157-162.

4. Anderlei, T., Zang, W., Papaspyrou, M., Büchs, J. **2004**. Online respiration activity measurement (OTR, CTR, RQ) in shake flasks. *Biochem Eng J*, 17(3), 187-194.

5. Antoni, D., Zverlov, V.V., Schwarz, W.H. **2007**. Biofuels from microbes. *Appl Microbiol Biotechnol*, 77(1), 23-35.

6. Anvari, M., Pahlavanzadeh, H., Vasheghani-Farahani, E., Khayati, G. **2009**. In situ recovery of 2,3-butanediol from fermentation by liquid-liquid extraction. *J Ind Microbiol Biotechnol*, 36(2), 313-317.

7. Auchinvole, C.A., Richardson, P., McGuinnes, C., Mallikarjun, V., Donaldson, K., McNab, H., Campbell, C.J. **2012**. Monitoring intracellular redox potential changes using SERS nanosensors. *ACS Nano*, 6(1), 888-896.

8. Beronio, P.B., Tsao, G.T. **1993**. Optimization of 2,3-butanediol production by *Klebsiella oxytoca* through oxygen transfer rate control. *Biotechnol Bioeng*, 42, 1263-1269.

9. Bialkowska, A.M. **2016**. Strategies for efficient and economical 2,3-butanediol production: new trends in this field. *World J Microbiol Biotechnol*, 32(200).

10. Bialkowska, A.M., Gromek, E., Krysiak, J., Sikora, B., Kalinowska, H., Jedrzejczak-Krzepkowska, M., Kubik, C., Lang, S., Schütt, F., Turkiewicz, M. **2015**. Application of enzymatic apple pomace hydrolysate to production of 2,3-butanediol by alkaliphilic *Bacillus licheniformis* NCIMB 8059. *J Ind Microbiol Biotechnol*, 42(12), 1609-1621.

11. Bisset, K.A., Street, J. **1973**. Morphological phases in the swarm of *Bacillus licheniformis*. *J Gen Microbiol*, 76, 369-373.

12. Blaschek, H.P., Ezeji, T.C., Scheffran, J. **2010**. Biofuels from agricultural wastes and byproducts: an introduction. in: *Biofuels from agricultural wastes and byproducts*, (Eds.) H.P. Blaschek, T.C. Ezeji, J. Scheffran, Wiley-Blackwell. Hoboken, USA.

13. BP. **2019**. Statistical Review of World Energy 68th edition.

14. Brandberg, T., Gustafsson, L., Franzén, C.J. **2007**. The impact of severe nitrogen limitation and microaerobic conditions on extended continuous cultivations of *Saccharomyces cerevisiae* with cell recirculation. *Enzyme Microb Technol*, 40(4), 585-593.

15. Büchs, J. **2001**. Introduction to advantages and problems of shaken cultures. *Biochem Eng J*, 7, 91-98.

16. Celinska, E., Grajek, W. **2009**. Biotechnological production of 2,3-butanediol-current state and prospects. *Biotechnol Adv*, 27(6), 715-725.

17. Chen, C., Wei, D., Shi, J., Wang, M., Hao, J. **2014**. Mechanism of 2,3-butanediol stereoisomer formation in *Klebsiella pneumoniae*. *Appl Microbiol Biotechnol*, 98(10), 4603-4613.

18. Chen, X., Xiu, Z., Wang, J., Zhang, D., Xu, P. **2003**. Stoichiometric analysis and experimental investigation of glycerol bioconversion to 1,3-propanediol by *Klebsiella pneumoniae* under microaerobic conditions. *Enzyme Microb Technol*, 33(4), 386-394.

19. Cho, S., Kim, T., Woo, H.M., Kim, Y., Lee, J., Um, Y. **2015a**. High production of 2,3-butanediol from biodiesel-derived crude glycerol by metabolically engineered *Klebsiella oxytoca* M1. *Biotechnol Biofuels*, 8(146).

20. Cho, S., Kim, T., Woo, H.M., Lee, J., Kim, Y., Um, Y. **2015b**. Enhanced 2,3-butanediol production by optimizing fermentation conditions and engineering *Klebsiella oxytoca* M1 through overexpression of acetoin reductase. *PLoS One*, 10(9).

21. Chu, H., Xin, B., Liu, P., Wang, Y., Li, L., Liu, X., Zhang, X., Ma, C., Xu, P., Gao, C. **2015**. Metabolic engineering of *Escherichia coli* for production of (2S,3S)-butane-2,3-diol from glucose. *Biotechnol Biofuels*, 8(143).

22. Converti, A., Perego, P., Del Borghi, M. **2003**. Effect of specific oxygen uptake rate on *Enterobacter aerogenes* energetics: carbon and reduction degree balances in batch cultivations. *Biotechnol Bioeng*, 82(3), 370-377.

23. D'Autreaux, B., Toledano, M.B. **2007**. ROS as signalling molecules: mechanisms that generate specificity in ROS homeostasis. *Nat Rev Mol Cell Biol*, 8(10), 813-824.

24. Dai, J.J., Cheng, J.S., Liang, Y.Q., Jiang, T., Yuan, Y.J. **2014**. Regulation of extracellular oxidoreduction potential enhanced (R,R)-2,3-butanediol production by *Paenibacillus polymyxa* CJX518. *Bioresour Technol*, 167, 433-440.

25. Dai, J.Y., Zhao, P., Cheng, X.L., Xiu, Z.L. **2015**. Enhanced production of 2,3-butanediol from sugarcane molasses. *Appl Biochem Biotechnol*, 175(6), 3014-3024.

26. Dauner, M., Storni, T., Sauer, U. **2001**. *Bacillus subtilis* metabolism and energetics in carbon-limited and excess-carbon chemostat culture. *J Bacteriol*, 183(24), 7308-7317.

27. de Graef, M.R., Alexeeva, S., Snoep, J.L., de Mattos, M.J.T. **1999**. The steady-state internal redox state (NADH/NAD) reflects the external redox state and is correlated with catabolic adaptation in *Escherichia coli*. *J Bacteriol*, 181(8), 2351-2357.

28. de Mas, C., Jansen, N.B., Tsao, G.T. **1988**. Production of optically active 2,3-butanediol by *Bacillus polymyxa*. *Biotech Bioeng*, 31, 366-377.

29. Devi, T.T., Kumar, B. **2017**. Mass transfer and power characteristics of stirred tank with Rushton and curved blade impeller. *Eng Sci Technol Int J*, 20(2), 730-737.

30. Dewhirst, M.W., Cao, Y., Moeller, B. **2008**. Cycling hypoxia and free radicals regulate angiogenesis and radiotherapy response. *Nat Rev Cancer*, 8(6), 425-437.

31. Drabo, P., Tiso, T., Heyman, B., Sarikaya, E., Gaspar, P., Förster, J., Büchs, J., Blank, L.M., Delidovich, I. **2017**. Anionic extraction for efficient recovery of biobased 2,3-butanediol - a platform for bulk and fine chemicals. *Chem Sus Chem*, 10, 3252-3259.

32. Erian, A.M., Gibisch, M., Pflügl, S. **2018**. Engineered *E. coli* W enables efficient 2,3-butanediol production from glucose and sugar beet molasses using defined minimal medium as economic basis. *Microb Cell Fact*, 17(190).

33. Fages, J., Mulard, D., Rouquet, J.J., Wilhelm, J.L. **1986**. 2,3-Butanediol production from jerusalem artichoke, *Helianthus tuberosus*, by *Bacillus polymyxa* ATCC 12321. Optimization of kLa profile. *Appl Microbiol Biotechnol*, 25, 197-202.

34. Franzén, C.J. **2003**. Metabolic flux analysis of RQ-controlled microaerobic ethanol production by *Saccharomyces cerevisiae*. *Yeast*, 20(2), 117-132.

35. Franzén, C.J., Albers, E., Niklasson, C. **1996**. Use of the inlet gas composition to control the respiratory quotient in microaerobic bioprocesses. *Chem Eng Sci*, 51(13), 3391-3402.

36. Frazer, F.R., McCaskey, T.A. **1989**. Wood hydrolyzate treatments for improved fermentation of wood sugars to 2,3-butanediol. *Biomass*, 31-42.

37. Gao, J., Xu, H., Li, Q.J., Feng, X.H., Li, S. **2010**. Optimization of medium for one-step fermentation of inulin extract from Jerusalem artichoke tubers using *Paenibacillus polymyxa* ZJ-9 to produce R,R-2,3-butanediol. *Bioresour Technol*, 101(18), 7087-7093.

38. Garg, S.K., Jain, A. **1995**. Fermentative production of 2,3-butanediol: a review. *Bioresour Technol*, 51, 103-109.

39. Ge, Y., Li, K., Li, L., Gao, C., Zhang, L., Ma, C., Xu, P. **2016**. Contracted but effective: production of enantiopure 2,3-butanediol by thermophilic and GRAS *Bacillus licheniformis*. *Green Chem*, 18(17), 4693-4703.

40. Giesecke, U.E., Bierbaum, G., Rudde, H., Spohn, U., Wandrey, C. **1991**. Production of alkaline protease with *Bacillus licheniformis* in a controlled fed-batch process. *Appl Microbiol Biotechnol*, 35, 720-724.

41. Gutscher, M., Pauleau, A.L., Marty, L., Brach, T., Wabnitz, G.H., Samstag, Y., Meyer, A.J., Dick, T.P. **2008**. Real-time imaging of the intracellular glutathione redox potential. *Nat Methods*, 5(6), 553-559.

42. Hässler, T., Schieder, D., Pfaller, R., Faulstich, M., Sieber, V. **2012**. Enhanced fed-batch fermentation of 2,3-butanediol by *Paenibacillus polymyxa* DSM 365. *Bioresour Technol*, 124, 237-244.

43. Hermann, H.G., Patel, M. **2007**. Today's and tomorrow's bio-based bulk chemicals from white biotechnology a techno-economic analysis. *Appl Biochem Biotechnol*, 136(3), 361-388.

44. Heyman, B., Lamm, R., Tulke, H., Regestein, L., Büchs, J. **2019**. Shake flask methodology for assessing the influence of the maximum oxygen transfer capacity on 2,3-butanediol production. *Microb Cell Fact*, 18(78).

45. Heyman, B., Tulke, H., Putri, S.P., Fukusaki, E., Büchs, J. **2020**. Online monitoring of the respiratory quotient reveals metabolic phases during microaerobic 2,3-butanediol production with *Bacillus licheniformis*. *Eng Life Sci*, 20, 133-144.

46. Hill, R. **1973**. A note on some old and some possible new redox indicators. *J Bioenerg*, 4, 229-237.

47. Hoppe, F., Burke, U., Thewes, M., Heufer, A., Kremer, F., Pischinger, S. **2016**. Tailor-Made Fuels from Biomass: potentials of 2-butanone and 2-methylfuran in direct injection spark ignition engines. *Fuel*, 167, 106-117.

48. Horowitz, S., Gilbert, J.N., Griffin, W.M. **1990**. Isolation and characterization of a surfactant produced by *Bacillus licheniformis* 86. *J Indust Microbiol*, 6, 243-248.

49. Hung, Y.P., Albeck, J.G., Tantama, M., Yellen, G. **2011**. Imaging cytosolic NADH-NAD(+) redox state with a genetically encoded fluorescent biosensor. *Cell Metab*, 14(4), 545-554.

50. Hwang, H.J., Lee, S.Y., Lee, P.C. **2018**. Engineering and application of synthetic *nar* promoter for fine-tuning the expression of metabolic pathway genes in *Escherichia coli*. *Biotechnol Biofuels*, 11(103).

51. Ishizaki, A., Shibai, H., Hirose, Y. **1974**. Basic aspects of electrode potential change in submerged fermentation. *Agr Biol Chem*, 38(12), 2399-2406.

52. Jansen, N., Flickinger, M.C., Tsao, G.T. **1984**. Production of 2,3-butanediol from D-xylose by *Klebsiella oxytoca* ATCC 8724. *Biotech Bioeng*, 26, 362-369.

53. Jeon, B.Y., Park, D.H. **2010**. Improvement of ethanol production by electrochemical redox combination of *Zymomonas mobilis* and *Saccharomyces cerevisiae*. *J Microbiol Biotechnol*, 20(1), 94-100.

54. Ji, X.J., Huang, H., Du, J., Zhu, J.G., Ren, L.J., Hu, N., Li, S. **2009**. Enhanced 2,3-butanediol production by *Klebsiella oxytoca* using a two-stage agitation speed control strategy. *Bioresour Technol*, 100(13), 3410-3414.

55. Ji, X.J., Huang, H., Ouyang, P.K. **2011**. Microbial 2,3-butanediol production: a state-of-the-art review. *Biotechnol Adv*, 29(3), 351-364.

56. Jurchescu, I.M., Hamann, J., Zhou, X., Ortmann, T., Kuenz, A., Prüße, U., Lang, S. **2013**. Enhanced 2,3-butanediol production in fed-batch cultures of free and immobilized *Bacillus licheniformis* DSM 8785. *Appl Microbiol Biotechnol*, 97(15), 6715-6723.

57. Kallbach, M. **2018**. Biotechnische 2,3-Butandiol-Produktion aus Birkenholz-Hemicellulose. Fakultät für Lebenswissenschaften (Dissertation). Technischen Universität Carolo-Wilhelmina zu Braunschweig.

58. Kallbach, M., Horn, S., Kuenz, A., Prüße, U. **2017**. Screening of novel bacteria for the 2,3-butanediol production. *Appl Microbiol Biotechnol*, 101(3), 1025-1033.

59. Karimi, A., Golbabaei, F., Mehrnia, M.R., Neghab, M., Mohammad, K., Nikpey, A., Pourmand, M.R. **2013**. Oxygen mass transfer in a stirred tank bioreactor using different impeller configurations for environmental purposes. *Iranian J Environ Health Sci Eng*, 10(6).

60. Kastner, J.R., Eiteman, M.A., Lee, S.A. **2003**. Effect of redox potential on stationary-phase xylitol fermentations using *Candida tropicalis*. *Appl Microbiol Biotechnol*, 63, 96-100.

61. Kim, S.J., Kim, J.W., Lee, Y.G., Park, Y.C., Seo, J.H. **2017**. Metabolic engineering of *Saccharomyces cerevisiae* for 2,3-butanediol production. *Appl Microbiol Biotechnol*, 101(6), 2241-2250.

62. Kjaergaard, L. **1976**. Influence of redox potential on the glucose catabolism of chemostat grown *Bacillus licheniformis*. *Eur J Appl Microbiol*, 2, 215-220.

63. Kjaergaard, L. **1977**. The redox potential: its use and control in biotechnology. in: *Advances in biochemical engineering*, Vol. 7, Springer. Berlin, Germany, pp. 131-150.

64. Klöckner, W., Büchs, J. **2012**. Advances in shaking technologies. *Trends Biotechnol*, 30(6), 307-314.

65. Koutinas, A.A., Yepez, B., Kopsahelis, N., Freire, D.M.G., de Castro, A.M., Papanikolaou, S., Kookos, I.K. **2016**. Techno-economic evaluation of a complete bioprocess for 2,3-butanediol production from renewable resources. *Bioresour Technol*, 204, 55-64.

66. Kreyenschulte, D., Emde, F., Regestein, L., Büchs, J. **2016**. Computational minimization of the specific energy demand of large-scale aerobic fermentation processes based on small-scale data. *Chem Eng Sci*, 153, 270-283.

67. Lee, S., Kim, B., Yang, J., Jeong, D., Park, S., Lee, J. **2015**. A non-pathogenic and optically high concentrated (R,R)-2,3-butanediol biosynthesizing *Klebsiella* strain. *J Biotechnol*, 209, 7-13.

68. Li, L., Li, K., Wang, Y., Chen, C., Xu, Y., Zhang, L., Han, B., Gao, C., Tao, F., Ma, C., Xu, P. **2015a**. Metabolic engineering of *Enterobacter cloacae* for high-yield production of enantiopure (2R,3R)-2,3-butanediol from lignocellulose-derived sugars. *Metab Eng*, 28, 19-27.

69. Li, L., Zhang, L., Li, K., Wang, Y., Gao, C., Han, B., Ma, C., Xu, P. **2013**. A newly isolated *Bacillus licheniformis* strain thermophilically produces 2,3-butanediol, a platform and fuel bio-chemical. *Biotechnol Biofuels*, 6(123).

70. Li, Y., He, D., Niu, D., Zhao, Y. **2015b**. Acetic acid production from food wastes using yeast and acetic acid bacteria micro-aerobic fermentation. *Bioprocess Biosyst Eng*, 38(5), 863-869.

71. Liang, X.S., Liu, C., Long, Z., Guo, X.H. **2018**. Rapid and simple detection of endospore counts in probiotic *Bacillus* cultures using dipicolinic acid (DPA) as a marker. *AMB Express*, 8, 101.

72. Liu, C.G., Hao, X.M., Lin, Y.H., Bai, F.W. **2016**. Redox potential driven aeration during very-high-gravity ethanol fermentation by using flocculating yeast. *Sci Rep*, 6(25763).

73. Liu, C.G., Xue, C., Lin, Y.H., Bai, F.W. **2013**. Redox potential control and applications in microaerobic and anaerobic fermentations. *Biotechnol Adv*, 31(2), 257-265.

74. Liu, H., Kang, J., Qi, Q., Chen, G. **2011**. Production of lactate in *Escherichia coli* by redox regulation genetically and physiologically. *Appl Biochem Biotechnol*, 164(2), 162-169.

75. Liu, J., Cao, L., Chen, J., Song, S., Lee, I.H., Quijano, C., Liu, H., Keyvanfar, K., Chen, H., Cao, L.Y., Ahn, B.H., Kumar, N.G., Rovira, II, Xu, X.L., van Lohuizen, M., Motoyama, N., Deng, C.X., Finkel, T. **2009**. Bmi1 regulates mitochondrial function and the DNA damage response pathway. *Nature*, 459(7245), 387-392.

76. Ma, C., Wang, A., Qin, J., Li, L., Ai, X., Jiang, T., Tang, H., Xu, P. **2009**. Enhanced 2,3-butanediol production by *Klebsiella pneumoniae* SDM. *Appl Microbiol Biotechnol*, 82, 49-57.

77. Magee, R.J., Kosaric, N. **1987**. The microbial production of 2,3-butanediol. in: *Advances in applied microbiology*, (Ed.) A.I. Laskin, Vol. 32, Academic press Inc. Somerset, USA, pp. 89-162.

78. Maier, U., Büchs, J. **2001**. Characterisation of the gas-liquid mass transfer in shaking bioreactors. *Biochem Eng J*, 7, 99-106.

79. Mao, W., Pan, R., Freedman, D. **1992**. High production of alkaline protease by *Bacillus licheniformis* in a fed-batch fermentation using a synthetic medium. *J Indust Microbiol*, 11, 1-6.

80. Martinov, M., Gancel, F., Jacques, P., Nikov, I., Vlaev, S. **2008**. Surfactant effects on aeration performance of stirred tank reactors. *Chem Eng Technol*, 31(10), 1494-1500.

81. McDaniel, L.E., Bailey, E.G., Zimmerli, A. **1965**. Effect of oxygen-supply rates on growth of *Escherichia coli*: I. studies in unbaffled and baffled shake flasks. *Appl Microbiol*, 13, 109-114.

82. Meissner, L., Kauffmann, K., Wengeler, T., Mitsunaga, H., Fukusaki, E., Büchs, J. **2015**. Influence of nitrogen source and pH value on undesired poly(gamma-glutamic acid) formation of a protease producing *Bacillus licheniformis* strain. *J Ind Microbiol Biotechnol*, 42(9), 1203-1215.

83. Memmert, K., Wandrey, C. **1987**. Continuous production of *Bacillus* exoenzymes through redox-regulation. *Ann N Y Acad Sci*, 506, 631-636.

84. Menon, S.G., Goswami, P.C. **2007**. A redox cycle within the cell cycle: ring in the old with the new. *Oncogene*, 26(8), 1101-1109.

85. Nakashimada, Y., Kanai, K., Nishio, N. **1998**. Optimization of dilution rate, pH and oxygen supply on optical purity of 2,3-butanediol produced by *Paenibacillus polymyxa* in chemostat culture. *Biotechnol Lett*, 20(12), 1133-1138.

86. Nguyen, D., Khanal, S.K. **2018**. A little breath of fresh air into an anaerobic system: how microaeration facilitates anaerobic digestion process. *Biotechnol Adv*, 36(7), 1971-1983.

87. Nilegaonkar, S., Bhosale, S.B., Kshirsagar, D.C., Kapadi, A.H. **1992**. Production of 2,3-butanediol from glucose by *Bacillus licheniformis*. *World J Microbiol Biotechnol*, 8, 378-381.

88. Oh, D.K., Kim, S.-Y., Kim, J.H. **1997**. Increase of xylitol production rate by controlling redox potential in *Candida parapsilosis*. *Biotech Bioeng*, 58(4), 440-444.

89. Parawira, W., Murto, M., Read, J.S., Mattiasson, B. **2004**. Volatile fatty acid production during anaerobic mesophilic digestion of solid potato waste. *J ChemTechnol Biotechnol*, 79(7), 673-677.

90. Park, D.H., Zeikus, J.G. **1999**. Utilization of electrically reduced neutral red by *Actinobacillus succinogenes*: physiological function of neutral red in membrane-driven fumarate reduction and energy conservation. *J Bacteriol*, 181(8), 2403–2410.

91. Park, J.M., Song, H., Lee, H.J., Seung, D. **2013**. In silico aided metabolic engineering of *Klebsiella oxytoca* and fermentation optimization for enhanced 2,3-butanediol production. *J Ind Microbiol Biotechnol*, 40(9), 1057-1066.

92. Partridge, J.D., Sanguinetti, G., Dibden, D.P., Roberts, R.E., Poole, R.K., Green, J. **2007**. Transition of *Escherichia coli* from aerobic to micro-aerobic conditions involves fast and slow reacting regulatory components. *J Biol Chem*, 282(15), 11230-11237.

93. Paulsen, C.E., Carroll, K.S. **2010**. Orchestrating redox signaling networks through regulatory cysteine switches. *ACS Chem Biol*, 5(1), 47-62.

94. Penner, D., Redepenning, C., Mitsos, A., Viell, J. **2017**. Conceptual design of methyl ethyl ketone production via 2,3-butanediol for fuels and chemicals. *Ind Eng Chem Res*, 56(14), 3947-3957.

95. Perego, P., Converti, A., Del Borghi, A., Canepa, P. **2000**. 2,3-Butaendiol production by *Enterobacter aerogenes:* selection of the optimal conditions and application to food industry residues. *Bioprocess Eng*, 23, 613-620.

96. Pflügl, S., Marx, H., Mattanovich, D., Sauer, M. **2014**. Heading for an economic industrial upgrading of crude glycerol from biodiesel production to 1,3-propanediol by *Lactobacillus diolivorans*. *Bioresour Technol*, 152, 499-504.

97. Pham, T.H., Mauvais, G., Vergoignan, C., De Coninck, J., Dumont, F., Lherminier, J., Cachon, R., Feron, G. **2008**. Gaseous environments modify physiology in the brewing yeast *Saccharomyces cerevisiae* during batch alcoholic fermentation. *J Appl Microbiol*, 105(3), 858-874.

98. Priya, A., Dureja, P., Talukdar, P., Rathi, R., Lal, B., Sarma, P.M. **2016**. Microbial production of 2,3-butanediol through a two-stage pH and agitation strategy in 150 l bioreactor. *Biochem Eng J*, 105, 159-167.

99. Qiu, Y., Zhang, J., Li, L., Wen, Z., Nomura, C.T., Wu, S., Chen, S. **2016**. Engineering *Bacillus licheniformis* for the production of meso-2,3-butanediol. *Biotechnol Biofuels*, 9(117).

100. Qureshi, N., Meagher, M.M., Hutkins, R.W. **1994**. Recovery of 2,3-butanediol by vacuum membrane distillation. *Sep Sci Technol*, 29(13), 1733-1748.

101. Rados, D., Carvalho, A.L., Wieschalka, S., Neves, A.R., Blombach, B., Eikmanns, B.J., Santos, H. **2015**. Engineering *Corynebacterium glutamicum* for the production of 2,3-butanediol. *Microb Cell Fact*, 14(171).

102. Ramachandran, K.B., Goma, G. **1987**. Effect of oxygen supply and dilution rate on the production of 2,3-butanediol in continuous bioreactor by *Klebsiella pneumoniae*. *Enzyme Microb Technol*, 9, 107-111.

103. Ramachandran, K.B., Hashim, M.A., Fernandez, A.A. **1990**. Kinetic study of 2,3-butanediol production by *Klebsiella oxytoca*. *J Ferm Bioeng*, 70(4), 235-240.

104. Raspoet, D., Pot, B., De Deyn, D., De Vos, P., Kersters, K., De Ley, J. **1991**. Differentiation between 2,3-butanediol producing *Bacillus licheniformis* and *B. polymyxa* strains by fermentation product profiles and whole-cell protein electrophoretic patterns. *Syst Appl Microbiol*, 14, 1-7.

105. Rebecchi, S., Pinelli, D., Zanaroli, G., Fava, F., Frascari, D. **2018**. Effect of oxygen mass transfer rate on the production of 2,3-butanediol from glucose and agro-industrial byproducts by *Bacillus licheniformis* ATCC9789. *Biotechnol Biofuels*, 11(145).

106. Rey, M.W., Ramaiya, P., Nelson, B.A., Brody-Karpin, S.D., Zaretsky, E.J., Tang, M., L., d.L.A., H., X., Gusti, V., Clausen, I.G., Olsen, P.B., Rasmussen, M.D., T., A.J., Jørgensen, P.L., S., L.T., Sorokin, A., A., B., Lapidus, A., Galleron, N., D., E.S., M., B.R. **2004**. Complete genome sequence of the industrial bacterium *B licheniformis* and comparisons with closely related *Bacillus species*. *Genome Biol*, 5(10).

107. Rodriguez, A., Ripoll, V., Santos, V.E., Gomez, E., Garcia-Ochoa, F. **2017**. Effect of fluid dynamic conditions on 2,3-butanediol production by *Raoultella terrigena* in SBTR: oxygen transfer and uptake rates. *J Chem Technol Biotechnol*, 92(6), 1266-1275.

108. Rybicka, J.M., Balce, D.R., Khan, M.F., Krohn, R.M., Yates, R.M. **2010**. NADPH oxidase activity controls phagosomal proteolysis in macrophages through modulation of the lumenal redox environment of phagosomes. *Proc Natl Acad Sci*, 107(23), 10496-10501.

109. Sabra, W., Groeger, C., Zeng, A.P. **2016**. Microbial cell factories for diol production. *Adv Biochem Eng Biotechnol*, 155, 165-197.

110. Saisaard, K., Angelidaki, I., Prasertsan, P. **2011**. Micro-aerobic, anaerobic and two-stage condition for ethanol production by *Enterobacter aerogenes* from biodiesel-derived crude glycerol. *World Acad Sci Eng Technol*, 77.

111. Sardinas, J., **1973**, Fermentation process for the production of citric acid, U. Patent, US3708399A.

112. Schaepe, S., Kuprijanov, A., Sieblist, C., Jenzsch, M., Simutis, R., Lubbert, A. **2013**. kLa of stirred tank bioreactors revisited. *J Biotechnol*, 168(4), 576-583.

113. Schallmey, M., Singh, A., Ward, O.P. **2004**. Developments in the use of *Bacillus* species for industrial production. *Can J Microbiol*, 50.

114. Schuldiner, S., Piersma, B.J., Warner, T.B. **1966**. Potential of a platinum electrode at low partial pressures of hydrogen and oxygen II. an improved gas-tight system with a negligible oxygen leak. *J Electrochem Soc*, 113(6), 573-577.

115. Schwarzländer, M., Dick, T.P., Meyer, A.J., Morgan, B. **2016**. Dissecting redox biology using dluorescent protein sensors. *Antioxid Redox Signal*, 24(13), 680-712.

116. Shariati, P., Mitchel, W.J., Boyd, A., Priest, F.G. **1995**. Anaerobic metabolism in *Bacillus licheniformis* NClB 6346. *Microbiol*, 141, 1117-1124.

117. Shen, C.R., Lan, E.I., Dekishima, Y., Baez, A., Cho, K.M., Liao, J.C. **2011**. Driving forces enable high-titer anaerobic 1-butanol synthesis in *Escherichia coli*. *Appl Environ Microbiol*, 77(9), 2905-2915.

118. Shibai, H., Ishizaki, A., Kobayashi, K., Hirose, Y. **1974**. Simultaneous measurement of dissolved oxygen and oxidation reduction potentials in the aerobic cultures. *Agr Biol Chem*, 38(12), 2407-2411.

119. Sonenshein, A.L., Hoch, J.A., Losick, R. **2002**. *Bacillus subtilis* and its closest relatives: from genes to cells. American Society for Microbiology, Washington D.C., USA.

120. Sun, L.H., Wang, X.D., Dai, J.Y., Xiu, Z.L. **2009**. Microbial production of 2,3-butanediol from Jerusalem artichoke tubers by *Klebsiella pneumoniae*. *Appl Microbiol Biotechnol*, 82(5), 847-852.

121. Syu, M.J. **2001**. Biological production of 2,3-butanediol. *Appl Microbiol Biotechnol*, 55, 10-18.

122. Takesono, S., Onodera, M., Ito, A., Yoshida, M., Yamagiwa, K., Ohkawa, A. **2001**. Mechanical control of foaming in stirred-tank reactors. *J Chem Technol Biotechnol*, 76, 355-362.

123. Tian, X., Wang, Y., Chu, J., Zhuang, Y., Zhang, S. **2015**. Improvement of L-lactic acid production with a two-step OUR control strategy. *J´Chem Technol Biotechnol*, 91(9), 2496-2502.

124. Veith, B., Herzberg, C., Steckel, S., Feesche, J., Maurer, K.H., Ehrenreich, P., Baumer, S., Henne, A., Liesegang, H., Merkl, R., Ehrenreich, A., Gottschalk, G. **2004**. The complete genome sequence of *Bacillus licheniformis* DSM13, an organism with great industrial potential. *J Mol Microbiol Biotechnol*, 7(4), 204-211.

125. Wang, Q., Chen, T., Zhao, X., Chamu, J. **2012**. Metabolic engineering of thermophilic *Bacillus licheniformis* for chiral pure D-2,3-butanediol production. *Biotechnol Bioeng*, 109(7), 1610-1621.

126. Wright, A.F., Chakarova, C.F., Abd El-Aziz, M.M., Bhattacharya, S.S. **2010**. Photoreceptor degeneration: genetic and mechanistic dissection of a complex trait. *Nat Rev Genet*, 11(4), 273-284.

127. Wu, J., Wang, Z., Duan, X., Zhou, P., Liu, P., Pang, Z., Wang, Y., Wang, X., Li, W., Dong, M. **2019**. Construction of artificial micro-aerobic metabolism for energy- and carbon-efficient synthesis of medium chain fatty acids in *Escherichia coli*. *Metab Eng*, 53, 1-13.

128. Xiu, Z.L., Chen, X., Sun, Y.Q., Zhang, D. **2007**. Stoichiometric analysis and experimental investigation of glycerol-glucose co-fermentation in *Klebsiella pneumoniae* under microaerobic conditions. *Biochem Eng J*, 33(1), 42-52.

129. Xiu, Z.L., Zeng, A.P. **2008**. Present state and perspective of downstream processing of biologically produced 1,3-propanediol and 2,3-butanediol. *Appl Microbiol Biotechnol*, 78(6), 917-926.

130. Xu, Y., Chu, H., Gao, C., Tao, F., Zhou, Z., Li, K., Li, L., Ma, C., Xu, P. **2014**. Systematic metabolic engineering of *Escherichia coli* for high-yield production of fuel bio-chemical 2,3-butanediol. *Metab Eng*, 23, 22-33.

131. Yakimov, M.M., Timmis, K.N., Wray, V., Fredrickson, H.L. **1995**. Characterization of a new lipopeptide surfactant produced by thermotolerant and halotolerant subsurface *Bacillus licheniformis* BAS50. *Appl Environ Microbiol*, 61(5), 1706-1713.

132. Yamada, R., Nishikawa, R., Wakita, K., Ogino, H. **2018**. Rapid and stable production of 2,3-butanediol by an engineered *Saccharomyces cerevisiae* strain in a continuous airlift bioreactor. *J Ind Microbiol Biotechnol*, 45(5), 305-311.

133. Yang, J., Kim, B., Kim, H., Kweon, Y., Lee, S., Lee, J. **2015**. Industrial production of 2,3-butanediol from the engineered *Corynebacterium glutamicum*. *Appl Biochem Biotechnol*, 176(8), 2303-2313.

134. Yang, S., Mohagheghi, A., Franden, M.A., Chou, Y.C., Chen, X., Dowe, N., Himmel, M.E., Zhang, M. **2016**. Metabolic engineering of *Zymomonas mobilis* for 2,3-butanediol production from lignocellulosic biomass sugars. *Biotechnol Biofuels*, 9(189).

135. Yang, T., Rao, Z., Zhang, X., Lin, Q., Xia, H., Xu, Z., Yang, S. **2011**. Production of 2,3-butanediol from glucose by GRAS microorganism *Bacillus amyloliquefaciens*. *J Basic Microbiol*, 51(6), 650-658.

136. Zeng, A.P., Biebl, H., Deckwer, W.D. **1991a**. Production of 2,3-butanediol in a membrane bioreactor with cell recycle. *Appl Microbiol Biotechnol*, 34, 463-468.

137. Zeng, A.P., Byun, T.G., Deckwer, W.D. **1991b**. On-line estimation of viable biomass of a microaerobic culture using exit gas analysis. *Biotechnol Tech*, 5(4), 247-250.

138. Zeng, A.P., Byun, T.G., Posten, C., Deckwer, W.D. **1994**. Use of respiratory quotient as a control parameter for optimum oxygen supply and scale-up of 2,3-butanediol production under microaerobic conditions. *Biotech Bioeng*, 44, 1107-1114.

139. Zeng, A.P., Deckwer, W.D. **1996**. Bioreaction techniques under microaerobic conditions: from molecular level to pilot plant reactors. *Chem Eng Sci*, 51(10), 2305-2314.

140. Zeng, A.P., Sabra, W. **2011**. Microbial production of diols as platform chemicals: recent progresses. *Curr Opin Biotechnol*, 22(6), 749-757.

141. Zhang, L., Yang, Y., Sun, J., Shen, Y., Wei, D., Zhu, J., Chu, J. **2010**. Microbial production of 2,3-butanediol by a mutagenized strain of *Serratia marcescens* H30. *Bioresour Technol*, 101(6), 1961-1967.

142. Zhang, Y.P., Du, C.Y., Rao, Z., Cao, Z.A. **2005**. Regulation of vitamin c and vitamin e on the biosynthesis of 1,3-propanediol by *Klebsiella pneumoniae*. *Chin J Process Eng*, 5(2), 197-200.

Appendix

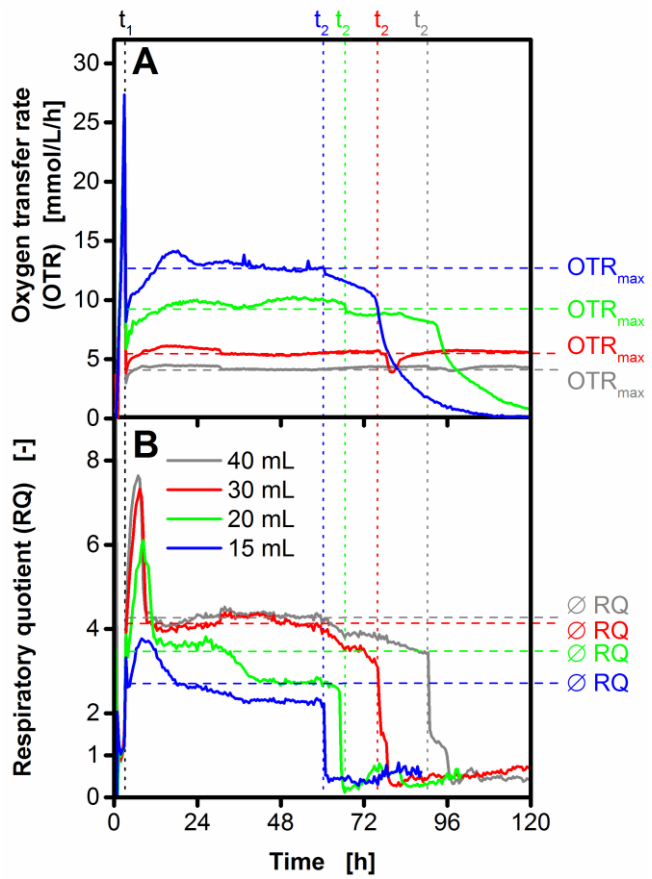

Appendix 1: Cultivation of *Bacillus licheniformis* DSM 8785 at different maximum oxygen transfer capacities. The courses of oxygen transfer rates (OTR) (A) and the respiratory quotients (RQ) (B) are shown for cultivations with different filling volumes. The shaking frequency was reduced from 350 to 100 rpm after 3 h (vertical dotted line at t_1). 2,3-Butanediol production begins upon reduction of the shaking frequency (t_1) and ends when the RQ drops (t_2). The average RQ during 2,3-butanediol production (Ø RQ) and the maximum oxygen transfer capacity (OTR_{max}) are depicted. Cultivation conditions: 250 mL unbaffled shake flasks, temperature: 37 °C, shaking frequency: 350/100 rpm, shaking diameter: 50 mm, Nakashimada medium with 100 mM MES buffer.

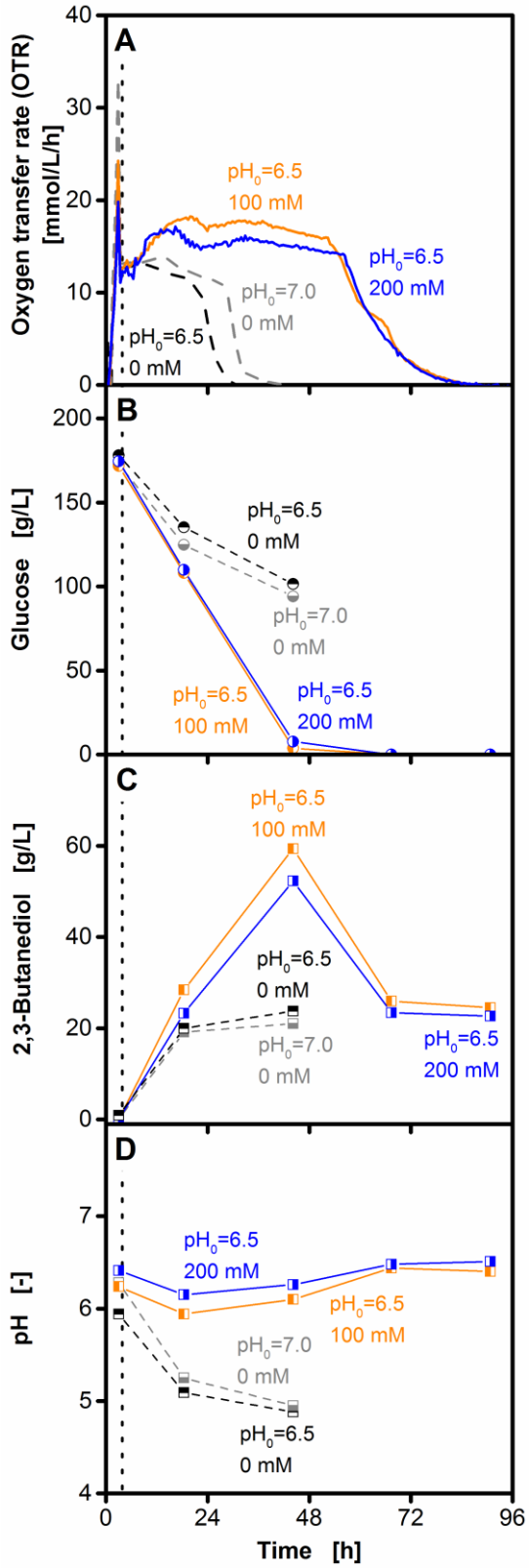

Appendix 2: Reduced acidification during the cultivation of *Bacillus licheniformis* DSM 8785. Cultivations in 10 mL Nakashimada medium with addition of different MES buffer concentrations (0, 100 and 200 mM as indicated in the figure) and different initial pH values (6.5 and 7.0 as indicated in the figure) are compared. Without addition of MES buffer, acetate formation was observed (up to 4.0

and 5.8 g/L for the cultivations with initial pH of 6.5 and 7, respectively). No acetate was measured in the cultures with MES addition. As indicated by the vertical dotted line, the shaking frequency was reduced from 350 to 100 rpm after 3 h. Thereby, oxygen-limited conditions are induced at the same time for all cultivations. Data on oxygen transfer rate (OTR) (A), glucose (B) and total 2,3-butanediol concentration (C) and pH (D) are depicted. 2,3-Butanediol is shown as sum of the stereoisomers. To account for the increase of metabolite concentrations due to evaporation of water, all concentrations were corrected accordingly and referred to the initial filling volume. Cultivation conditions: 250 mL unbaffled shake flasks, temperature: 37 °C, shaking frequency: 350/100 rpm, shaking diameter: 50 mm, filling volume: 10 mL.

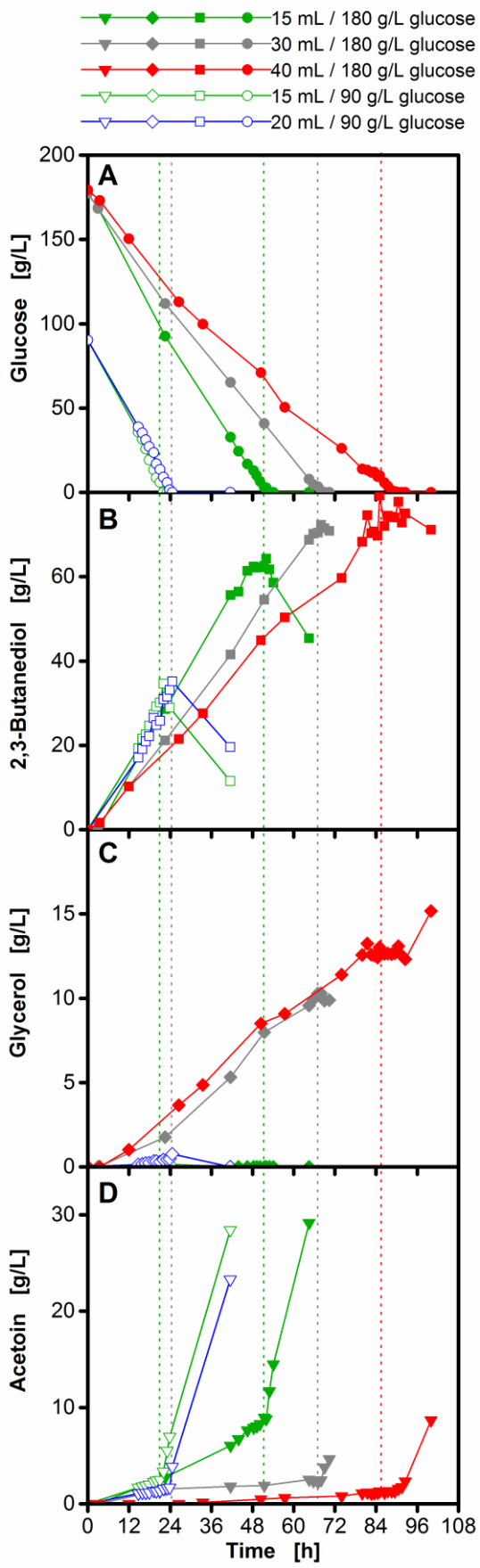
15 mL / 180 g/L glucose
30 mL / 180 g/L glucose
40 mL / 180 g/L glucose
15 mL / 90 g/L glucose
20 mL / 90 g/L glucose
A
B
C
D
Glucose [g/L]
2,3-Butanediol [g/L]
Glycerol [g/L]
Acetoin [g/L]
Time [h]
0
12
24
36
48
60
72
84
96
108

Appendix 3: Glucose consumption and product formation during different cultivations of *Bacillus licheniformis* DSM 8785. Cultivations with varied filling volumes and glucose concentrations are compared as described in the figure legend. Variation of the filling volume results in different maximum oxygen transfer capacities (OTR_{max}) in shake flask cultivations. The shaking frequency was reduced from 350 to 100 rpm after 3 h. Thereby, oxygen-limited conditions are induced at the same time for all cultivations. Data on glucose (A) total 2,3-butanediol (B) glycerol (C) and acetoin concentration (D) are depicted. 2,3-Butanediol is shown as sum of the stereoisomers. The vertical dotted lines represent the time of glucose depletion derived from the sharply decreasing respiratory quotient (data not shown) as described in Figure 3-3. At this point the average deviation between the calculated and measured 2,3-butanediol concentration was 3.6% (2.4, 8.8, 0.7, 3.4 and 2.7% for the individual cultivations from top to bottom of the legend). To account for the increase of metabolite concentrations due to evaporation of water, all concentrations were corrected accordingly and referred to the initial filling volume. Cultivation conditions: 250 mL unbaffled shake flasks, temperature: 37 °C, shaking frequency: 350/100 rpm, shaking diameter: 50 mm, Nakashimada medium with 100 mM MES buffer (90 or 180 g/L glucose).

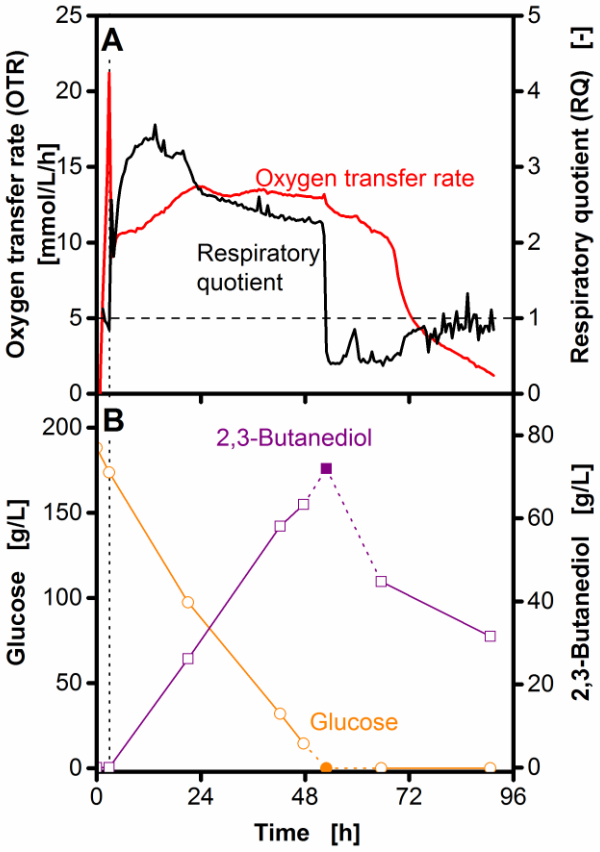

Appendix 4: 2,3-Butanediol formation and subsequent consumption during the cultivation of *Bacillus licheniformis* DSM 8785. As indicated by the vertical dotted line, the shaking frequency was reduced from 350 to 100 rpm after 3 h. Data on oxygen transfer rate (OTR) and respiratory quotient (RQ) (A), and total 2,3-butanediol and glucose concentration (B) are depicted. In addition to offline samples (open symbols), the concentrations upon glucose depletion were calculated as illustrated in Figure 3-3 (closed symbols). For clarity, the connection between the measured and calculated values is shown as dotted line. 2,3-Butanediol is shown as sum of the stereoisomers. The RQ is only shown for OTR > 1 mmol/L/h. To account for the increase of metabolite concentrations due to evaporation of water, all concentrations were corrected accordingly and referred to the initial filling volume. Cultivation conditions: 250 mL unbaffled shake flasks, temperature: 37 °C, shaking frequency: 350/100 rpm, shaking diameter: 50 mm, filling volume: 30 mL, Nakashimada medium with 100 mM MES buffer.

Appendix 5: Calculation of the average respiratory quotient from offline samples. This table provides additional information to Figure 4-5. The metabolite formation during the 2,3-butanediol production phase (between t_1 and t_2 in Appendix 1) is shown for 19 individual shake flask cultivations with different maximum oxygen transfer capacity (OTR_{max}). The algebraic sign indicates if the metabolite was formed (positive) or consumed (negative) in the observed cultivation period. The average RQ was calculated from these values according to Equation 2-9.

OTR_{max}	**Metabolite and cell dry weight formation [g/L]**									**average RQ [-]**	
[mmol/L/h]	Glucose	CDW	BDO	Glycerol	Acetoin	Lactate	Ethanol	Succinate	Acetate	calculated	measured
4.3	-171.3	2.0	70.7	10.6	3.9	1.3	n.d.	n.d.	-0.2	4.6	4.1
4.4	-163.8	-2.2	69.7	12.2	1.2	-3.5	-0.5	n.d.	n.d.	6.0	4.2
4.7	-198.1	5.6	86.3	17.8	1.0	2.1	1.4	n.d.	n.d.	4.3	4.3
5.4	-161.2	5.9	65.0	7.9	1.6	2.0	1.3	n.d.	n.d.	5.0	4.4
5.7	-196.6	7.0	80.3	12.0	1.3	0.6	1.3	n.d.	n.d.	5.1	4.2
6.2	-170.8	3.2	68.7	7.8	4.5	1.7	n.d.	n.d.	-0.3	4.6	3.9
6.4	-161.6	-2.0	68.1	7.2	1.8	-2.4	-0.5	n.d.	n.d.	5.3	3.9
7.2	-165.6	6.2	67.8	4.2	1.4	5.5	2.9	n.d.	n.d.	4.0	3.7
9.0	-165.3	6.1	71.0	1.6	2.9	2.6	2.5	n.d.	n.d.	3.4	3.4
9.2	-169.1	4.9	66.1	2.8	6.0	1.6	n.d.	n.d.	-0.3	4.4	3.7
9.3	-171.4	-0.7	70.0	0.9	4.9	-7.1	-2.5	n.d.	n.d.	5.6	3.5
9.4	-181.9	8.0	80.2	0.7	6.4	n.d.	n.d.	n.d.	n.d.	3.1	3.4
10.1	-163.5	2.6	71.2	1.2	5.0	-5.5	-0.7	n.d.	n.d.	4.0	3.1
12.7	-161.7	6.6	66.6	n.d.	8.6	-0.9	1.1	n.d.	n.d.	2.7	2.7
12.8	-188.6	7.4	75.9	n.d.	10.0	n.d.	n.d.	n.d.	n.d.	2.9	2.6
12.9	-170.1	3.7	61.9	0.4	7.4	-5.8	-2.9	n.d.	n.d.	4.4	2.9
13.4	-172.9	4.9	60.2	0.2	10.4	-3.1	-2.7	-0.1	n.d.	4.2	2.6
15.5	-169.3	5.4	55.8	n.d.	16.0	-1.2	-1.6	n.d.	n.d.	3.3	2.7
16.0	-165.3	-1.2	55.9	n.d.	23.6	n.d.	-0.7	-0.7	n.d.	2.5	2.4

CDW: Cell dry weight; BDO: 2,3-butanediol; n.d.: not detected

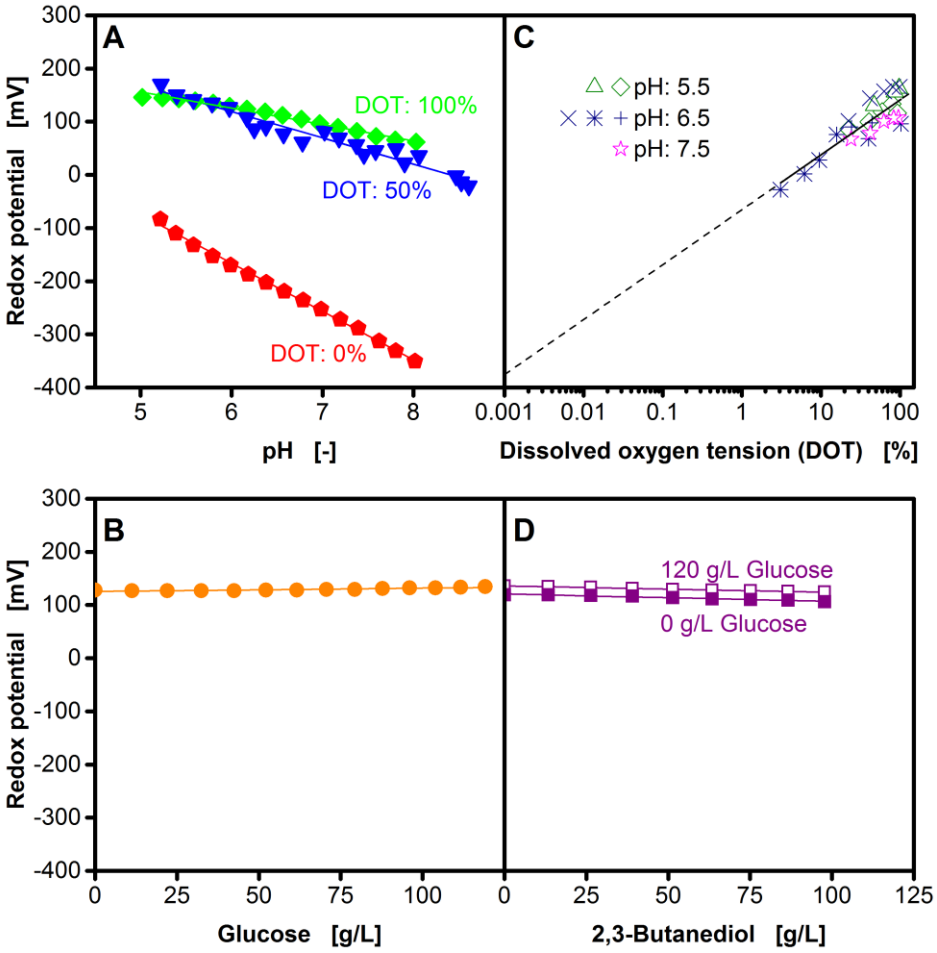

Appendix 6: Comparison of different influences on the absolute value of the redox potential. The influence of pH (A), dissolved oxygen tension (DOT) (C), glucose (B) and 2,3-butanediol (D) on the redox potential is compared. The same data as in Figure 5-9 are shown, but the absolute redox potential is shown instead of the redox potential shift. Solid lines represent linear correlations in the range of the measured data. The dashed line in (C) visualizes the approach to interpolate the correlation to determine low DOTs via redox potential measurements.

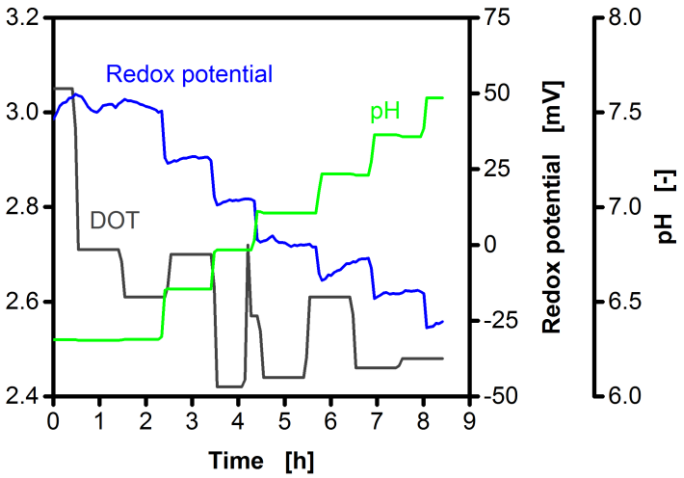

Appendix 7: Influence of the pH on the redox potential at a dissolved oxygen tension of 3%. To exclude any effects of microbial growth, sterile cultivation medium was used to investigate the redox potential. The reactor was constantly gassed with a mixture of nitrogen and pressurized air and the pH was adjusted by NaOH titration. Experimental setup: Temperature: 37 °C, 2 L stirred tank reactor, filling volume: 1.5 L, Nakashimada medium without MES buffer addition.

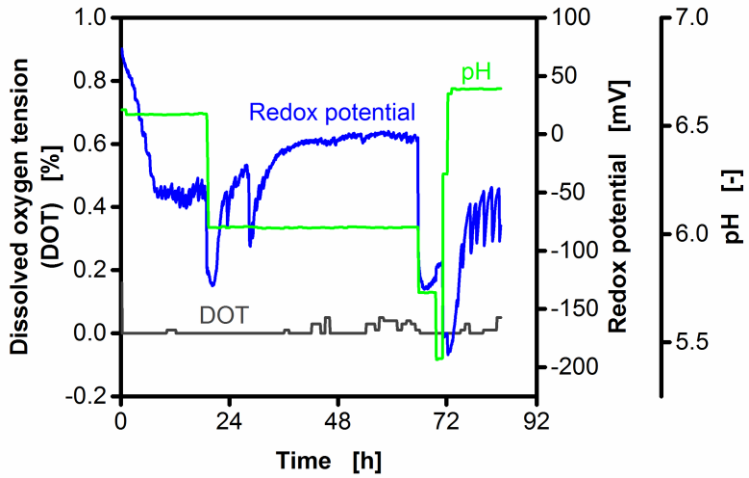

Appendix 8: Redox potential measurements in phosphate buffer. Redox potential, pH and dissolved oxygen tension (DOT) measurements in sterile phosphate buffer (80 mM) are shown. The reactor was constantly gassed with nitrogen and the pH was adjusted by NaOH or H_2SO_4 titration. Experimental setup: Temperature: 37 °C, 2 L stirred tank reactor, filling volume: 1.5 L.

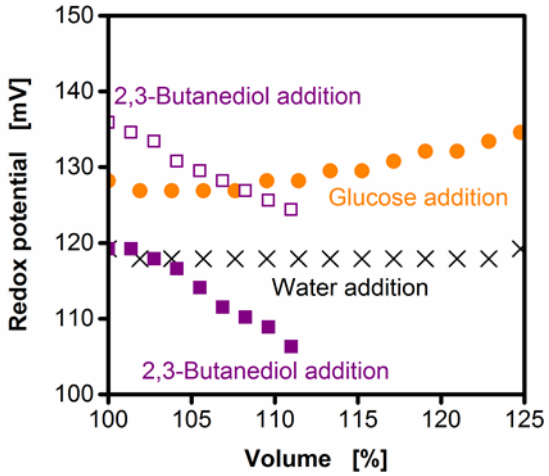

Appendix 9: Influence of glucose, 2,3-butanediol and water addition on the redox potential. The influence of 2,3-butanediol was tested in the presence and absence of glucose. Experimental setup: Sterile Nakashimada medium (without MES buffer addition) was mixed in a beaker glass with a magnetic stirrer at room temperature and water, glucose or 2,3-butanediol solutions were added gradually. Data pairs were recorded when the redox potential reached constant values.

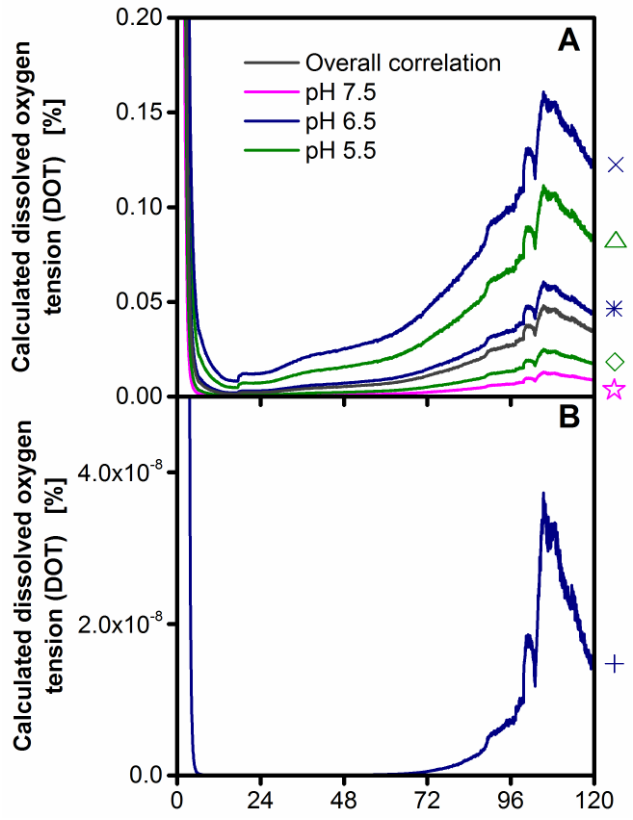

Appendix 10: Calculation of the dissolved oxygen tension from the redox potential. The dissolved oxygen tension (DOT) was calculated based on the course of the redox potential shown in Figure 5-10. The calculation is based on the ΔE_{DOT} derived from each individual experiment shown in Figure 5-7 as indicated by the respective symbol behind each curve. The overall correlation that is also used for the calculation of the DOT in Figure 5-10 is shown as reference. Different scalings of the ordinate are used in A and B. At the beginning of the cultivation, an agitation rate of 400 rpm was applied. At 18 h, the agitation rate was shortly adjusted to 500 rpm for 0.5 h and then reduced to 450 rpm for the rest of the cultivation. Cultivation conditions: Temperature: 37 °C, 2 L stirred tank reactor, filling volume: 1.5 L, aeration rate: 0.5 L/min (0.33 vvm), Nakashimada medium without MES buffer addition.

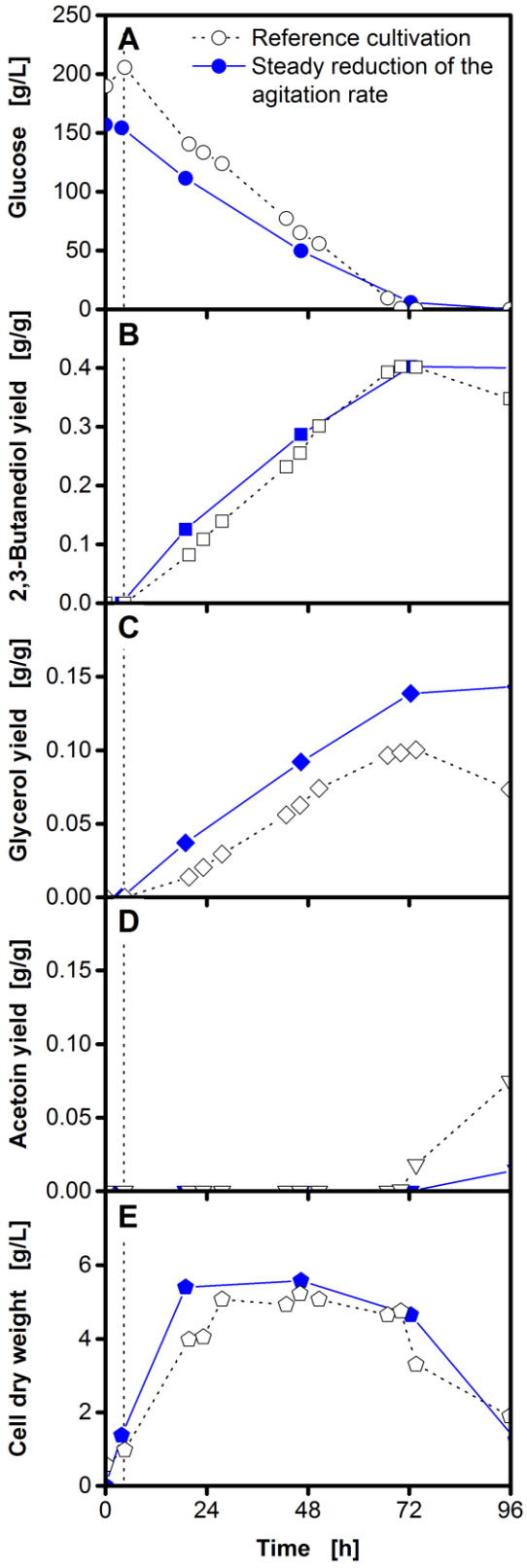

Appendix 11: Reduction of the agitation rate during the cultivation of *Bacillus licheniformis* DSM 8785. The corresponding offline samples to the reference cultivation (black) and a cultivation with steadily decreased agitation rate (blue) shown in Figure 5-11 are presented. The courses of glucose concentration (A), 2,3-butanediol (B), glycerol (C), acetoin (D) yields and the cell dry weight (E)

are shown. At the beginning of the cultivation, oxygen unlimited growth conditions were assured using an agitation rate control (DOT ≥ 30%) (black) or a manually adjusted high agitation rate (blue). To induce oxygen-limited conditions the agitation rate was then reduced to 500 rpm. After 19 h the agitation rate was steadily decreased to counteract the increasing DOT in (E). Cultivation conditions: Temperature: 37 °C, 2 L stirred tank reactor, filling volume: 1.5 L, aeration rate: 0.5 L/min (0.33 vvm), Nakashimada medium without MES buffer addition.